Tissue-specific expression of SMALL AUXIN UP RNA41 differentially regulates cell expansion and root meristem patterning in Arabidopsis

Kong, Yingying ; Zhu, Yubin ; Gao, Chen ; She, Wenjing ; Lin, Weiqiang ; Chen, Yong ; Han, Ning ; Bian, Hongwu ; Zhu, Muyuan ; Wang, Junhui

Abstract: Among the three primary auxin-induced gene families, Auxin/Indole-3-Acetic Acid (Aux/IAA), Gretchen Hagen3 (GH3) and SMALL AUXIN UP RNA (SAUR), the function of SAUR genes remains unclear. Arabidopsis SAUR genes have been phylogenetically classified into three clades. Recent work has suggested that SAUR19 (clade II) and SAUR63 (clade I) promote cell expansion through the modulation of auxin transport. Herein, we present our work on SAUR41, a clade III SAUR gene with a distinctive expression pattern in root meristems. SAUR41 was normally expressed in the quiescent center and cortex/endodermis initials; upon auxin stimulation, the expression was provoked in the endodermal layer. During lateral root development, SAUR41 was expressed in prospective stem cell niches of lateral root primordia and in expanding endodermal cells surrounding the primordia. SAUR41-EGFP (enhanced green fluorescent protein) fusion proteins localized to the cytoplasm. Overexpression of SAUR41 from the Cauliflower mosaic virus 35S promoter led to pleiotropic auxin-related phenotypes, including long hypocotyls, increased vegetative biomass and lateral root development, expanded petals and twisted inflorescence stems. Ectopic SAUR41 proteins were able to promote auxin transport in hypocotyls. Tissue-specific expression of SAUR41 from the PIN1, WOX5, PLT2 and ACR4 promoters induced the formation of new auxin accumulation/signaling peaks above the quiescent centers, whereas tissue-specific expression of SAUR41 from the PIN2 and PLT2 promoters enhanced root gravitropic growth. Cells in the root stem cell niches of these transgenic seedlings were differentially enlarged. The distinctive expression pattern of the SAUR41 gene and the explicit function of SAUR41 proteins implied that further investigations on the loss-of-function phenotypes of this gene in root development and environmental responses are of great interest.

DOI: https://doi.org/10.1093/pcp/pct028

Tissue-specific Expression of SMALL AUXIN UP RNA41 Differentially Regulates Cell Expansion and Root Meristem Patterning in Arabidopsis

Journal:	*Plant and Cell Physiology*
Manuscript ID:	PCP-2012-E-00558.R1
Manuscript Type:	Regular Paper
Date Submitted by the Author:	n/a
Complete List of Authors:	Kong, Yingying; Zhejiang University, College of Life Sciences Zhu, Yubin; Zhejiang University, College of Life Sciences Gao, Chen; Zhejiang University, College of Life Sciences She, Wenjing; Zhejiang University, College of Life Sciences Lin, Weiqiang; Zhejiang University, College of Life Sciences Chen, Yong; Zhejiang University, College of life Sciences ning, han; Zhejiang University, College of life sciences hongwu, bian; Zhejiang University, College of life sciences muyuan, zhu; Zhejiang University, College of life sciences Wang, Junhui; Zhejiang University, College of life sciences
Keywords:	SAUR, Arabidopsis, Auxin transport, Cell expansion, Root meristem patterning

Running title: SAUR41 in cell expansion and root development

Manuscript type: Regular paper

***Correspondence author:**
Junhui Wang
Institute of Genetics, College of Life Sciences, Zhejiang University, 368 Yuhangtang Road, Hangzhou 310058, China
Tel: 0086-571-88206495; Fax: 0086-571-88206535
E-mail: junhuiwang@zju.edu.cn.

Subject area: growth and development

Number of black and white figures: 1
Number of color figures: 5
Number of table: 0
Supplementary data: 1 table.

Tissue-specific Expression of *SMALL AUXIN UP RNA41* Differentially Regulates Cell Expansion and Root Meristem Patterning in Arabidopsis

Yingying Kong[1,2,3], Yubin Zhu[1,2,3], Chen Gao[1], Wenjing She[1], Weiqiang Lin[1], Yong Chen[1], Ning Han[1], Hongwu Bian[1], Muyuan Zhu[1] and Junhui Wang[1]*

[1]*Institute of Genetics, College of Life Sciences, Zhejiang University, Zijingang Campus, Hangzhou 310058, China*

[2]*Sir Run Run Shaw Hospitol, School of Medicine, Zhejiang University, Hangzhou 310016, China*

[3]*These authors contributed equally to this work.*

Abbreviations: ARF, AUXIN RESPONSE FACTOR; ACR4, ARABIDOPSIS CRINKLY4; Aux/IAA, AUXIN/INDOLE-3-ACETIC ACID; CaMV, Cauliflower Mosaic Virus; DIC, differential-interference-contrast; EGFP, enhanced green fluorescent protein; GA, gibberellins; GH3, Gretchen Hagen3; GUS, beta-glucuronidase; LRC, lateral root cap; NAA, 1-naphthaleneacetic acid; PI, propidium iodide; PIN, PINFORM; PLT2, PLETHORA2; SAUR, SMALL AUXIN UP RNA; TIR1/AFB, TRANSPORT INHIBITOR RESPONSE1/AUXIN-BINDING F-BOX PROTEIN; WOX5, WUSCHEL-RELATED HOMEOBOX 5.

ABSTRACT

Among the three primary auxin-induced gene families, *Aux/IAA*, *GH3*, and *SAUR*, the function of *SAUR* genes remains unclear. Arabidopsis *SAUR* genes have been phylogenetically classified into three clades. Recent work has suggested that *SAUR19* (clade II) and *SAUR63* (clade I) promote cell expansion through the modulation of auxin transport. Herein, we present our work on *SAUR41,* a clade III *SAUR* gene with a distinctive expression pattern in root meristems. *SAUR41* was normally expressed in the quiescent center and cortex/endodermis initials; upon auxin stimulation, the expression was provoked in the endodermis layer. During lateral root development, *SAUR41* was expressed in prospective stem cell niches of lateral root primordia and in expanding endodermal cells surrounding the primordia. SAUR41-EGFP fusion proteins localized to the cytoplasm. Overexpression of *SAUR41* from the CaMV *35S* promoter led to pleiotropic auxin-related phenotypes, including long hypocotyls, increased vegetative biomass and lateral root development, expanded petals and twisted inflorescence stems. Ectopic SAUR41 proteins were able to promote auxin transport in hypocotyls. Tissue-specific expression of *SAUR41* from the *PIN1*, *WOX5*, *PLT2*, and *ACR4* promoters induced the formation of new auxin accumulation/signaling peaks above the quiescent centers, whereas tissue-specific expression of *SAUR41* from the *PIN2* and *PLT2* promoters enhanced root gravitropic growth. Cells in the root stem cell niches of these transgenic seedlings were differentially enlarged. The distinctive expression pattern of *SAUR41* gene and the explicit function of SAUR41 proteins implied that further investigations on the loss-of-function phenotypes of this gene in root development and environmental responses are of great interest.

Key words: SAUR; Arabidopsis; Auxin transport; Cell expansion; Root meristem patterning

Introduction

The plant hormone auxin modulates many aspects of plant growth and development, and recent decades have seen rapid progress in our understanding of the molecular mechanism of auxin biology (Woodward and Bartel, 2005; Santner and Estelle, 2009; Vanneste and Friml, 2009). For instance, in the field of auxin control of root development, numerous fundamental insights have been achieved on the contribution of shoot-derived auxin and root-generated auxin in root development (Overvoorde et al., 2010), establishment and maintenance of root stem cell niches (Aichinger et al., 2012; Perilli et al., 2012; Petricka et al., 2012), hormone interactions in coordinated root growth (Petricka et al., 2012; Ubeda-Tomás et al., 2012), and root growth in response to the environment (Jones and Ljung, 2012; Petricaka et al., 2012).

Auxin regulates cell division, differentiation and elongation in part by changing gene expression (Woodward and Bartel, 2005; Paponov et al., 2008; Santner and Estelle, 2009; Vanneste and Friml, 2009; Hayashi, 2012). Primary auxin response genes consist of members of three gene families (Hagen and Guilfoyle, 2002): *Aux/IAA* (*Auxin/Indole-3-Acetic Acid*), *GH3* (*Gretchen Hagen3*), and *SAUR* (*SMALL AUXIN UP RNA*). Aux/IAA proteins are transcription repressors (Ulmasov et al., 1997; Worley et al., 2000; Gray et al., 2001; Ouellet, et al., 2001; Ramos et al., 2001; Reed, 2001; Rogg et al., 2001; Tiwari et al., 2001). Their domain II interacts with the TIR1/AFB family of auxin receptors, while their domains III and IV dimerize with the ARF family transcription factors (Kim et al., 1997; Gray et al., 2001). Upon an auxin stimulus, Aux/IAA proteins are ubiquitinated by the TIR1/AFB proteins and then degraded, which release the activity of ARF proteins (Dharmasiri et al., 2005; Kepinski and Leyser, 2005; Tan et al., 2007). The GH3 family of acyl acid amido synthetases contributes to the amino acid conjugation of indole acetic acid, jasmonic acid, or salicylic acid (Ljung et al., 2002; Staswick et al., 2005; Park et al., 2007). The crystal structure and putative mechanisms of two GH3 proteins had been reported recently (Westfall et al., 2012). In contrast to Aux/IAA and GH3 proteins, the function of SAUR proteins remains unclear, most likely due to genetic redundancy within the

large SAUR gene family (Hagen and Guilfoyle, 2002; Jain et al., 2006).

Recent studies have begun to address the function of SAUR proteins in rice (*Oryza sativa*) and Arabidopsis. *OsSAUR39* has been identified as a negative regulator of auxin synthesis and transport, since rice plants overexpressing *OsSAUR39* exhibit reduced lateral root development and shoot and root length (Kant et al., 2009). The SAUR19 subfamily proteins (SAUR19-24) of Arabidopsis have been reported to be highly unstable; however, the addition of an N-terminal tag increases the stability of these proteins (Spartz et al., 2012). Arabidopsis plants overexpressing these stabilized SAUR fusion proteins exhibited increased hypocotyl elongation and larger leaf size, while seedlings expressing an artificial microRNA targeting the *SAUR19* subfamily genes exhibit opposite phenotypes (Franklin et al., 2011; Spartz et al., 2012). In another report on Arabidopsis, transgenic plant lines overexpressing *SAUR63:GFP* or *SAUR63:GUS* displayed long hypocotyls, petals and stamen filaments; in contrast, transgenic plants expressing artificial microRNA constructs targeting to the *SAUR63* subfamily genes (*SAUR61-68* and *SAUR75*) had slightly reduced hypocotyl and stamen filament elongation (Chae et al., 2012). The *SAUR19* subfamily genes were expressed in elongating tissues, including the root elongation zone (Spartz et al., 2012) while the *SAUR63* subfamily genes were not expressed in roots (Chae et al., 2012). As far as the mechanism is concerned, Arabidopsis SAUR proteins have been proposed to promote cell expansion through the modulation of auxin transport (Spartz et al., 2012; Chae et al., 2012).

The *SAUR* gene family could be phylogenetically classified into three clades (Kodira et al., 2011). The genes in clades I and II had a tendency to display higher expression levels in leaves and lower expressions in roots, while the genes in clade III demonstrated opposite expression patterns (Kodira et al., 2011). The *SAUR63* subfamily and the *SAUR19* subfamily were clade I and clade II *SAUR* genes, respectively (Kodira et al., 2011). Herein, we presented our work on *SAUR41*, a clade III *SAUR* gene displayed a distinctive expression pattern in Arabidopsis root meristems.

The *SAUR41* subfamily contained four members: *SAUR41* (At1g16510), *SAUR40*

(At1g79130), *SAUR71* (At1g56150) and *SAUR72* (At3g12830). Their amino acid sequences differed from other SAUR families in the N-terminus. In prior microarray experiments, the expression of *SAUR41* has been reported to be regulated by circadian rhythm (Mazzella et al., 2005; Darrah et al., 2006), biotic stress (Zhang et al., 2007; Peltier et al., 2011), and mitochondrial dysfunction and reactive oxygen species (Carrie et al., 2010; Gleason et al., 2011). The expression of *SAUR40* and *SAUR71* was responsive to abscisic acid signaling (Leondardt et al., 2004; Zeng et al., 2012) and the functional status of chloroplasts (Bosco et al., 2004; Estavillo et al., 2011). *SAUR71* and *SAUR72* were expressed in the vascular development (Nagawa et al., 2006; Shirakawa et al., 2009).

We found that *SAUR41* was normally expressed in the quiescent center and cortex/endodermis initials, but it was provoked in the endodermis layer upon an auxin or gravitropic stimulation. During lateral root development, *SAUR41* was distinctively expressed in prospective stem cell niches of lateral root primordia and in expanding endodermal cells surrounding the primordia. SAUR41-EGFP fusion proteins localized to the cytoplasm, unlike EGFP-SAUR19 and SAUR63-EGFP which localized predominantly to the plasma membrane. Interestingly, although the gene expression pattern and the protein localization pattern of *SAUR41* were different from *SAUR19* and *SAUR63*, the phenotypes resulting from overexpression of *SAUR41* driven by the CaMV *35S* promoter shared many similarities with those of *SAUR19* and *SAUR63* subfamily genes. Tissue-specific expression of *SAUR41* from promoters of auxin transporter genes and root meristem patterning genes differentially modulated root meristem development, root cell expansion, and root gravitropic growth. The distinctive expression pattern of *SAUR41* gene and the explicit function of ectopic SAUR41 proteins implied that further investigations on the loss-of-function phenotypes of this gene family in root development are of great interest.

Results

SAUR41 had a distinctive expression pattern in Arabidopsis root meristems

Previously, to counteract possible position effects in plant promoter analysis, we used the *gypsy*-Su(Hw) system of *Drosophila* in a novel approach that facilitated high and precise expression of reporter genes (She et al., 2010). Using this system, together with the GATEWAY recombination approach, we generated sets of promoter reporter lines for the *PIN* gene family encoding auxin carriers and the *TIR1/AFB* gene family encoding auxin receptors (She et al., 2010). We extended this system to promoter analysis of certain *SMALL AUXIN UP RNA* (*SAUR*) genes, and found that the *SAUR41* (At1g16510) gene showed a distinctive expression pattern in root meristems.

In generating promoter reporter lines for *SAUR41*, an ~1800 bp DNA fragment upstream of the ATG start codon of *SAUR41,* as predicted by AtcisDB (Davuluri et al., 2003), was fused with the *EGFP-GUS* reporter gene. Viewed by confocal microscopy, *SAUR41* was found to be specifically expressed in the quiescent center and cortex/endodermis initials of root stem niches (Fig. 1A). Considering that *SAUR* genes had been proposed to function in auxin-mediated growth events, we examined the expression of *SAUR41* under gravitropic stimulation and auxin treatment. Gravitropism allows plant roots to grow directionally, whereas auxin is an essential regulator in this process (Harrison and Masson, 2008). During the gravitropic response, the expression of *SAUR41* was provoked on both sides of the endodermis at the proximal meristem region and on the upper side of the endodermis at distal elongation zone, indicating that this gene might act to coordinate root elongation rather than simply respond to auxin redistribution (Fig. 1B). *SAUR41* was specifically induced in the endodermis with 1 h of auxin (10 μM 1-naphthaleneaacetic acid, NAA) treatment (Fig. 1C). Since the endodermis was recently reported as the primary responsive tissure for gibberellins (GA) to coordinate root growth (Ubeda-Tomás et al., 2008, 2009, 2012), we then tested whether or not *SAUR41* was a GA-responsive gene. As shown in Fig. 1D, *SAUR41* was unresponsive to GA treatment. This result was in agreement with the results of a microarray experiment (Josse et al., 2011).

Extending the duration of auxin treatment to 12 h, and detected by overnight

histochemical staining, *SAUR41* was found to be induced in multiple cell layers at the root meristem and transition zone (Fig. 1E). However, in the elongation zone, it was specifically induced in the endodermal cells (Fig. 1F).

During lateral root development, *SAUR41* was expressed in the prospective quiescent center of lateral root primordia (Fig. 1G, H). Interestingly, *SAUR41* was also specifically expressed in the endodermal cells surrounding the lateral root primordia during the process of the lateral root primordia breaking through the endodermis (Fig. 1G). In the newly formed lateral roots, *SAUR41* was strongly expressed in the quiescent center and initial cells, and weakly expressed in the endodermis (Fig. 1I). In hypocotyls, petioles and cotyledons, *SAUR41* was predominantly expressed in the vascular tissues (Fig. 1J, K and L).

SAUR41-EGFP fusion protein accumulated in the cytoplasm

To check the subcellular localization of the SAUR41 protein, we generated a transgenic construct in which the CaMV (Cauliflower Mosaic Virus) *35S* promoter drove a C-terminal translational fusion between the full-length SAUR41 and the EGFP protein. Location of the fusion protein in hypocotyls and root tips of stably-transformed Arabidopsis plants was examined by confocal microscopy. Results showed that the EGFP fluorescence was identified at the cytoplasm of epidermal and cortical cells in hypocotyls (Fig. 1M, N); and at the cytoplasm of all types of cells in root tips, including quiescent center cells, cortex/endodermis initial cells and epidermal cells (Fig. 1O, P).

Overexpression of *SAUR41* conferred pleiotropic auxin-related phenotypes

To explore potential roles for *SAUR41* in Arabidopsis growth and development, we first screened T-DNA and transposon insertion lines from the Arabidopsis Biological Resource Center (ABRC) and the Rikagaku Kenkyusho Bioresource Center (RIKEN-BRC), respectively. The line SALK_056968 from the ABRC stocks

contained a T-DNA at the promoter region of *SAUR41*. However, RT-PCR analysis revealed that this insertion did not impair the expression of *SAUR41* (data not shown). In three additional lines (SALK_121397, PST_11030 and PST_17947), we failed to identify DNA insertions inside the *SAUR41* gene.

We then used a gain-of-function approach and generated transgenic Arabidopsis plants overexpressing untagged (*35S::SAUR41*) or MYC-tagged (*35S::SAUR41-MYC*) *SAUR41* gene, in addition to the *35S::SAUR41-EGFP* plants described above. More than 20 independent lines were obtained for each transgenic construct. Plants overexpressing untagged *SAUR41* had strong phenotypes, similar to that of MYC-tagged *SAUR41*. In contrast, plants overexpressing EGFP-tagged *SAUR41* had the weakest phenotypes. We chose *35S::SAUR41* plants for detailed study.

The *35S::SAUR41* transgenic lines displayed pleiotropic auxin-related phenotypes. Light-grown seedlings exhibited 1.7-2.0-fold longer hypocotyls than wild-type controls (Fig. 2A, B, E; $P<0.01$, *t*-test). Surprisingly, these seedlings also displayed 1.3-1.5-fold longer primary roots compared to wild-type controls (Fig. 2C, D, F; $P<0.05$, *t*-test). In addition, overexpression of *SAUR41* increased root waving on vertically-oriented agar plates (Fig. 2D). After 10 d of growth, *35S::SAUR41* seedlings had 1.5-1.9-fold increase in lateral root numbers ($P<0.05$, *t*-test) and 20-30% increase in vegetative biomass as measured by the fresh weight of shoots (Fig. 2G, H; $P<0.05$, *t*-test).

Adult *35S::SAUR41* plants had twisted inflorescence stems (Fig. 2I). Furthermore, the petals of transgenic flower organs were over-expanded and defective in opening completely (Fig. 2J, K and L), resulting in reduced seed setting in many siliques (Fig. 2I).

To determine if the elongated hypocotyl phenotype induced by ectopic SAUR41 was due to increased cell expansion, we measured hypocotyl epidermal cell length in 6-d-old seedlings. The change in hypocotyl epidermal cell length was parallel to the change in hypocotyl length (Fig. 3A, Fig. 2E). We then directly measured ^{3}H IAA transport in hypocotyls and detected a 40-70% increase in basipetal IAA transport in hypocotyls of *35S::SAUR41-EGFP*, *35S::SAUR41-MYC*, and *35S::SAUR41* seedlings

(Fig. 3B).

Tissue-specific expression of *SAUR41* from the *PIN1* promoter induced alterations in root meristem patterning

As *SAUR41* had a distinctive expression pattern in Arabidopsis root meristems, and rice and Arabidopsis SAUR proteins have been proposed to modulate auxin transport (Kant et al., 2009; Spartz et al., 2012; Chae et al., 2012), we next implemented tissue-specific expression of *SAUR41* from promoters of auxin transporter genes and root meristem patterning genes. To facilitate the examination of auxin signaling and distribution, all transgenic plants were generated in a *DR5rev::GFP* background (Friml et al., 2003; Fig. 4B).

We first expressed *SAUR41* from the *PIN1* and *PIN2* promoters. In Arabidopsis roots, *PIN1* promoter activity was strong in stele cells and weak in endodermis and the quiescent center (She et al., 2010; Fig. 4C). Ectopic expression of *SAUR41* driven by the *PIN1* promoter led to auxin retention in stele initials transporting auxin, resulting in a large auxin accumulation/signaling peak (Fig. 4D-G). In addition, *PIN1::SAUR41* roots had additional tiers of distal stem cells (Fig. 4E, G), while wild-type roots typically had one tier of distal stem cells (Ding and Friml, 2010; Fig. 4A, B). Non-differentiated distal stem cells below the quiescent center were characterized by the absence of starch grains (Ding and Friml, 2010; Fig. 4H, L). Finally, *PIN1::SAUR41* roots had supernumerary cell layers (Fig. 4E, G), while wild-type roots exhibited distinctive root radial patterns (Fig. 4A, B). Statistically, 80-90% *PIN1::SAUR41* roots displayed abnormalities in root meristem patterning (n=40, $P<0.05$, *t*-test).

PIN2 promoter activity was detected in the epidermis, cortex and lateral root cap (She et al., 2010; Fig. 4I). Ectopic expression of *SAUR41* from the *PIN2* promoter induced expansion of epidermal and cortical cells, but the auxin accumulation/signaling pattern appeared normal (Fig. 4J). *PIN2::SAUR41* roots exhibited a root-waving phenotype on vertically-oriented agar plates, and the

epidermal and cortical cells in the two sides of root transition zones were irregularly and asymmetrically elongated (Fig. 4K).

Comparison of tissue-specific expression of *SAUR41* and *IAA2^{P65S}* from promoters of root meristem patterning genes

We also expressed *SAUR41* from the promoters of root meristem patterning genes. Three promoters were chosen: *WOX5*, *ACR4*, and *PLT2*. *WOX5* encoded a homeodomain transcription factor (Sarkar et al., 2007), *PLT2* encoded an AP-2 type transcription factor (Aida et al., 2004; Galinha et al., 2007), and *ACR4* encoded a receptor-like kinase (De Smet et al., 2008). They were three of the major regulators of root stem cell activity (Aichinger et al., 2012; Perilli et al., 2012; Petricka et al., 2012). To compare the effects between tissue-specific expression of a SAUR protein and a stabilized AUX/IAA protein, we introduced IAA2^{P65S} that harbored a site-directed mutation in the proline residue of conserved domain II. As one of 29 *Aux/IAA* genes of Arabidopsis, *IAA2* was highly auxin inducible and expressed in vascular tissues and auxin accumulation/signaling peaks (Swarup et al., 2001).

WOX5 was expressed in the quiescent center of root stem cell niches (Sarkar et al., 2007; Fig. 5A). Tissue-specific expression of *SAUR41* from the *WOX5* promoter induced the formation of additional auxin accumulation/signaling peaks in stele initials above the quiescent center (Fig. 5B-F). In addition, *WOX5::SAUR41* roots had supernumerary cell layers (Fig. 5C, D, F), like those observed in *PIN1::SAUR41* roots (Fig. 4E, G). As expected, tissue-specific expression of *IAA2^{P65S}* driven by the *WOX5* promoter inhibited auxin accumulation/signaling in the quiescent center (Fig. 5G, H). Interestingly, it also inhibited auxin accumulation/signaling in the stele initials (Fig. 5G, H), opposite to the effects observed in tissue-specific expression of *SAUR41* from the *WOX5* promoter (Fig. 5B-F).

ACR4 was expressed in the root stem cell niche and its surrounding cells, including young epidermal cells, cortical cells and columella cells (De Smet et al., 2008; Fig. 5I). Ectopic expression of *SAUR41* from the *ACR4* promoter led to the expansion of

cells expressing *ACR4* (Fig. 5J, K). Formation of auxin accumulation/signaling peaks in stele initials was visible (Fig. 5J, K), but not as dramatically as that in the *WOX5::SAUR41* roots (Fig. 5B-F), indicating that the balanced expression of *SAUR41* in the entire root stem cell niche attenuated the effects of ectopic SAUR proteins on auxin transport, compared to the selected expression of *SAUR41* in the quiescent center by the *WOX5* promoter. On the other hand, tissue-specific expression of $IAA2^{P65S}$ from the *ACR4* promoter had a more remarkable impact on root meristem development compared to that seen in $WOX5::IAA2^{P65S}$ roots. As shown in Fig. 5, $ACR4::IAA2^{P65S}$ roots had two separate auxin accumulation/signaling maxima: one in the quiescent center, the other in the young columella cells (Fig. 5L).

PLT2 was gradiently expressed in root meristems and lateral cap cells (Aida et al., 2004; Galinha et al., 2007; Fig. 5M). Tissue-specific expression of *SAUR41* from the *PLT2* promoter exhibited triple effects as addressed above: additional auxin accumulation/signaling peaks in stele initials, and supernumerary cell layers in the proximal meristem zone (Fig. 5N, O). On the other hand, tissue-specific expression of $IAA2^{P65S}$ from the *PLT2* promoter inhibited auxin accumulation/signaling in the quiescent center, promoted auxin accumulation/signaling in stele initials, and led to establishment of new auxin accumulation/signaling peaks in the adjacent provascular cells (Fig. 5P), similar to that seen for relocalization of auxin accumulation/signaling peaks upon polar auxin transport inhibitor treatment (Sabatini et al., 1999).

Ectopic SAUR41 proteins differentially regulated root cell expansion and root gravitropic growth

We measured cell areas of stele initial cells, quiescent center cells, and distal stem cells in root meristems of transgenic seedlings expressing *SAUR41* from promoters of auxin transporter genes and root meristem patterning genes. Results showed that *PIN1::SAUR41*, *WOX5::SAUR41*, and *PLT2::SAUR41* roots had a 30-60% increase in cell areas of stele initial cells and quiescent center cells, while *ACR4::SAUR41* roots had enlarged quiescent center cells and distal stem cells (Fig. 6A, $P<0.05$, *t*-test).

The root gravitropic responses in these transgenic seedlings were also analyzed. *ACR4::SAUR41* roots showed delayed gravitropic growth (Fig. 6B), coinciding with their higher auxin accumulation/signaling in young columella cells but lower auxin accumulation/signaling in root lateral cap cells (Fig. 5I). *PIN2::SAUR41* roots had advanced gravitropic growth 2 h after the gravitropic stimulation, while *PLT2::SAUR41* roots displayed enhanced gravitropic growth 3 h after the gravitropic stimulation (Fig. 6B). It has been suggested that auxin transport in lower side of lateral cap cells and auxin accumulation in lower side of epidermal and cortical cells were essential for root gravitropic response (Ottenschläger, et al., 2003). Our results were consistent with the expression pattern of *PIN2* and *PLT2* promoters. *PIN2* was expressed in both lateral cap cells and epidermal and cortical cells (Fig. 4I), while *PLT2* was expressed in lateral cap cells (Fig. 5M)

Discussion

The expression pattern of *SAUR41* in root meristems was distinctive. *SAUR19* subfamily genes were expressed in growing hypocotyls in response to shade avoidance, and in root elongation zones in response to auxin treatment (Spartz et al., 2012). *SAUR63* and members of its clade were expressed in growing regions of hypocotyls, cotyledons, petiole, young rosette leaves and inflorescence stems, but not in roots (Chae et al., 2012). Herein, we found that the expression of *SAUR41* was normally restricted to the quiescent center and cortex/endodermis initials of root meristems; upon an auxin or gravitropic stimulation, it was provoked in the endodermis at proximal meristem region and transition zone of Arabidopsis roots (Fig. 1A-F). Furthermore, *SAUR41* was differentially expressed during lateral root development, as manifested by GUS activity in prospective stem cell niches of lateral root primordia, and in expanding endodermal cells surrounding the lateral root primordia (Fig. 1G-I). In prior microarray experiments, the expression of *SAUR41* has been reported to be regulated by multiple environmental signals (Mazzella et al., 2005; Darrah et al., 2006; Zhang et al., 2007; Peltier et al., 2011). Taken together, it seemed

that *SAUR41* was actively expressed in response to both developmental and environmental cues.

SAUR41-EGFP fusion proteins localize to the cytoplasm (Fig. 1M-P), while EGFP-SAUR19 and SAUR63-EGFP localize predominantly to the plasma membrane (Spartz et al., 2012; Chae et al., 2012). Although the protein localization pattern and the gene expression pattern of *SAUR41* were different from *SAUR19* and *SAUR63*, the phenotypes resulting from overexpression of *SAUR41* driven by the CaMV *35S* promoter shared many similarities with those of *SAUR19* and *SAUR63* subfamily genes. In all three cases, transgenic seedlings had elongated hypocotyls, expanded hypocotyl epidermal cells, and enhanced hypocotyl basipetal IAA transport, compared to wild type (Fig. 2A, B, E; Fig. 3; Spartz et al., 2012; Chae et al., 2012). In the cases of *SAUR41* and *SAUR19*, transgenic seedlings displayed waving roots and increased vegetative biomass (Fig. 2C, D, H; Spartz et al., 2012); while in the cases of *SAUR41* and *SAUR63*, transgenic plants had expanded petals and twisted inflorescence stems (Fig. 2I-L; Chae et al., 2012). Interestingly, only in the case of *SAUR41* did the transgenic seedlings have increased primary root length and lateral root development compared to wild-type controls (Fig. 2F, G). Thus, it seems likely that Arabidopsis SAUR proteins have some similarities but also specificity in terms of molecular functions. Alternatively, SAUR proteins may share a similar molecular function, but different SAUR proteins require different tissue-specific partners.

Tissue-specific expression of *SAUR41* from *PIN1*, *WOX5, ACR4* or *PLT2* promoters caused new auxin accumulation/signaling peaks in stele initial cells transporting auxin (Fig. 4D-G; Fig. 5B-F, N, O). Roots of *PIN1::SAUR41* seedlings had additional tiers of distal stem cells below the quiescent center and supernumerary cell layers in root meristems (Fig. 4D-G, H, L, Q). It has been reported that auxin regulates distal stem cell differentiation in Arabidopsis roots, and defects in auxin transport would lead to additional tiers of distal stem cells (Ding and Friml, 2010). Thus, it seemed likely that SAUR41 induced perturbation of auxin transport in root meristems as it was expressed above the stem cell niches (from the *PIN1* promoter). In contrast, tissue-specific expression of *SAUR41* from the *PIN2* promoter did not

induce alterations in root meristem patterning, but caused alterations in cell expansion in the corresponding cell lineages (Fig. 4J, K). In addition, *PIN2::SAUR41* and *PLT2::SAUR41* roots had enhanced gravitropic growth (Fig. 6B), indicating that ectopic SAUR41 proteins promoted root basipetal auxin transport for root gravitropic responses. Taken together, it seems likely that ectopic SAUR41 proteins retard auxin transport in root stem cell niches, but promote auxin transport in root lateral cap cells and epidermal and cortical cells.

Previously, it has been proposed that rice *SAUR39* acted as a negative regulator of organ growth and auxin transport (Kant et al. 2009), while Arabidopsis *SAUR19* and *SAUR63* acted as positive regulators of cell expansion and auxin transport (Spartz, et al., 2012; Chae et a., 2012). Herein, in terms of cell expansion, we found that *SAUR41* promoted cell expansion, as it was constitutively expressed from the CaMV *35S* promoter (Fig. 2, 3). In addition, stele initial cells, quiescent center cells, and distal stem cells in root meristems of transgenic seedlings expressing *SAUR41* from promoters of auxin transporter genes and root meristem patterning genes were differentially enlarged (Fig. 6A). Thus, similar to SAUR19 with N-terminal tags and SAUR63 with C-terminal tags, untagged SAUR41 promoted cell expansion, as it was ectopically expressed. However, in terms of auxin transport, the functions of SAUR proteins appeared to be more complicated. The observed higher flow rate of labeled IAA in hypocotyls could be an indirect effect of SAUR protein overexpression. Two questions, why ectopic SAUR41 proteins retarded auxin transport in root stem cell niches but promoted basipetal auxin transport, and why rice OsSAUR39 (analogous to Arabidopsis SAUR63, clade I) inhibited auxin transport but Arabidopsis SAUR63 promoted auxin transport, remained unanswered. It should be noticed that the *DR5::GFP* marker basically indicated the status of auxin signaling but not the auxin transport. Currently, direct measurement of auxin transport in root stem cell niches is unavailable. It was tempting to speculate that SAUR41 proteins used different mechanism to regulate auxin transport for cell elongation and for root meristem patterning.

Tissue-specific expression of $IAA2^{P65S}$ from *WOX5*, *ACR4* and *PLT2* promoters

displayed fundamentally different effects on root meristem patterning compared to that observed for *SAUR41* (Fig. 5). The mechanism of stabilized Aux/IAA proteins is clear. They impaired the SCF^{TIR1} pathway of auxin signaling to regulate cell division, differentiation and elongation. They also disturbed auxin transport by transcriptional modification of the auxin export machinery (Hayashi, 2012; Scherer et al., 2012). On the contrary, the precise mechanism by which SAUR proteins regulate cell expansion and auxin transport remains unclear. It will be interesting to learn whether there exist epistatic interactions between the *IAA2* and the *SAUR41* gain of function phenotypes. We are currently crossing the $IAA2^{P65S}$ lines with the corresponding *SAUR41* lines to answer this question.

The *SAUR41* function reported here was solely depends on the ectopic expression data, while its endogenous role in stem cell maintenance remained unclear. The gene could be involved in the regulation of cell sizes of quiescent center and cortex/endodermis initials, and/or in the modulation of auxin transport in these cells. In addition, the *SAUR41* subfamily contains four members: *SAUR40*, *SAUR41*, *SAUR71*and *SAUR72*. Further investigations on promoter activity and protein localization patterns of other *SAUR41* subfamily members, as well as on loss-of-function phenotypes of the *SAUR41* gene family, are required and of great interest.

Materials and methods

Plant materials and growth conditions

Arabidopsis thaliana ecotype Columbia-0 and the *DR5rev::GFP* background (Friml et al., 2003) were used as sources of wild-type plant materials. Promoter reporter lines for the *PIN* gene family and the *TIR1/AFB* gene family (She et al., 2010) have been donated to ABRC. Seeds were surface-sterilized and cultured aseptically on 9 cm Petri dishes containing Gamborg's B5 medium with 1% (w/v) sucrose and 1% (w/v) agar. The plates were maintained at 4˚C for 2 d, and then transferred to a culture room (23˚C, 80 μM m^{-2} s^{-1} irradiance with a 16-h photoperiod, 30-40% RH).

Vector construction and plant transformation

We used the GATEWAY™ system for vector construction. Entry vectors were created using the pENTR™/D-TOPO kits (Invitrogen). The PCR primers for construction of entry vectors for the coding region of *SAUR41*and for promoter regions of *SAUR41*, *WOX5*, *ACR4* and *PLT2* were listed in Table S1. *IAA2*^{P65S} was generated by overlapping PCR using primers in Table S1. Each entry clone was confirmed by DNA sequencing. GATEWAY™ compatible destination vectors for protein subcellular localization, overexpression, MYC tagging and promoter analysis were used (Karimi et al., 2002; Earley et al., 2006; She et al., 2010). The LR Reaction was conducted to generate different expression vectors.

To facilitate tissue-specific gene expression from various promoters, the CaMV *35S* promoter in the overexpression constructs (*35S::SAUR41* and the *35S::IAA2*^{P65S}) was replaced with a *ccdB* fragment by a method described previously (Yang et al., 2012). Briefly, the *ccdB* fragment was PCR-amplified using pH7FWG2,0 as a template, with the primers ccdB-Up and ccdB-Dn, containing an introduced *HindIII* and *SpeI* site, respectively. The *ccdB* fragment was then digested to replace the 35S promoter sequence, thus forming new destination vectors for tissue-specific expression.

All of the expression vectors were electroporated into *Agrobacterium tumefaciens* strain GV3101. Plants were transformed using the vacuum infiltration method

(Bechtold et al., 1993). Transgenic plants were selected on B5 plates with 12.5 μg/mL hygromycin or 25 μg/mL kanamycin depending on the selection markers. Single-locus and homozygous transgenic lines were characterized as we described previously (She et al., 2010).

Microscopic analysis and Histochemical detection

For histochemical detection of GUS activities, young seedlings at different developmental stages and different parts from transgenic plants were collected. They were stained at 37˚C overnight in 1 mM 5-bromo-4-chloro-3-indolyl-b-D-glucuronic acid (X-Gluc), 1 mM potassium ferricyanide, 0.1% Triton X-100, and 0.1 M sodium phosphate buffer, pH 7.0 with 10 mM EDTA. Samples were washed in 70% ethanol to remove chlorophyll. DIC (differential-interference-contrast) images were visualized using a microscope (Nikon Eclipse 80i, Japan) with DXM1200 CCD camera and EclipseNet software. For the localization of fluorescence fusion proteins, a confocal microscope system (Zeiss LSM510, Germany) was used. Without specification, 5-d-old seedlings were mounted in water. Starch grains in columella cells were stained with I_2-KI as described previously (Ding and Friml, 2010).

Hypocotyl IAA transport assay

IAA transport in hypocotyls was measured as previously described (Chae, 2012). [^{3}H] IAA was a product of American Radiolabeled Chemicals, Inc. (St. Louis, MO, USA). The radioisotope counts of [^{3}H] IAA was detected using a low-noise scintillation counter (MicroBeta 2, Perkin Elmer).

Growth and cell measurement, statistical analysis, and image processing

After incubations for the durations indicated in the text, the plates were digitally photographed. Root and hypocotyl length was measured using magnified images. Lateral root (>1 mm) numbers were counted using each seedling as an individual sample. For hormone treatment, seedlings were transferred onto a medium containing 10 μM NAA or GA_3 for 1 or 12 h. For gravitropism assays, the protocol of Weijers et

al. (2005) was adopted. The mean hypocotyl epidermal cell length and the cell area of root stem cell niches were measured as described by Spartz et al. (2012). Each treatment contained 30-50 seedlings and was replicated 3 times. Statistical analysis of the data was performed using Microsoft Excel and Student's *t*-test. Images were processed using Adobe Photoshop CS2.

Supplementary data

Supplementary data are available at PCP online.

Funding

This work was supported by funding from the National Natural Science Foundation of China (grant no. 31170211 to J.W.).

Acknowledgements

We are grateful to ABRC and RIKEN-BRC for the distribution of Arabidopsis materials. No conflict of interest is declared.

References

Aichinger, E., Kornet, N., Friedrich, T., and Laux, T. (2012) Plant stem cell niches. *Annu. Rev. Plant Biol.* 63: 625-636.

Aida, M., Beis, D., Heidstra, R., Willemsen, V., Blilou, I., Galinha, C., et al. (2004) The *PLETHORA* genes mediate patterning of the *Arabidopsis* root stem cell niche. *Cell,* 119: 109-120.

Bechtold, N., Ellis, J., and Pelletier, G. (1993) *In planta* Agrobacterium-mediated gene-transfer by infiltration of adult *Arabidopsis thaliana* plants. *Compt Rend Acad Sci Serie III De La Vie-Life Sci.* 316: 1194-1199

Bosco, C.D., Lezhneva., L., Biehl, A., Leister, D., Strotmann, H., Wanner., G., and Meurer, J. (2004) Inactivation of the chloroplast ATP synthase gamma subunit results in high non-photochemical fluorescence quenching and altered nuclear gene expression in *Arabidopsis thaliana*. *J. Biol. Chem.* 279: 1060-1069

Carrie, C., Giraud, E., Duncan, O., Xu, L., Wang, Y., Huang, S., et al. (2010) Conserved and novel functions for *Arabidopsis thaliana* MIA40 in assembly of proteins in mitochondria and peroxisomes. *J. Biol. Chem.* 285: 36138-36148.

Chae, K., Lsaacs, C.G., Reeves, P.H., Msloney, G.S., Muday, G.K., Nagpal, P., and Reed, J.W. (2012) *Arabidopsis SMALL AUXIN UP RNA63* promotes hypocotyl and stamen filament elongation. *Plant J* 71 6: 84-697.

Darrah, C., Taylor, B.L., Edwards, K.D., Brown, P.E., Hall, A., and McWatters, H.G. (2006) Analysis of phase of *LUCIFERASE* expression reveals novel circadian quantitative trait loci in *Arabidopsis*. *Plant Physiol.* 140: 1464-1474.

Davuluri, R.V., Sun, H., Palaniswamy, S.K., Matthews, N., Molina, C., Kurtz, M., and Grotewold, E. (2003) AGRIS, Arabidopsis Gene Regulatory Information Server, an information resource of Arabidopsis cis-regulatory elements and transcription factors. *BMC Bioinform.* 4: 25.

De Smet, I., Vassileva, V., De Rybel, B., Levesque, M.P., Grunewald, W., Van Damme, D., et al. (2008) Receptor-like kinase ACR4 restricts formative cell divisions in the Arabidopsis root. *Science* 322: 594-597.

Dharmasiri, N., Dharmasiri, S., and Estelle, M. (2005) The F-box protein TIR1 is an auxin receptor. *Nature* 435: 441-445

Ding, Z., and Friml, J. (2010) Auxin regulates distal stem cell differentiation in *Arabidopsis* roots. *Proc. Natl. Acad. Sci. U S A*. 107: 12046-12051.

Earley, K.W., Haag, J.R., Pontes, O., Opper, K., Juehne, T., Song, K., and Pikaard, C.S. (2006). Gateway-compatible vectors for plant functional genomics and proteomics. *Plant J* 45: 616-629.

Estavillo, G.M., Crisp, P.A., Pornsiriwong, W., Wirtz, M., Collinge, D., Carrie, C., et al. (2011) Evidence for a SAL1-PAP chloroplast retrograde pathway that functions in drought and high light signaling. *Plant Cell* 23: 3992-4012

Franklin, K.A., Lee, S.H., Patel, D., Kumar, S.V., Spartz, A.K., Gu, C., et al. (2011) PHYTOCHROME-INTERACTING FACTOR 4 (PIF4) regulates auxin biosynthesis at high temperature. *Proc. Natl. Acad. Sci. U S A.* 108: 20231-20235.

Friml, J., Vieten, A., Sauer, M., Weijers, D., Schwarz, H., Hamann, T., et al. (2003) Efflux-dependent auxin gradients establish the apical-basal axis of Arabidopsis. *Nature* 426: 147–153.

Galinha, C., Hofhuis, H., Luijten, M., Willemsen, V., Blilou, I., Heidstra, R., and Scheres, B. (2007) PLETHORA proteins as dose-dependent master regulators of Arabidopsis root development. *Nature* 449: 1053-1057.

Gleason, C., Huang, S., Thatcher, L.F., Foley, R.C., Anderson, C.R., Carroll, A.J., et al.

(2011) Mitochondrial complex Ⅱ has a key role in mitochondrial-derived reactive oxygen species influence on plant stress gene regulation and defense. *Proc. Natl. Acad. Sci. U S A.* 108: 10768-10773.

Gray, W.M,, Kepinski, S., Rouse, D., Leyser, O., and Estelle, M. (2001) Auxin regulates SCF^{TIR1} –dependent degradation of AUX/IAA proteins. *Nature* 414: 271-276

Hagen, G. and Guilfoyle, T. (2002) Auxin-responsive gene expression: genes, promoters and regulatory factors. *Plant Mol. Biol.* 49: 373-385.

Harrison, B.R., and Masson, P.H. (2008) ARL2, ARG1 and PIN3 define a gravity signal transduction pathway in root statocytes. *Plant J* 53: 380-392.

Hayashi, K. (2012) The interaction and integration of auxin signaling components. *Plant Cell Physiol.* 53: 965-975

Jain, M., Tyagi, A.K., and Khurana, J.P. (2006) Genome-wide analysis, evolutionary expansion, and expression of early auxin-responsive *SAUR* gene family in rice (*Oryza sativa*). *Genomics* 88: 360-371.

Jones, B. and Ljung K. (2012) Subterranean space exploration: the development of root system architecture. *Curr. Opin. Plant Biol.* 15: 97-102.

Josse, E.-M., Gan, Y., Bou-Torrent, J., Stewart, K.L., Gilday, A.D., Jeffree, C.E., et al. (2011) A DELLA in disguise: SPATULA restrains the growth of the developing *Arabidopsis* seedling. *Plant Cell* 23: 1337-1351.

Kant, S., Bi, Y.M., Zhu, T. and Rothstein, S.J. (2009) SAUR39, a small auxin-up RNA gene, acts as a negative regulator of auxin synthesis and transport in rice. *Plant Physiol.* 151: 691-701.

Karimi, M., Inzé, D., and Depicker, A. (2002) GATEWAYTM vectors for Agrobacterium-mediated plant transformation. *Trends Plant Sci.* 7: 193-195

Kepinski, S., and Leyser, O. (2005) The Arabidopsis F-box protein TIR1 is an auxin receptor. *Nature* 435: 446-451.

Kim, J., Harter, K., and Theologis, A. (1997) Protein-protein interactions among the Aux/IAA proteins. *Proc. Natl. Acad. Sci. U S A. 94:* 11786-11791

Kodaira K.-S., Qin, F., Tran, L.-S.P., Maruyama, K., Kidokoro, S., Fujita, Y. et al.

(2011) Arabidopsis Cys2/His2 zinc-finger proteins AZF1 and AZF2 negatively regulate abscisic acid-repressive and auxin-inducible geness under abiotic stress conditions. *Plant Physiol.* 157: 742-756

Leonhardt, N., Kwak J.M., Robert, N., Waner, D., Leonhardt, G., and Schroeder, J.I. (2004) Microarray expression analyses of Arabidopsis guard cells and isolation of a recessive abscisic acid hypersensitive protein phosphatase 2C mutant. *Plant Cell* 16: 596-615

Ljung, K., Hull, A.K., Kowalczyk, M., Marchant, A., Celenza, J., Cohen, J.D., and Sandberg, G. (2002) Biosynthesis, conjugation, catabolism and homeostasis of indole-3-acetic acid in *Arabidopsis thaliana*. *Plant Mol. Biol.* 50: 309–332.

Mazzella, M.A., Arana, M.V., Staneloni, R.J., Perelman, S., Batiller, M.J.R., Muschietti, J., et al. (2005) Phytochrome control of the *Arabidopsis* transcriptome anticipates seedling exposure to light. *Plant Cell* 17: 2507-2516.

Nagawa, S., Sawa, S., Sato, S., Kato, T., Tabata, S., Fukuda, H. (2006) Gene trapping in Arabidopsis reveals genes involved in vascular development. *Plant Cell Physiol.* 47: 1394-1405

Ouellet, F., Overvoorde, P.J., and Theologis, A. (2001) IAA17/AXR3, Biochemical insight into an auxin mutant phenotype. *Plant Cell* 13: 829-841

Overvoorde, P., Fukaki, H., and Beeckman, T. (2010) Auxin control of root development. *Cold Spring Harb. Perspect. Biol.* 10.1101/cshperspect.a001537.

Ottenschläger, I., Wolff, P., Wolverton, C., Bhalerao, R.P., Sandberg, G., Ishikawa, H., et al. (2003) Gravity-regulated differential auxin transport from columella to lateral root cap cells. *Proc. Natl. Acad. Sci. U S A.* 100: 2987-2991

Paponov, I.A., Paponov, M., Teala, W., Menges, M., Chakrabortee, S., Murray, J.A.H. and Palme K. (2008) Comprehensive transcriptome analysis of auxin responses in *Arabidopsis*. *Molecular Plant* 12: 321-337.

Park, J.-E., Park, J.-Y., Kim, Y.-S., Sraswick, P.E., Jeon, J., Yun, J., et al. (2007) GH3-mediated auxin homeostasis links growth regulation with stress adaptation response in *Arabidopsis*. *J. Biol. Chem.* 282: 10036-10046.

Peltier, C., Schmidlin, L., Klein, E., Tsconnat, L., Prinsen, E., Erhardt, M., et al. (2011)

Expression of Beet necrotic yellow vein virus p25 protein induces hormonal changes and a root branching phenotype in *Arabidopsis thaliana*. *Transgenic Res.* 20: 443-466.

Perilli, S., Mambro, R.D., and Sabatini, S. (2012) Growth and development of the root apical meristem. *Curr. Opin. Plant Biol.* 15: 17-23.

Petricka, J.J., Winter, C.M., and Benfey, P.N. (2012) Control of *Arabidopsis* root development. *Annu. Rev. Plant Biol.* 63: 563-564.

Ramos, J., Zenser, N., Leyser, O., and Callis, J. (2001) Rapid degradation of auxin/indoleacetic acid proteins requires conserved amino acids of domain II and is proteasome dependent. *Plant Cell* 13: 2349-2360

Reed, J.W. (2001) Roles and activities of Aux/IAA proteins in Arabidopsis. *Trends Plant Sci.* 6: 420-425

Rogg, L.E., Lasswell, J., and Bartel, B. (2001) A gain-of-function mutation in *IAA28* suppresses lateral root development. *Plant Cell* 13: 465-480

Sabatini, S., Beis, D., Wolkenfelt, H., Murfett, J., Guilfoyle, T., Malamy, J., et al. (1999) An Auxin-Dependent distal organizer of pattern and polarity in the *Arabidopsis* root. *Cell* 99: 463-472.

Santner, A., and Estelle, M. (2009) Recent advances and emerging trends in plant hormone signaling. *Nature* 459: 1071-1078

Sarkar, A.K., Luijten, M., Miyashima, S., Lenhard, M., Hashimoto, T., Nakajima, K., Scheres, B., Heidstra, R., and Laux, T. (2007) Conserved factors regulate signaling in *Arabidopsis thaliana* shoot and root stem cell organizers. *Nature* 446: 811-814.

Scherer, G.F.E., Labusch, C. and Effendi, Y. (2012) Phospholipases and the network of auxin signal transduction with ABP1 and TIR1 as two receptors: a comprehensive and provocative model. *Front. Plant Sci.* 3: doi: 10.3389/fpls.2012.00056.

She, W., Lin, W., Zhu, Y., Chen, Y., Jin, W., Yang, Y., et al. (2010) The gypsy insulator of *Drosophila melanogaster* together with its binding protein Su(Hw) (Suppressor of Hairy-wing) facilitate high and precise expression of transgenes in *Arabidopsis thaliana. Genetics* 185: 1141-1150

Shirakawa, M., Ueda, H., Shimada, T., Nishiyama., C., and Hara-Nishimura, I. (2009)

Vacuolar SNAREs function in the formation of the leaf vascular network by regulating auxin distribution. *Plant Cell Physiol.* 50: 1319-1328

Spartz, A.K., Lee, S.H., Wenger, J.P., Gonzalez, N., Itoh, H., Inzé, D., et al. (2012) The *SAUR19* subfamily of *SMALL AUXIN UP RNA* genes promote cell expension. *Plant J* 70: 978-990.

Staswick, P.E., Serban, B., Rowe, M., Tiryaki, I., Maldonado, M.T., Maldonado, M.C., and Suza, W. (2005) Characterization of an Arabidopsis enzyme family that conjugates amino acids to indole-3-acetic acid. *Plant Cell* 17: 616-627

Swarup, R., Friml, J., Marchant, A., Ljung, K., Sandberg, G., Palme, K., and Bennett, M. (2001) Localization of the auxin permease AUX1 suggests two functionally distinct hormone transport pathways operate in the Arabidopsis root apex. *Gene Dev.* 15: 2648-2653

Tan, X., Calderon-Villalobos, L.I.A., Sharon, M., Zheng, C., Robinson, C.V., Estelle, M., and Zheng, N. (2007). Mechanism of auxin perception by the TIR1 ubiquitin ligase. *Nature* 446: 640-645

Tiwari, S.B., Wang, X.J., Hagen, G., and Guilfoyle, T.J. (2001) AUX/IAA proteins are active repressors, and their stability and activity are modulated by auxin. *Plant Cell* 13: 2809-2822

Ubeda-Tomás, S., Beemster, G.T.S., and Bennett, M.J. (2012) Hormonal regulation of root growth: integrating local activities into global behavior. *Trends Plant Sci.* 17: 326-331.

Ubeda-Tomás, S., Federici, F., Casimiro, I., Beemster, G.T., Bhalerao, R., Swarup, R., et al. (2009) Gibberellin signaling in the endodermis controls Arabidopsis root meristem size. *Curr. Biol.* 19: 1194-1199.

Ubeda-Tomás, S., Swarup, R., Coates, J., Swarup, K., Laplaze, L., Beemster, G.T., et al. (2008) Root growth in Arabidopsis requires gibberellin/DELLA singaling in the endodermis. *Nat. Cell Biol.* 10: 625-628.

Ulmasov, T., Murfett, J., Hagen, G., and Guilfoyle, T. (1997) Aux/IAA proteins repress expression of reporter genes containing natural and highly active synthetic auxin response elements. *Plant Cell* 9: 1963-1971.

Vanneste, S. and Friml, J. (2009) Auxin: a trigger for change in plant development. *Cell* 136: 1005-1016.

Weijers, D., Benkova ,E., Jäger, K.E., Schlereth, A., Hamann, T., Kientz, M., et al. (2005) Developmental specificity of auxin response by pairs of ARF and Aux/IAA transcriptional regulators. *EMBO J.* 24: 1874-1885

Westfall, C.S., Zubieta, C., Herrmann, J., Kapp, U., Nanao, M.H., and Jez, J.M. (2012) Structural basis for prereceptor modulation of plant hormones by GH3 proteins. *Science* 336: 1708-1711.

Woodward, A.W., and Bartel, B. (2005) Auxin: regulation, action, and interaction. Ann. Bot. 95: 707-735.

Worley, C.K., Zenser, N., Ramos, J., Rouse, D., Leyser, O., Theologis, A., and Callis, J. (2000) Degradation of Aux/IAA proteins is essential for normal auxin signaling. *Plant J.* 21: 553–562

Yang, Y., Jin, H., Chen, Y., Lin, W., Wang, C., et al. (2011) A chloroplast envelope membrane protein containing a putative LrgB domain related to the control of bacterial death and lysis is required for chloroplast development in *Arabidopsis thaliana. New Phytol.* 193: 81-95.

Zeng, Y., Zhao, T., Kermode, A.R. (2012) A conifer ABI3-interacting protein plays important roles during key transition of the plant lifecycle. *Plant Physiol.* Doi:10.1104/pp.112.206946

Zhang, H., Kim, M., Krishnamachari, V., Payton, P., Sun, Y., Grimson, M., et al. (2007) Rhizobacterial volatile emissions regulate auxin homeostasis and cell expansion in *Arabidopsis*. *Planta*. 226: 839-851.

Figure legends

Fig. 1. The expression pattern of the *SAUR41* gene, and the subcellular localization of SAUR41 fusion protein. An ~1800 bp promoter region of *SAUR41* was fused with the *EGFP-GUS* reporter gene. Green EGFP (enhanced green fluorescent protein) signals and red PI (propidium iodide, staining cell wall here) signals were viewed by confocal microscopy. GUS (beta-glucuronidase) activity stained in blue was viewed by DIC (differential-interference-contrast) microscopy. *SAUR41* was normally restricted to the quiescent center and cortex/endodermis initials at the root meristems (A). Upon a gravitropic (B) or auxin (C) stimulation, *SAUR41* was provoked in the endodermis layer. (D) *SAUR41* was unresponsive to GA treatment. After extended auxin treatment, *SAUR41* was induced in multiple cell layers at the root meristem (E); however, in the elongation zone, it was specifically induced in the endodermal cells (F). During lateral root development, *SAUR41* was expressed in the prospective quiescent center and initial cells of lateral root primordia (G, H) and in the endodermal cells surrounding the lateral root primordia (G). Insets are enlargements of lateral root primordia. In a new lateral root, *SAUR41* was strongly expressed in quiescent center and initial cells (I). *SAUR41* was predominantly expressed in the vascular tissues of hypocotyls (J), petioles (K) and cotyledons (L). SAUR41-EGFP fusion proteins localized to the cytoplasm of epidermal cells and cortical cells in hypocotyls (1M, N) and to the cytoplasm of quiescent center cells, cortex/endodermis initial cells and epidermal cells in root tips (O, P). LRC, lateral root cap; Ep, epidermis; C, Cortex; En, endodermis. Bars: 25 μm.

Fig. 2. Overexpression of *SAUR41* from the CaMV *35S* promoter confered pleiotropic auxin- or cell expansion-related phenotypes. (A-E) Light-grown 6-d-old seedlings. (F-H) Light-grown 10-d-old seedlings. (I-L) Adult plants. Hypocotyls of wild-type controls (A) and *35S::SAUR41* seedlings (B). Roots of wild-type controls (C) and *35S::SAUR41* seedlings (D). (E-H) Statistical comparison of hypocotyl length (E), primary root length (F), lateral root number (G) and vegetative biomass (H) of wild

type controls with *35S::SAUR41* seedlings. (I-L) Adult *35S::SAUR41* plants had twisted inflorescence stems (I) and over-expanded petals (J-L). Roots or flowers marked by arrows were enlarged in the subsequent images. **, $P<0.01$; *, $P<0.05$, *t*-test.

Fig. 3. Ectopic *SAUR41* promoted hypocotyl epidermal cell expansion and IAA transport. (A) Mean hypocotyl epidermal cell length in 6-d-old seedlings. (B) Relative ^{3}H IAA basipetal transport in hypocotyls of 7-d-old seedlings. **, $P<0.01$; *, $P<0.05$, *t*-test.

Fig. 4. Tissue-specific expression of *SAUR41* from the *PIN1* and *PIN2* promoters. Green EGFP (enhanced green fluorescent protein) signals and red PI (propidium iodide, staining cell wall here) signals were viewed by confocal microscopy. Purple starch grains stained by Lugol's solution were viewed by DIC (differential-interference-contrast) microscopy. (A) The root stem cell niches. (B) Auxin accumulation/signaling pattern in root meristems of the *DR5rev::GFP* background line. White arrow indicated the quiescent center, while blue arrow indicates the tier of distal stem cells. Boxed areas were magnified in the subsequent images. Insects were enlargements of root stem cell niches. (C) Promoter activity of *PIN1*. (D-F) Tissue-specific expression of *SAUR41* from the *PIN1* promoter led to auxin retention in stele initials transporting auxin (pink arrow), additional tiers of distal stem cells (blue arrow), and supernumerary cell layers (white bracket). (H, L) Differentiation status of columella cells in control roots (H) and *PIN1::SAUR41* roots (L) determined by Lugol's solution staining. (I) Promoter activity of *PIN2*. (J-K) Tissue-specific expression of *SAUR41* from the *PIN2* promoter did not induce auxin retention but caused irregular cell expansion in the corresponding cells. LRC, lateral root cap; Ep, epidermis; C, Cortex; En, endodermis. Bars: 25 μm.

Fig. 5. Tissue-specific expression of *SAUR41* and $IAA2^{P65S}$ from promoters of root meristem patterning genes. Green EGFP (enhanced green fluorescent protein) signals

and red PI (propidium iodide, staining cell wall here) signals were viewed by confocal microscopy. Boxed areas were magnified in the subsequent images. Insects were enlargements of root stem cell niches. (A) Auxin accumulation/signaling pattern in root meristems of the *DR5rev::GFP* background line (left) and the promoter activity of *WOX5* (right). (B-F) Tissue-specific expression of *SAUR41* from the *WOX5* promoter. (G, H) Tissue-specific expression of $IAA2^{P65S}$ from the *WOX5* promoter. (I) Promoter activity of *ACR4*. (J, K) Tissue-specific expression of *SAUR41* from the *ACR4* promoter. (L) Tissue-specific expression of $IAA2^{P65S}$ from the *ACR4* promoter. (M) Promoter activity of *PLT2*. (N, O) Tissue-specific expression of *SAUR41* from the *PLT2* promoter. (P) Tissue-specific expression of $IAA2^{P65S}$ from the *PLT2* promoter. Arrow indicatef the division of endodermal cells. < indicated additional auxin accumulation/signaling peaks; * indicated the quiescent center; + indicated tiers of distal stem cells; and **[** indicated the supernumerary cell layers. Bars: 25 μm.

Fig. 6. Ectopic SAUR41 proteins differentially regulated root cell expansion and root gravitropic growth. (A) Cell areas of stele initial cells, quiescent center cells and distal stem cells in roots of 5-d-old seedlings. (B) Root gravitropic respones in 6-d-old seedlings. *, $P<0.05$, *t*-test.

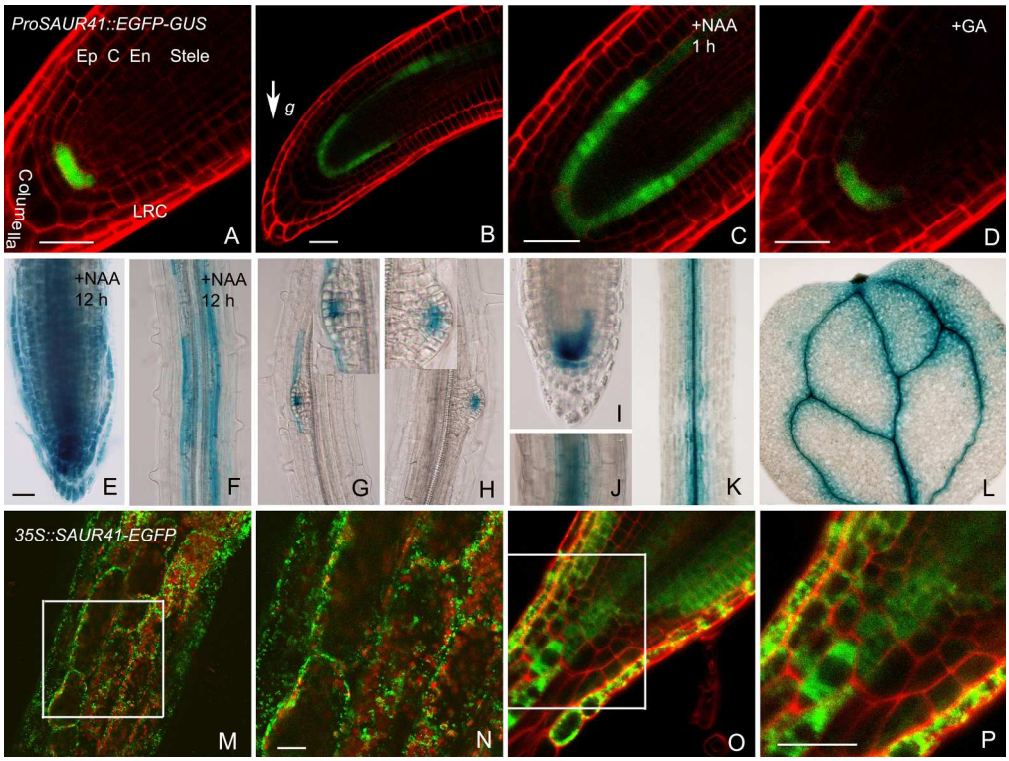

Fig. 1. The expression pattern of the SAUR41 gene, and the subcellular localization of SAUR41 fusion protein. An ~1800 bp promoter region of SAUR41 was fused with the EGFP-GUS reporter gene. Green EGFP (enhanced green fluorescent protein) signals and red PI (propidium iodide, staining cell wall here) signals were viewed by confocal microscopy. GUS (beta-glucuronidase) activity stained in blue was viewed by DIC (differential-interference-contrast) microscopy. SAUR41 was normally restricted to the quiescent center and cortex/endodermis initials at the root meristems (A). Upon a gravitropic (B) or auxin (C) stimulation, SAUR41 was provoked in the endodermis layer. (D) SAUR41 was unresponsive to GA treatment. After extended auxin treatment, SAUR41 was induced in multiple cell layers at the root meristem (E); however, in the elongation zone, it was specifically induced in the endodermal cells (F). During lateral root development, SAUR41 was expressed in the prospective quiescent center and initial cells of lateral root primordia (G, H) and in the endodermal cells surrounding the lateral root primordia (G). Insets are enlargements of lateral root primordia. In a new lateral root, SAUR41 was strongly expressed in quiescent center and initial cells (I). SAUR41 was predominantly expressed in the vascular tissues of hypocotyls (J), petioles (K) and cotyledons (L). SAUR41-EGFP fusion proteins localized to the cytoplasm of epidermal cells and cortical cells in hypocotyls (1M, N) and to the cytoplasm of quiescent center cells, cortex/endodermis initial cells and epidermal cells in root tips (O, P). LRC, lateral root cap; Ep, epidermis; C, Cortex; En, endodermis. Bars: 25 μm.
109x82mm (600 x 600 DPI)

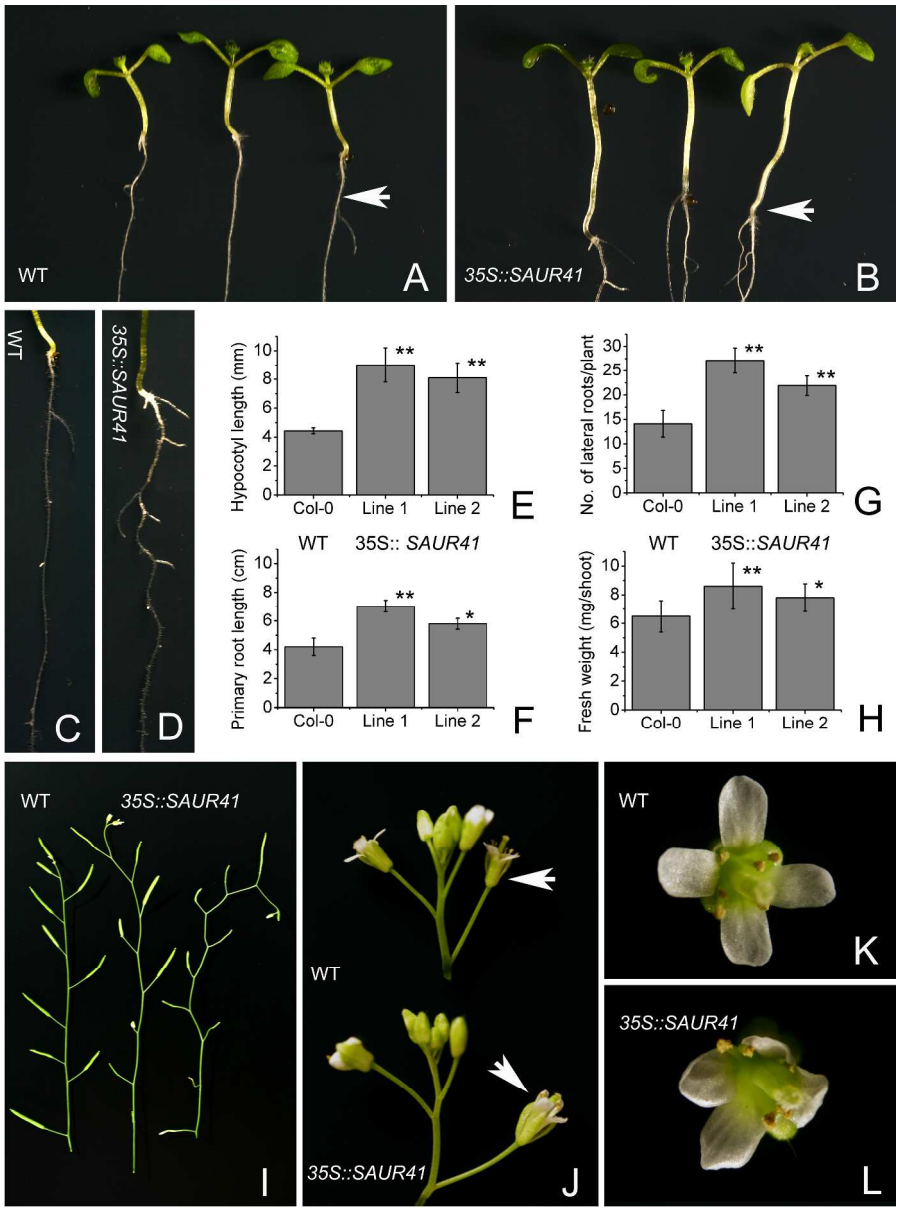

Fig. 2. Overexpression of SAUR41 from the CaMV 35S promoter confered pleiotropic auxin- or cell expansion-related phenotypes. (A-E) Light-grown 6-d-old seedlings. (F-H) Light-grown 10-d-old seedlings. (I-L) Adult plants. Hypocotyls of wild-type controls (A) and 35S::SAUR41 seedlings (B). Roots of wild-type controls (C) and 35S::SAUR41 seedlings (D). (E-H) Statistical comparison of hypocotyl length (E), primary root length (F), lateral root number (G) and vegetative biomass (H) of wild type controls with 35S::SAUR41 seedlings. (I-L) Adult 35S::SAUR41 plants had twisted inflorescence stems (I) and over-expanded petals (J-L). Roots or flowers marked by arrows were enlarged in the subsequent images. **, P<0.01; *, P<0.05, t-test.

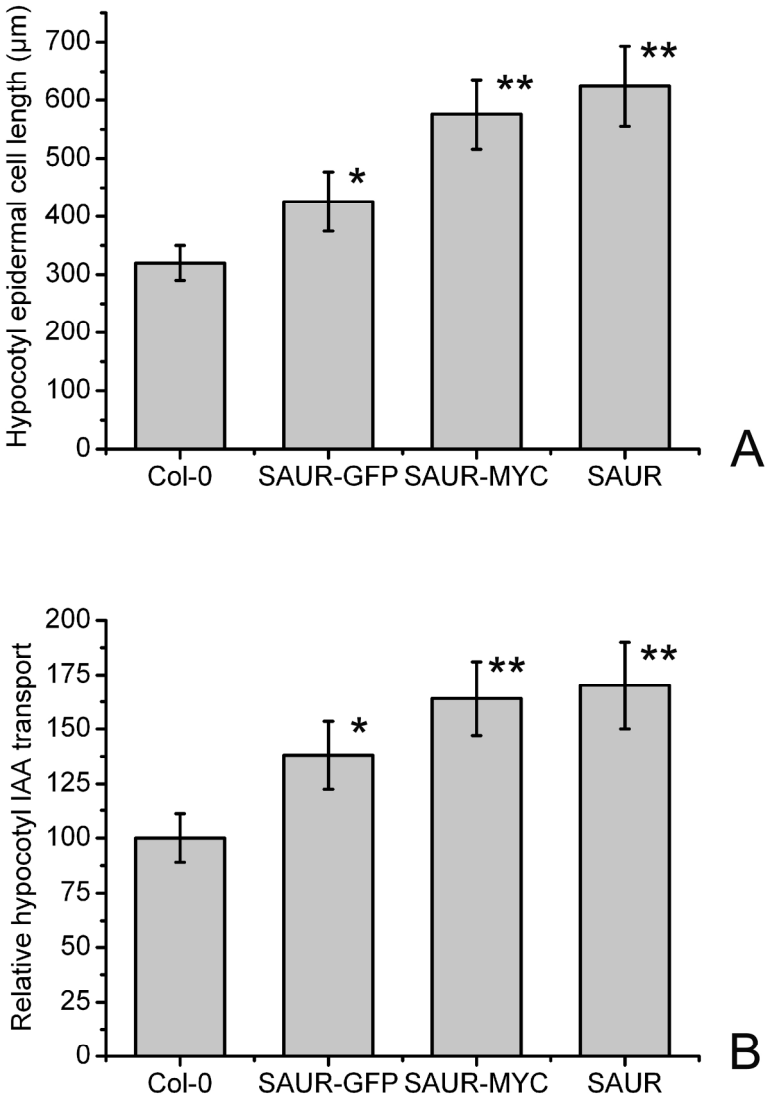

Fig. 3. Ectopic SAUR41 promoted hypocotyl epidermal cell expansion and IAA transport. (A) Mean hypocotyl epidermal cell length in 6-d-old seedlings. (B) Relative 3H IAA basipetal transport in hypocotyls of 7-d-old seedlings. **, P<0.01; *, P<0.05, t-test.
99x137mm (600 x 600 DPI)

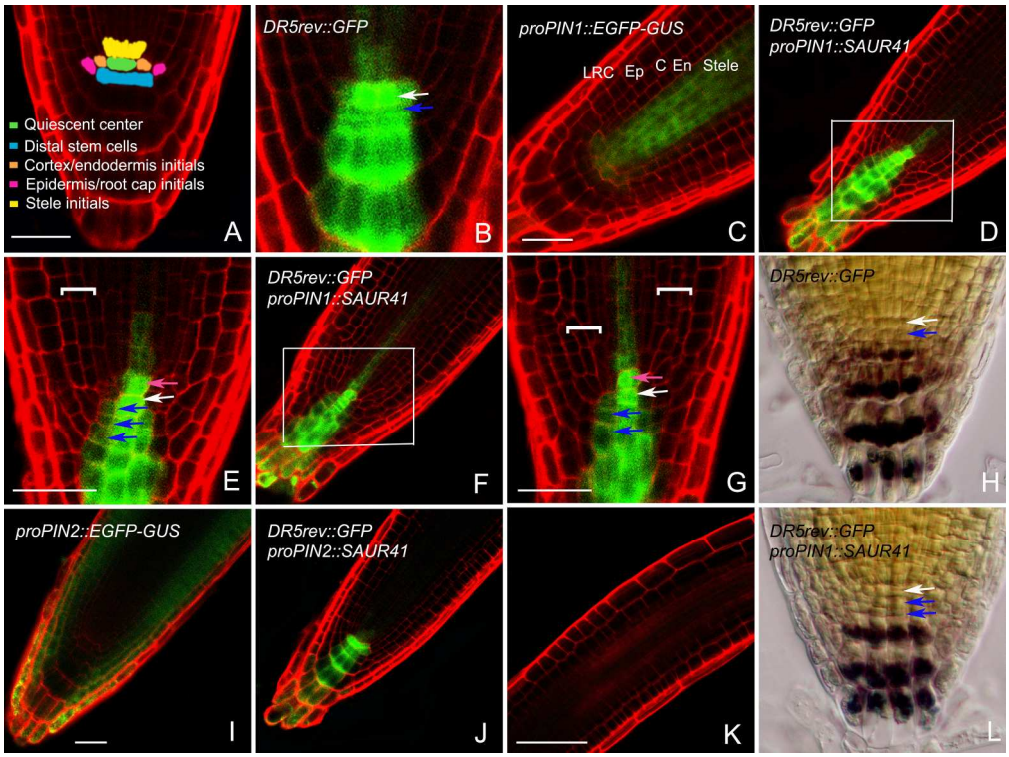

Fig. 4. Tissue-specific expression of SAUR41 from the PIN1 and PIN2 promoters. Green EGFP (enhanced green fluorescent protein) signals and red PI (propidium iodide, staining cell wall here) signals were viewed by confocal microscopy. Purple starch grains stained by Lugol's solution were viewed by DIC (differential-interference-contrast) microscopy. (A) The root stem cell niches. (B) Auxin accumulation/signaling pattern in root meristems of the DR5rev::GFP background line. White arrow indicated the quiescent center, while blue arrow indicates the tier of distal stem cells. Boxed areas were magnified in the subsequent images. Insects were enlargements of root stem cell niches. (C) Promoter activity of PIN1. (D-F) Tissue-specific expression of SAUR41 from the PIN1 promoter led to auxin retention in stele initials transporting auxin (pink arrow), additional tiers of distal stem cells (blue arrow), and supernumerary cell layers (white bracket). (H, L) Differentiation status of columella cells in control roots (H) and PIN1::SAUR41 roots (L) determined by Lugol's solution staining. (I) Promoter activity of PIN2. (J-K) Tissue-specific expression of SAUR41 from the PIN2 promoter did not induce auxin retention but caused irregular cell expansion in the corresponding cells. LRC, lateral root cap; Ep, epidermis; C, Cortex; En, endodermis. Bars: 25 μm.
109x81mm (600 x 600 DPI)

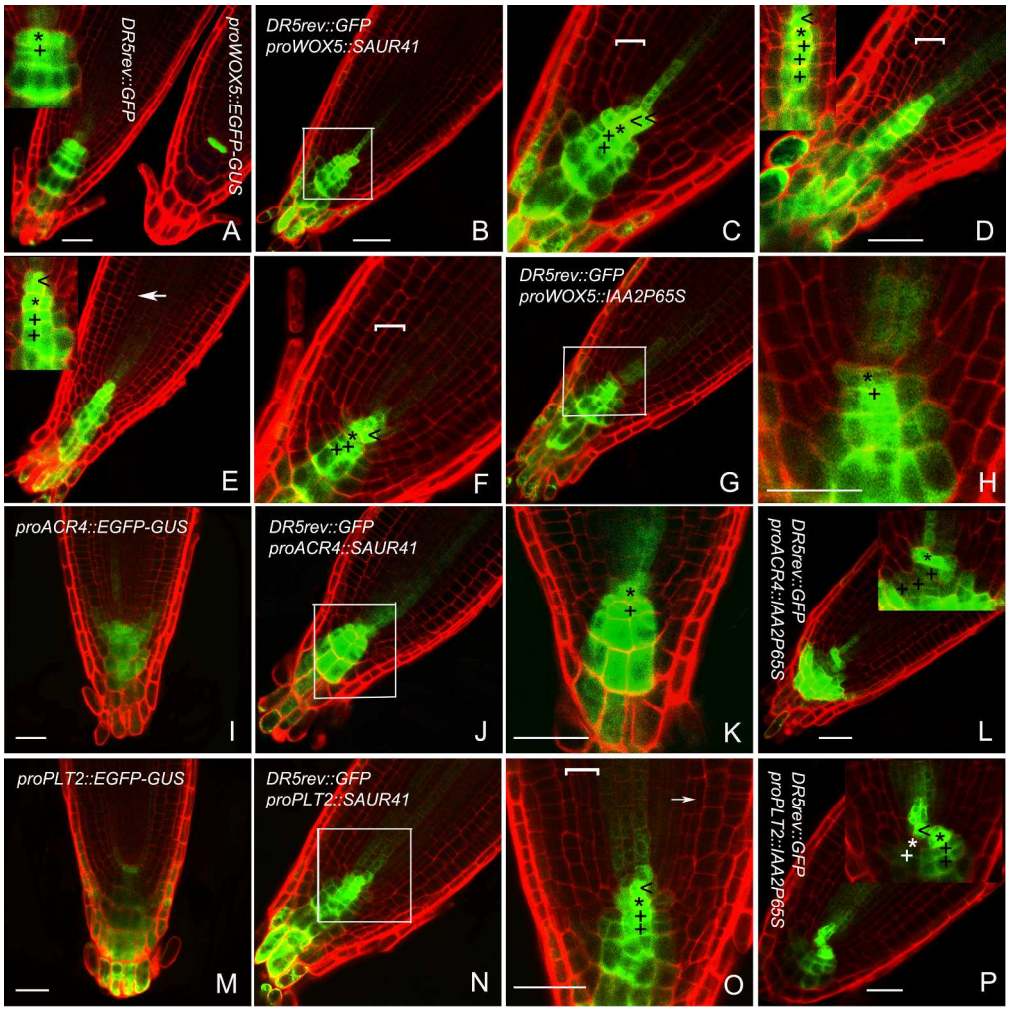

Fig. 5. Tissue-specific expression of SAUR41 and IAA2P65S from promoters of root meristem patterning genes. Green EGFP (enhanced green fluorescent protein) signals and red PI (propidium iodide, staining cell wall here) signals were viewed by confocal microscopy. Boxed areas were magnified in the subsequent images. Insects were enlargements of root stem cell niches. (A) Auxin accumulation/signaling pattern in root meristems of the DR5rev::GFP background line (left) and the promoter activity of WOX5 (right). (B-F) Tissue-specific expression of SAUR41 from the WOX5 promoter. (G, H) Tissue-specific expression of IAA2P65S from the WOX5 promoter. (I) Promoter activity of ACR4. (J, K) Tissue-specific expression of SAUR41 from the ACR4 promoter. (L) Tissue-specific expression of IAA2P65S from the ACR4 promoter. (M) Promoter activity of PLT2. (N, O) Tissue-specific expression of SAUR41 from the PLT2 promoter. (P) Tissue-specific expression of IAA2P65S from the PLT2 promoter. Arrow indicatef the division of endodermal cells. < indicated additional auxin accumulation/signaling peaks; * indicated the quiescent center; + indicated tiers of distal stem cells; and [indicated the supernumerary cell layers. Bars: 25 μm.
146x146mm (600 x 600 DPI)

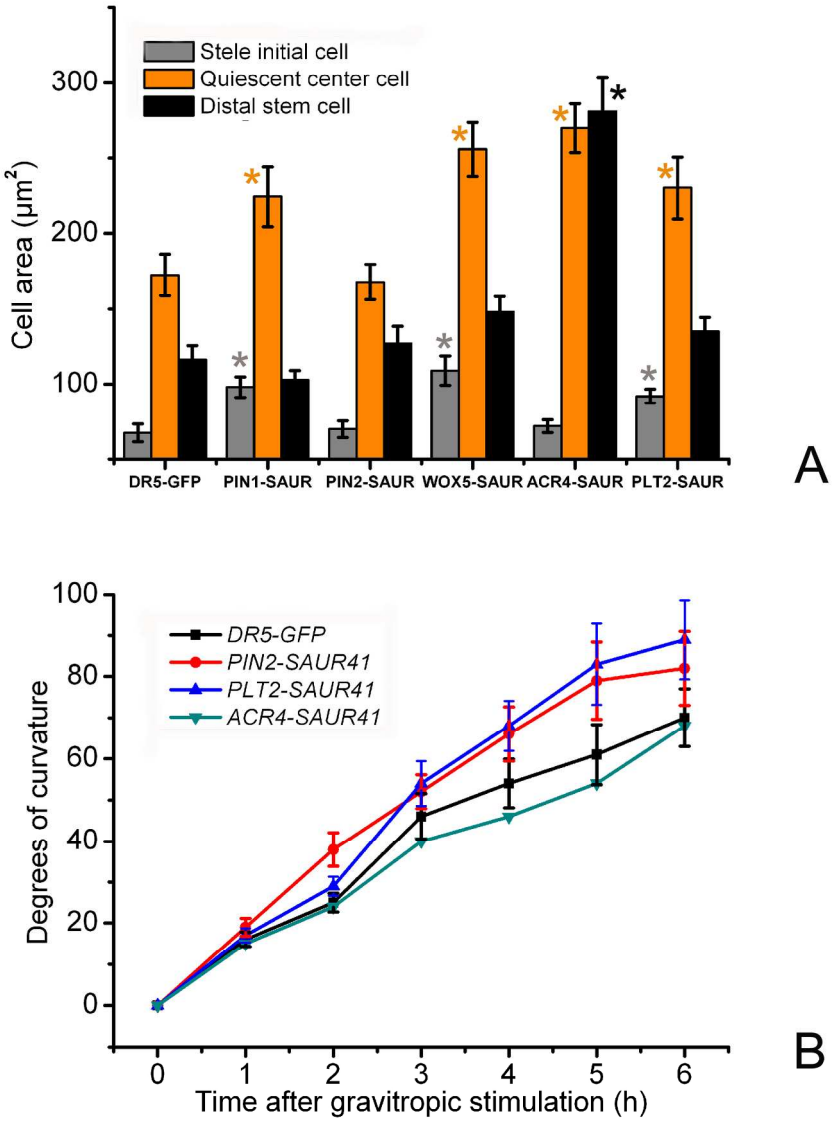

Fig. 6. Ectopic SAUR41 proteins differentially regulated root cell expansion and root gravitropic growth. (A) Cell areas of stele initial cells, quiescent center cells and distal stem cells in roots of 5-d-old seedlings. (B) Root gravitropic respones in 6-d-old seedlings. *, P<0.05, t-test.
99x133mm (600 x 600 DPI)

AUTHOR/EDITOR QUERIES

Please tick all check box to confirm that you have agreed or have made relevant changes for each query

ARTICLE ID : PCP-pct028				
Please respond to all queries and send any additional proof corrections. Failure to do so could result in delayed publication				
Query no	**Section**	**Paragraph**	**Query**	**Checked**
Q1	Author names		Please check that all names have been spelled correctly and appear in the correct order. Please also check that all initials are present. Please check that the author surnames (family name) have been correctly identified by a pink background. If this is incorrect, please identify the full surname of the relevant authors. Occasionally, the distinction between surnames and forenames can be ambiguous, and this is to ensure that the authors' full surnames and forenames are tagged correctly, for accurate indexing online. Please also check all author affiliations.	☐
Q2			Please check that the text is complete and that all figures, and their legends are included.	☐
Q3	Funding		Please provide a Funding statement, detailing any funding received. Remember that any funding used while completing this work should be highlighted in a separate Funding section. Please ensure that you use the full official name of the funding body, and if your paper has received funding from any institution, such as NIH, please inform us of the grant number to go into the funding section. We use the institution names to tag NIH-funded articles so they are deposited at PMC. If we already have this information, we will have tagged it and it will appear as coloured text in the funding paragraph. Please check the information is correct.	☐

Q4	Figures		Figures have been placed as close as possible to their first citation. Please check that they have no missing sections and that the correct figure legend is present.	☐

Making corrections to your proofs

- Please use the tools in the Annotation and Drawing Markups toolbars to correct your proofs. To access these, press 'Comment' in the top right hand corner.
- If you would like to save your comments and return at a later time, click **Publish Comments**.
- If applicable, to see new comments from other contributors, press **Check for New Comments**
- Once you have finished correcting your article, click **Finalize/Finalize PDF Comments**.
- The **Publish Comments** and **Finalize/Finalize PDF Comments** options are available either as:
    1. A pop up JavaScript Window, shown right, or
    2. By clicking 'Tools' in the top right hand corner, then clicking 'JavaScript Window', shown right.
    3. **Do not close the Javascript window.**

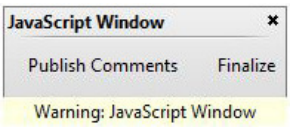

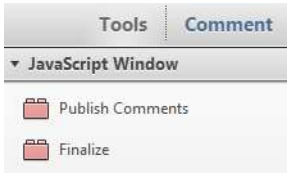

Annotation tools

Insert text at cursor: click to set the cursor location in the text and start typing to add text. You may cut and paste text from another file into the commenting box

Replace (Insert): click and drag the cursor over the text then type in the replacement text. You may cut and paste text from another file into the commenting box

Strikethrough (Delete): click and drag over the text to be deleted then press the delete button on your keyboard for text to be struck through

Comments list This provides a list of all comments and corrections made to the article. It can be sorted by date or person.

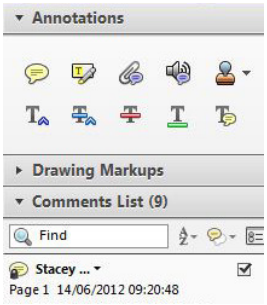

Underline: click to indicate text that requires underlining

Add sticky note: click to add a comment to the page. Useful for layout changes

Add note to text: click to add a note. Useful for layout changes

Highlight text: click to highlight specific text and make a comment. Useful for indicating font problems, bad breaks, and other textual inconsistences

Drawing tools There is the ability to draw shapes and lines, if required.

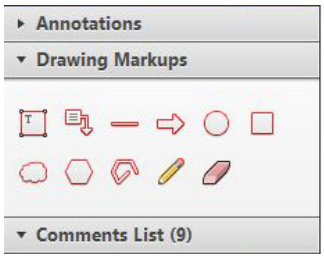

Attach file, Record audio, and Add stamp are not in use.

[20.2.2013-5:54pm] [1-13] Paper: OP-PCPJ130028
MANUSCRIPT CATEGORY: REGULAR PAPER

PCP
PLANT & CELL PHYSIOLOGY

Tissue-Specific Expression of *SMALL AUXIN UP RNA41* Differentially Regulates Cell Expansion and Root Meristem Patterning in Arabidopsis

Q1

Yingying Kong[1,2,3], Yubin Zhu[1,2,3], Chen Gao[1], Wenjing She[1], Weiqiang Lin[1], Yong Chen[1], Ning Han[1], Hongwu Bian[1], Muyuan Zhu[1] and Junhui Wang[1,*]

[1]Institute of Genetics, College of Life Sciences, Zhejiang University, Zijingang Campus, Hangzhou 310058, China
[2]Sir Run Run Shaw Hospitol, School of Medicine, Zhejiang University, Hangzhou 310016, China
[3]These authors contributed equally to this work.
*Corresponding author: E-mail, junhuiwang@zju.edu.cn; Fax: +86-571-88206535.
(Received August 20, 2012; Accepted February 3, 2013)

Regular Paper

Among the three primary auxin-induced gene families, *Auxin/Indole-3-Acetic Acid* (*Aux/IAA*), *Gretchen Hagen3* (*GH3*) and *SMALL AUXIN UP RNA* (*SAUR*), the function of *SAUR* genes remains unclear. Arabidopsis *SAUR* genes have been phylogenetically classified into three clades. Recent work has suggested that *SAUR19* (clade II) and *SAUR63* (clade I) promote cell expansion through the modulation of auxin transport. Herein, we present our work on *SAUR41*, a clade III *SAUR* gene with a distinctive expression pattern in root meristems. *SAUR41* was normally expressed in the quiescent center and cortex/endodermis initials; upon auxin stimulation, the expression was provoked in the endodermal layer. During lateral root development, *SAUR41* was expressed in prospective stem cell niches of lateral root primordia and in expanding endodermal cells surrounding the primordia. SAUR41–EGFP (enhanced green fluorescent protein) fusion proteins localized to the cytoplasm. Overexpression of *SAUR41* from the *Cauliflower mosaic virus* 35S promoter led to pleiotropic auxin-related phenotypes, including long hypocotyls, increased vegetative biomass and lateral root development, expanded petals and twisted inflorescence stems. Ectopic SAUR41 proteins were able to promote auxin transport in hypocotyls. Tissue-specific expression of *SAUR41* from the *PIN1*, *WOX5*, *PLT2* and *ACR4* promoters induced the formation of new auxin accumulation/signaling peaks above the quiescent centers, whereas tissue-specific expression of *SAUR41* from the *PIN2* and *PLT2* promoters enhanced root gravitropic growth. Cells in the root stem cell niches of these transgenic seedlings were differentially enlarged. The distinctive expression pattern of the *SAUR41* gene and the explicit function of SAUR41 proteins implied that further investigations on the loss-of-function phenotypes of this gene in root development and environmental responses are of great interest.

Keywords: Arabidopsis • Auxin transport • Cell expansion • Root meristem patterning • SAUR.

Abbreviations: ACR4, ARABIDOPSIS CRINKLY4; ARF, AUXIN RESPONSE FACTOR; Aux/IAA, AUXIN/INDOLE-3-ACETIC ACID; CaMV, *Cauliflower mosaic virus*; DIC, differential interference-contrast; EGFP, enhanced green fluorescent protein; GH3, Gretchen Hagen3; GUS, β-glucuronidase; LRC, lateral root cap; NAA, 1-naphthaleneacetic acid; PI, propidium iodide; PIN, PINFORM; PLT2, PLETHORA2; RT–PCR, reverse transcription–PCR; SAUR, SMALL AUXIN UP RNA; TIR1/AFB, TRANSPORT INHIBITOR RESPONSE1/AUXIN-BINDING F-BOX PROTEIN; WOX5, WUSCHEL-RELATED HOMEOBOX 5.

Introduction

The plant hormone auxin modulates many aspects of plant growth and development, and recent decades have seen rapid progress in our understanding of the molecular mechanism of auxin biology (Woodward and Bartel 2005, Santner and Estelle 2009, Vanneste and Friml 2009). For instance, in the field of auxin control of root development, numerous fundamental insights have been achieved on the contribution of shoot-derived auxin and root-generated auxin in root development (Overvoorde et al. 2010), establishment and maintenance of root stem cell niches (Aichinger et al. 2012, Perilli et al. 2012, Petricka et al. 2012), hormone interactions in coordinated root growth (Petricka et al. 2012, Ubeda-Tomás et al. 2012) and root growth in response to the environment (Jones and Ljung, 2012, Petricaka et al. 2012).

Auxin regulates cell division, differentiation and elongation in part by changing gene expression (Woodward and Bartel 2005, Paponov et al. 2008, Santner and Estelle 2009, Vanneste and Friml 2009, Hayashi 2012). Primary auxin response genes consist of members of three gene families (Hagen and Guilfoyle 2002): *Aux/IAA* (*Auxin/Indole-3-Acetic Acid*), *GH3* (*Gretchen Hagen3*) and *SAUR* (*SMALL AUXIN UP RNA*). Aux/IAA proteins are transcription repressors (Ulmasov et al. 1997, Worley et al. 2000, Gray et al. 2001, Ouellet, et al. 2001, Ramos et al. 2001,

Plant Cell Physiol. 0(0): 1–13 doi:10.1093/pcp/pct028, available online at www.pcp.oxfordjournals.org

Reed 2001, Rogg et al. 2001, Tiwari et al. 2001). Their domain II interacts with the TRANSPORT INHIBITOR RESPONSE1/AUXIN-BINDING F-BOX PROTEIN (TIR1/AFB) family of auxin receptors, while their domains III and IV dimerize with the AUXIN RESPONSE FACTOR (ARF) family transcription factors (Kim et al. 1997, Gray et al. 2001). Upon an auxin stimulus, Aux/IAA proteins are ubiquitinated by the TIR1/AFB proteins and then degraded, which releases the activity of ARF proteins (Dharmasiri et al. 2005, Kepinski and Leyser 2005, Tan et al. 2007). The GH3 family of acyl acid amido synthetases contributes to the amino acid conjugation of IAA, jasmonic acid or salicylic acid (Ljung et al. 2002, Staswick et al. 2005, Park et al. 2007). The crystal structure and putative mechanisms of two GH3 proteins had been reported recently (Westfall et al. 2012). In contrast to Aux/IAA and GH3 proteins, the function of SAUR proteins remains unclear, most probably due to genetic redundancy within the large SAUR gene family (Hagen and Guilfoyle 2002, Jain et al. 2006).

Recent studies have begun to address the function of SAUR proteins in rice (*Oryza sativa*) and Arabidopsis. *OsSAUR39* has been identified as a negative regulator of auxin synthesis and transport, since rice plants overexpressing *OsSAUR39* exhibit reduced lateral root development and shoot and root length (Kant et al. 2009). The SAUR19 subfamily proteins (SAUR19–SAUR24) of Arabidopsis have been reported to be highly unstable; however, the addition of an N-terminal tag increases the stability of these proteins (Spartz et al. 2012). Arabidopsis plants overexpressing these stabilized SAUR fusion proteins exhibited increased hypocotyl elongation and larger leaf size, while seedlings expressing an artificial microRNA targeting the *SAUR19* subfamily genes exhibit opposite phenotypes (Franklin et al. 2011, Spartz et al. 2012). In another report on Arabidopsis, transgenic plant lines overexpressing *SAUR63:GFP* or *SAUR63:GUS* displayed long hypocotyls, petals and stamen filaments; in contrast, transgenic plants expressing artificial microRNA constructs targeting the *SAUR63* subfamily genes (*SAUR61–SAUR68* and *SAUR75*) had slightly reduced hypocotyl and stamen filament elongation (Chae et al. 2012). The *SAUR19* subfamily genes were expressed in elongating tissues, including the root elongation zone (Spartz et al. 2012), while the *SAUR63* subfamily genes were not expressed in roots (Chae et al. 2012). As far as the mechanism is concerned, Arabidopsis SAUR proteins have been proposed to promote cell expansion through the modulation of auxin transport (Chae et al. 2012, Spartz et al. 2012).

The *SAUR* gene family could be phylogenetically classified into three clades (Kodaira et al. 2011). The genes in clades I and II had a tendency to display higher expression levels in leaves and lower expression in roots, while the genes in clade III demonstrated opposite expression patterns (Kodaira et al. 2011). The *SAUR63* subfamily and the *SAUR19* subfamily are clade I and clade II *SAUR* genes, respectively (Kodira et al. 2011). Herein, we present our work on *SAUR41*, a clade III *SAUR* gene displaying a distinctive expression pattern in Arabidopsis root meristems.

The *SAUR41* subfamily contained four members: *SAUR41* (At1g16510), *SAUR40* (At1g79130), *SAUR71* (At1g56150) and *SAUR72* (At3g12830). Their amino acid sequences differed from those of other SAUR families in the N-terminus. In previous microarray experiments, the expression of *SAUR41* has been reported to be regulated by circadian rhythm (Mazzella et al. 2005, Darrah et al. 2006), biotic stress (Zhang et al. 2007, Peltier et al. 2011), and mitochondrial dysfunction and reactive oxygen species (Carrie et al. 2010, Gleason et al. 2011). The expression of *SAUR40* and *SAUR71* was responsive to ABA signaling (Leondardt et al. 2004, Zeng et al. 2012) and the functional status of chloroplasts (Bosco et al. 2004, Estavillo et al. 2011). *SAUR71* and *SAUR72* were expressed in vascular development (Nagawa et al. 2006, Shirakawa et al. 2009).

We found that *SAUR41* was normally expressed in the quiescent center and cortex/endodermis initials, but it was provoked in the endodermal layer upon an auxin or gravitropic stimulation. During lateral root development, *SAUR41* was distinctively expressed in prospective stem cell niches of lateral root primordia and in expanding endodermal cells surrounding the primordia. SAUR41–enhanced green fluorescent protein (EGFP) fusion proteins localized to the cytoplasm, unlike EGFP–SAUR19 and SAUR63–EGFP which localized predominantly to the plasma membrane. Interestingly, although the gene expression pattern and the protein localization pattern of *SAUR41* were different from those of *SAUR19* and *SAUR63*, the phenotypes resulting from overexpression of *SAUR41* driven by the *Cauliflower mosaic virus* (CaMV) 35S promoter shared many similarities with those of *SAUR19* and *SAUR63* subfamily genes. Tissue-specific expression of *SAUR41* from promoters of auxin transporter genes and root meristem patterning genes differentially modulated root meristem development, root cell expansion and root gravitropic growth. The distinctive expression pattern of the *SAUR41* gene and the explicit function of ectopic SAUR41 proteins implied that further investigations on the loss-of-function phenotypes of this gene family in root development are of great interest.

Results

SAUR41 had a distinctive expression pattern in Arabidopsis root meristems

Previously, to counteract possible position effects in plant promoter analysis, we used the *gypsy*-Su(Hw) system of *Drosophila* in a novel approach that facilitated high and precise expression of reporter genes (She et al. 2010). Using this system, together with the GATEWAY recombination approach, we generated sets of promoter reporter lines for the *PIN* (*PINFORM*) gene family encoding auxin carriers and the *TIR1/AFB* gene family encoding auxin receptors (She et al. 2010). We extended this system to promoter analysis of certain *SAUR* genes, and found that the *SAUR41* (At1g16510) gene showed a distinctive expression pattern in root meristems.

In generating promoter reporter lines for *SAUR41*, an ~1,800 bp DNA fragment upstream of the ATG start codon of *SAUR41*, as predicted by AtcisDB (Davuluri et al. 2003), was fused with the *EGFP-GUS* reporter gene. Viewed by confocal microscopy, *SAUR41* was found to be specifically expressed in the quiescent center and cortex/endodermis initials of root stem niches (**Fig. 1A**). Considering that *SAUR* genes had been proposed to function in auxin-mediated growth events, we examined the expression of *SAUR41* under gravitropic stimulation and auxin treatment. Gravitropism allows plant roots to grow directionally, whereas auxin is an essential regulator in this process (Harrison and Masson 2008). During the gravitropic response, the expression of *SAUR41* was provoked on both sides of the endodermis at the proximal meristem region and on the upper side of the endodermis at the distal elongation zone, indicating that this gene might act to coordinate root elongation rather than simply respond to auxin redistribution (**Fig. 1B**). *SAUR41* was specifically induced in the endodermis with 1 h of auxin [10 μM 1-naphthalene acetic acid (NAA)] treatment (**Fig. 1C**). Since the endodermis was recently reported as the primary responsive tissure for gibberellins to coordinate root growth (Ubeda-Tomás et al. 2008, Ubeda-Tomás

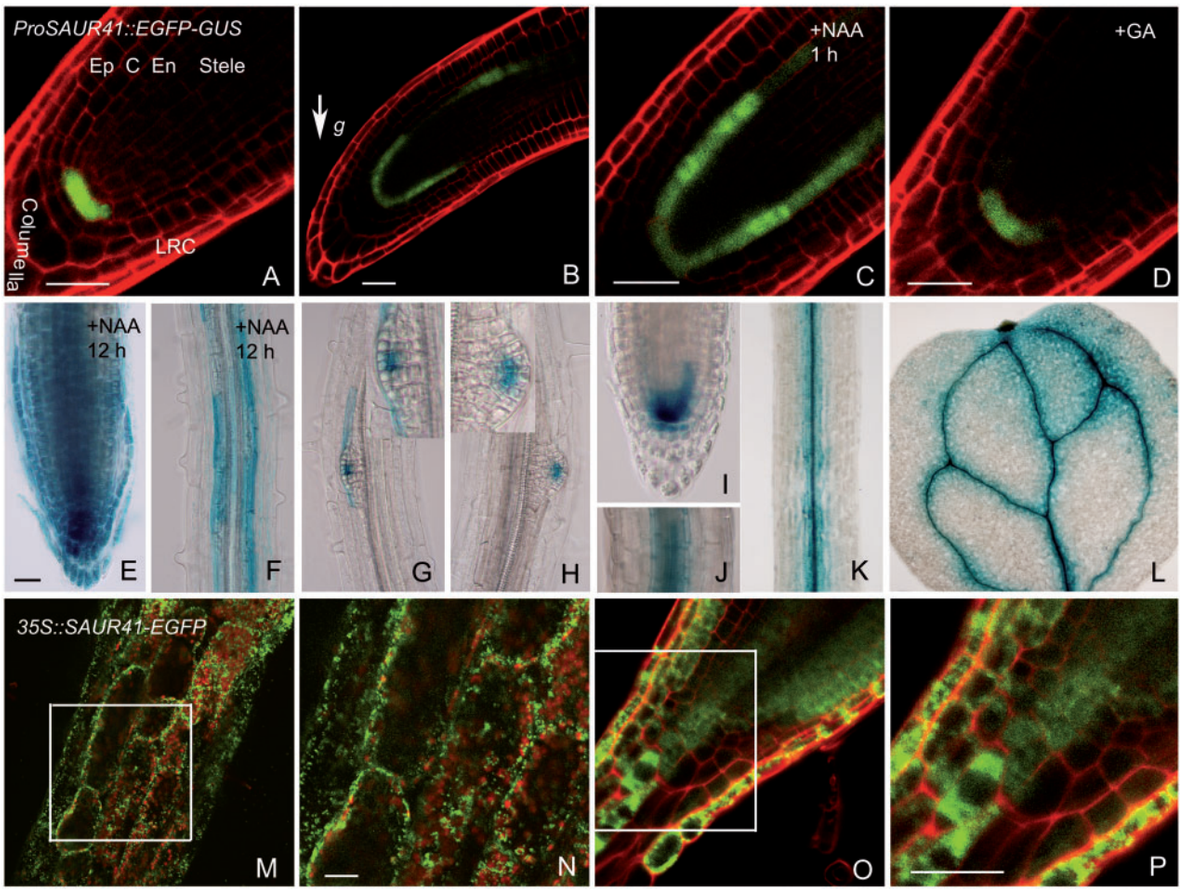

Fig. 1 The expression pattern of the *SAUR41* gene, and the subcellular localization of SAUR41 fusion protein. An ~1,800 bp promoter region of *SAUR41* was fused with the *EGFP-GUS* reporter gene. Green EGFP (enhanced green fluorescent protein) signals and red PI (propidium iodide, staining the cell wall here) signals were viewed by confocal microscopy. GUS (β-glucuronidase) activity stained in blue was viewed by DIC (differential interference contrast) microscopy. *SAUR41* was normally restricted to the quiescent center and cortex/endodermis initials at the root meristems (A). Upon a gravitropic (B) or auxin (C) stimulation, *SAUR41* was provoked in the endodermis layer. (D) *SAUR41* was unresponsive to gibberellin treatment. After extended auxin treatment, *SAUR41* was induced in multiple cell layers at the root meristem (E); however, in the elongation zone, it was specifically induced in the endodermal cells (F). During lateral root development, *SAUR41* was expressed in the prospective quiescent center and initial cells of lateral root primordia (G, H) and in the endodermal cells surrounding the lateral root primordia (G). Insets are enlargements of lateral root primordia. In a new lateral root, *SAUR41* was strongly expressed in the quiescent center and initial cells (I). *SAUR41* was predominantly expressed in the vascular tissues of hypocotyls (J), petioles (K) and cotyledons (L). SAUR41–EGFP fusion proteins localized to the cytoplasm of epidermal cells and cortical cells in hypocotyls (M, N) and to the cytoplasm of quiescent center cells, cortex/endodermis initial cells and epidermal cells in root tips (O, P). LRC, lateral root cap; Ep, epidermis; C, cortex; En, endodermis. Bars: 25 μm.

et al. 2009, Ubeda-Tomás et al. 2012), we then tested whether or not *SAUR41* was a gibberellin-responsive gene. As shown in **Fig. 1D**, *SAUR41* was unresponsive to gibberellin treatment. This result was in agreement with the results of a microarray experiment (Josse et al. 2011).

Extending the duration of auxin treatment to 12 h, and using detection by overnight histochemical staining, *SAUR41* was found to be induced in multiple cell layers at the root meristem and transition zone (**Fig. 1E**). However, in the elongation zone, it was specifically induced in the endodermal cells (**Fig. 1F**).

During lateral root development, *SAUR41* was expressed in the prospective quiescent center of lateral root primordia (**Fig. 1G, H**). Interestingly, *SAUR41* was also specifically expressed in the endodermal cells surrounding the lateral root primordia during the process of the lateral root primordia breaking through the endodermis (**Fig. 1G**). In the newly formed lateral roots, *SAUR41* was strongly expressed in the quiescent center and initial cells, and weakly expressed in the endodermis (**Fig. 1I**). In hypocotyls, petioles and cotyledons, *SAUR41* was predominantly expressed in the vascular tissues (**Fig. 1J–L**).

SAUR41–EGFP fusion protein accumulated in the cytoplasm

To check the subcellular localization of the SAUR41 protein, we generated a transgenic construct in which the CaMV *35S* promoter drove a C-terminal translational fusion between the full-length SAUR41 and the EGFP protein. Location of the fusion protein in hypocotyls and root tips of stably transformed Arabidopsis plants was examined by confocal microscopy. Results showed that the EGFP fluorescence was identified at the cytoplasm of epidermal and cortical cells in hypocotyls (**Fig. 1M, N**), and at the cytoplasm of all types of cells in root tips, including quiescent center cells, cortex/endodermis initial cells and epidermal cells (**Fig. 1O, P**).

Overexpression of *SAUR41* conferred pleiotropic auxin-related phenotypes

To explore potential roles for *SAUR41* in Arabidopsis growth and development, we first screened T-DNA and transposon insertion lines from the Arabidopsis Biological Resource Center (ABRC) and the Rikagaku Kenkyusho Bioresource Center (RIKEN-BRC), respectively. The line SALK_056968 from the ABRC stocks contained a T-DNA at the promoter region of *SAUR41*. However, reverse transcription–PCR (RT–PCR) analysis revealed that this insertion did not impair the expression of *SAUR41* (data not shown). In three additional lines (SALK_121397, PST_11030 and PST_17947), we failed to identify DNA insertions inside the *SAUR41* gene.

We then used a gain-of-function approach and generated transgenic Arabidopsis plants overexpressing the untagged (*35S::SAUR41*) or MYC-tagged (*35S::SAUR41-MYC*) *SAUR41* gene, in addition to the *35S::SAUR41-EGFP* plants described above. More than 20 independent lines were obtained for each transgenic construct. Plants overexpressing untagged *SAUR41* had strong phenotypes, similar to that of MYC-tagged *SAUR41*. In contrast, plants overexpressing EGFP-tagged *SAUR41* had the weakest phenotypes. We chose *35S::SAUR41* plants for detailed study.

The *35S::SAUR41* transgenic lines displayed pleiotropic auxin-related phenotypes. Light-grown seedlings exhibited 1.7- to 2.0-fold longer hypocotyls than wild-type controls (**Fig. 2A, B, E**; $P < 0.01$, *t*-test). Surprisingly, these seedlings also displayed 1.3- to 1.5-fold longer primary roots compared with wild-type controls (**Fig. 2C, D, F**; $P < 0.05$, *t*-test). In addition, overexpression of *SAUR41* increased root waving on vertically oriented agar plates (**Fig. 2D**). After 10 d of growth, *35S::SAUR41* seedlings had a 1.5- to 1.9-fold increase in lateral root numbers ($P < 0.05$, *t*-test) and a 20–30% increase in vegetative biomass as measured by the fresh weight of shoots (**Fig. 2G, H**; $P < 0.05$, *t*-test).

Adult *35S::SAUR41* plants had twisted inflorescence stems (**Fig. 2I**). Furthermore, the petals of transgenic flower organs were overexpanded and defective in opening completely (**Fig. 2J–L**), resulting in reduced seed setting in many siliques (**Fig. 2I**).

To determine if the elongated hypocotyl phenotype induced by ectopic SAUR41 was due to increased cell expansion, we measured hypocotyl epidermal cell length in 6-day-old seedlings. The change in hypocotyl epidermal cell length was parallel to the change in hypocotyl length (**Figs. 3A, 2E**). We then directly measured [^{3}H]IAA transport in hypocotyls and detected a 40–70% increase in basipetal IAA transport in hypocotyls of *35S::SAUR41-EGFP*, *35S::SAUR41-MYC* and *35S::SAUR41* seedlings (**Fig. 3B**).

Tissue-specific expression of *SAUR41* from the *PIN1* promoter induced alterations in root meristem patterning

As *SAUR41* had a distinctive expression pattern in Arabidopsis root meristems, and rice and Arabidopsis SAUR proteins have been proposed to modulate auxin transport (Kant et al. 2009, Chae et al. 2012, Spartz et al. 2012), we next implemented tissue-specific expression of *SAUR41* from promoters of auxin transporter genes and root meristem patterning genes. To facilitate the examination of auxin signaling and distribution, all transgenic plants were generated in a *DR5rev::GFP* background (Friml et al. 2003; **Fig. 4B**).

We first expressed *SAUR41* from the *PIN1* and *PIN2* promoters. In Arabidopsis roots, *PIN1* promoter activity was strong in stele cells and weak in endodermis and the quiescent center (She et al. 2010; **Fig. 4C**). Ectopic expression of *SAUR41* driven by the *PIN1* promoter led to auxin retention in stele initials transporting auxin, resulting in a large auxin accumulation/signaling peak (**Fig. 4D–G**). In addition, *PIN1::SAUR41* roots had additional tiers of distal stem cells (**Fig. 4E, G**), while wild-type roots typically had one tier of distal stem cells (Ding and Friml 2010; **Fig. 4A, B**). Non-differentiated distal stem cells below the quiescent center were characterized by

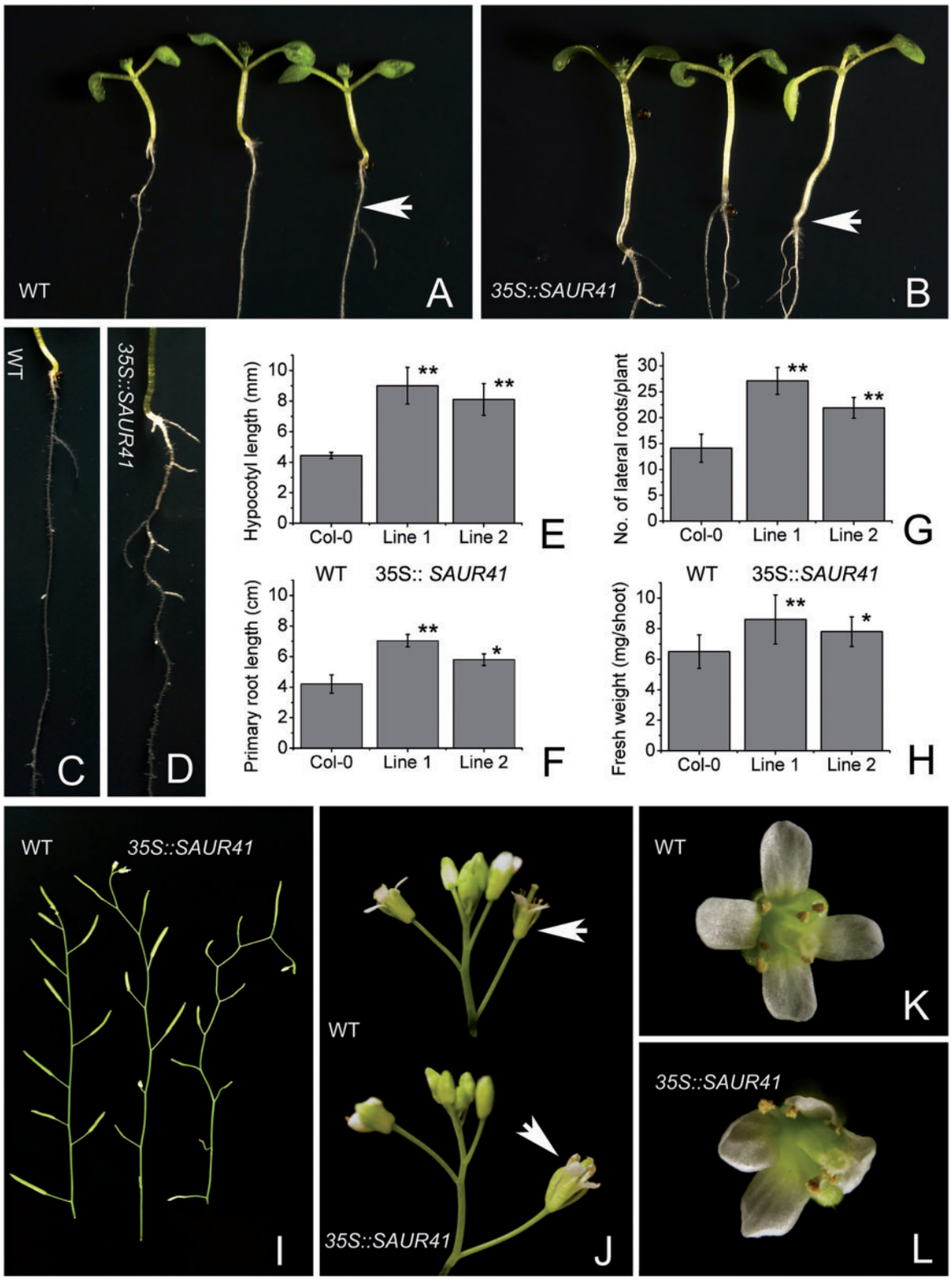

Fig. 2 Overexpression of *SAUR41* from the CaMV *35S* promoter conferred pleiotropic auxin- or cell expansion-related phenotypes. (A–E) Light-grown 6-day-old seedlings. (F–H) Light-grown 10-day-old seedlings. (I–L) Adult plants. Hypocotyls of wild-type controls (A) and *35S::SAUR41* seedlings (B). Roots of wild-type controls (C) and *35S::SAUR41* seedlings (D). (E–H) Statistical comparison of hypocotyl length (E), primary root length (F), lateral root number (G) and vegetative biomass (H) of wild-type controls with *35S::SAUR41* seedlings. (I–L) Adult *35S::SAUR41* plants had twisted inflorescence stems (I) and overexpanded petals (J–L). Roots or flowers marked by arrows were enlarged in the subsequent images. $^{**}P < 0.01$; $^{*}P < 0.05$, *t*-test.

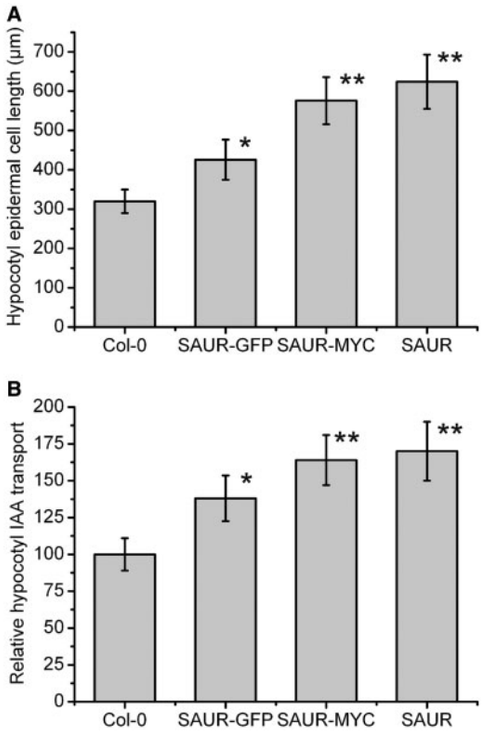

Fig. 3 Ectopic *SAUR41* promoted hypocotyl epidermal cell expansion and IAA transport. (A) Mean hypocotyl epidermal cell length in 6-day-old seedlings. (B) Relative [^{3}H]IAA basipetal transport in hypocotyls of 7-day-old seedlings. $^{**}P < 0.01$; $^{*}P < 0.05$, *t*-test.

the absence of starch grains (Ding and Friml 2010; **Fig. 4H, L**). Finally, *PIN1::SAUR41* roots had supernumerary cell layers (**Fig. 4E, G**), while wild-type roots exhibited distinctive root radial patterns (**Fig. 4A, B**). Statistically, 80–90% of *PIN1::SAUR41* roots displayed abnormalities in root meristem patterning ($n = 40$, $P < 0.05$, *t*-test).

PIN2 promoter activity was detected in the epidermis, cortex and lateral root cap (LRC; She et al. 2010; **Fig. 4I**). Ectopic expression of *SAUR41* from the *PIN2* promoter induced expansion of epidermal and cortical cells, but the auxin accumulation/signaling pattern appeared normal (**Fig. 4J**). *PIN2::SAUR41* roots exhibited a root-waving phenotype on vertically oriented agar plates, and the epidermal and cortical cells in the two sides of the root transition zones were irregularly and asymmetrically elongated (**Fig. 4K**).

Comparison of tissue-specific expression of *SAUR41* and *IAA2*^{P65S} from promoters of root meristem patterning genes

We also expressed *SAUR41* from the promoters of root meristem patterning genes. Three promoters were chosen: *WOX5* (*WUSCHEL-related homeobox 5*), *ACR4* (*ARABIDOPSIS CRINKLY4*) and *PLT2* (*PLETHORA2*). *WOX5* encoded a homeodomain transcription factor (Sarkar et al. 2007), *PLT2* encoded an AP-2 type transcription factor (Aida et al. 2004, Galinha et al. 2007) and *ACR4* encoded a receptor-like kinase (De Smet et al. 2008). They were three of the major regulators of root stem cell activity (Aichinger et al. 2012, Perilli et al. 2012, Petricka et al. 2012). To compare the effects between tissue-specific expression of a SAUR protein and a stabilized AUX/IAA protein, we introduced IAA2^{P65S} that harbored a site-directed mutation in the proline residue of conserved domain II. As one of 29 *Aux/IAA* genes of Arabidopsis, *IAA2* was highly auxin inducible and expressed in vascular tissues and auxin accumulation/signaling peaks (Swarup et al. 2001).

WOX5 was expressed in the quiescent center of root stem cell niches (Sarkar et al. 2007; **Fig. 5A**). Tissue-specific expression of *SAUR41* from the *WOX5* promoter induced the formation of additional auxin accumulation/signaling peaks in stele initials above the quiescent center (**Fig. 5B–F**). In addition, *WOX5::SAUR41* roots had supernumerary cell layers (**Fig. 5C, D, F**), like those observed in *PIN1::SAUR41* roots (**Fig. 4E, G**). As expected, tissue-specific expression of *IAA2*^{P65S} driven by the *WOX5* promoter inhibited auxin accumulation/signaling in the quiescent center (**Fig. 5G, H**). Interestingly, it also inhibited auxin accumulation/signaling in the stele initials (**Fig. 5G, H**), opposite to the effects observed in tissue-specific expression of *SAUR41* from the *WOX5* promoter (**Fig. 5B–F**). *ACR4* was expressed in the root stem cell niche and its surrounding cells, including young epidermal cells, cortical cells and columella cells (De Smet et al. 2008; **Fig. 5I**). Ectopic expression of *SAUR41* from the *ACR4* promoter led to the expansion of cells expressing *ACR4* (**Fig. 5J, K**). Formation of auxin accumulation/signaling peaks in stele initials was visible (**Fig. 5J, K**), but not as dramatically as that in the *WOX5::SAUR41* roots (**Fig. 5B–F**), indicating that the balanced expression of *SAUR41* in the entire root stem cell niche attenuated the effects of ectopic SAUR proteins on auxin transport, compared with the selected expression of *SAUR41* in the quiescent center by the *WOX5* promoter. On the other hand, tissue-specific expression of *IAA2*^{P65S} from the *ACR4* promoter had a more remarkable impact on root meristem development compared with that seen in *WOX5::IAA2*^{P65S} roots. As shown in **Fig. 5**, *ACR4::IAA2*^{P65S} roots had two separate auxin accumulation/signaling maxima: one in the quiescent center and the other in the young columella cells (**Fig. 5L**).

PLT2 was gradiently expressed in root meristems and lateral cap cells (Aida et al. 2004, Galinha et al. 2007; **Fig. 5M**). Tissue-specific expression of *SAUR41* from the *PLT2* promoter exhibited triple effects as addressed above: additional auxin accumulation/signaling peaks in stele initials and supernumerary cell layers in the proximal meristem zone (**Fig. 5N, O**). On the other hand, tissue-specific expression of *IAA2*^{P65S} from the *PLT2* promoter inhibited auxin accumulation/signaling in the quiescent center, promoted auxin accumulation/signaling in stele initials and led to establishment of new auxin accumulation/signaling peaks in the adjacent provascular cells (**Fig. 5P**), similar to that seen for relocalization of auxin accumulation/signaling peaks upon polar auxin transport inhibitor treatment (Sabatini et al. 1999).

[20.2.2013-5:54pm] [1–13] Paper: OP-PCPJ130028
MANUSCRIPT CATEGORY: REGULAR PAPER

PCP PLANT & CELL PHYSIOLOGY

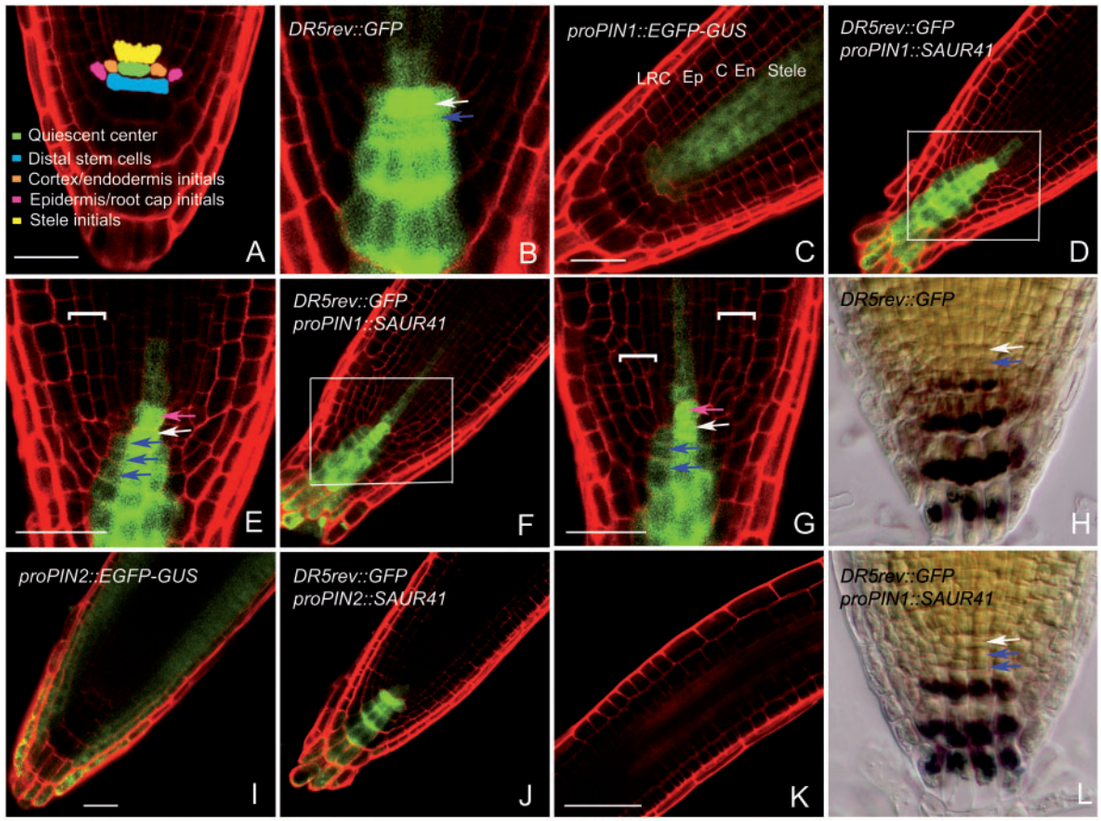

Fig. 4 Tissue-specific expression of *SAUR41* from the *PIN1* and *PIN2* promoters. Green EGFP (enhanced green fluorescent protein) signals and red PI (propidium iodide, staining the cell wall here) signals were viewed by confocal microscopy. Purple starch grains stained by Lugol's solution were viewed by DIC (differential interference contrast) microscopy. (A) The root stem cell niches. (B) Auxin accumulation/signaling pattern in root meristems of the *DR5rev::GFP* background line. A white arrow indicates the quiescent center, while a blue arrow indicates the tier of distal stem cells. Boxed areas were magnified in the subsequent images. ~~Insets were enlargements of root stem cell niches.~~ (C) Promoter activity of *PIN1*. (D–F) Tissue-specific expression of *SAUR41* from the *PIN1* promoter led to auxin retention in stele initials transporting auxin (pink arrow), additional tiers of distal stem cells (blue arrow) and supernumerary cell layers (white bracket). (H, L) Differentiation status of columella cells in control roots (H) and *PIN1::SAUR41* roots (L) determined by Lugol's solution staining. (I) Promoter activity of *PIN2*. (J, K) Tissue-specific expression of *SAUR41* from the *PIN2* promoter did not induce auxin retention but caused irregular cell expansion in the corresponding cells. LRC, lateral root cap; Ep, epidermis; C, cortex; En, endodermis. Bars: 25 μm.

Ectopic SAUR41 proteins differentially regulated root cell expansion and root gravitropic growth

We measured cell areas of stele initial cells, quiescent center cells and distal stem cells in root meristems of transgenic seedlings expressing *SAUR41* from promoters of auxin transporter genes and root meristem patterning genes. The results showed that *PIN1::SAUR41*, *WOX5::SAUR41* and *PLT2::SAUR41* roots had a 30–60% increase in cell areas of stele initial cells and quiescent center cells, while *ACR4::SAUR41* roots had enlarged quiescent center cells and distal stem cells (**Fig. 6A**; $P < 0.05$, *t*-test).

The root gravitropic responses in these transgenic seedlings were also analyzed. *ACR4::SAUR41* roots showed delayed gravitropic growth (**Fig. 6B**), coinciding with their higher auxin accumulation/signaling in young columella cells but lower auxin accumulation/signaling in LRC cells (**Fig. 5I**). *PIN2::SAUR41* roots had advanced gravitropic growth 2 h after the gravitropic stimulation, while *PLT2::SAUR41* roots displayed enhanced gravitropic growth 3 h after the gravitropic stimulation (**Fig. 6B**). It has been suggested that auxin transport in the lower side of lateral cap cells and auxin accumulation in the lower side of epidermal and cortical cells were essential for the root gravitropic response (Ottenschläger et al. 2003). Our results were consistent with the expression pattern of *PIN2* and *PLT2* promoters. *PIN2* was expressed in both lateral cap cells and epidermal and cortical cells (**Fig. 4I**), while *PLT2* was expressed in lateral cap cells (**Fig. 5M**).

Discussion

The expression pattern of *SAUR41* in root meristems was distinctive. *SAUR19* subfamily genes were expressed in growing hypocotyls in response to shade avoidance, and in root

[20.2.2013-5:54pm] [1–13] Paper: OP-PCPJ130028
MANUSCRIPT CATEGORY: REGULAR PAPER

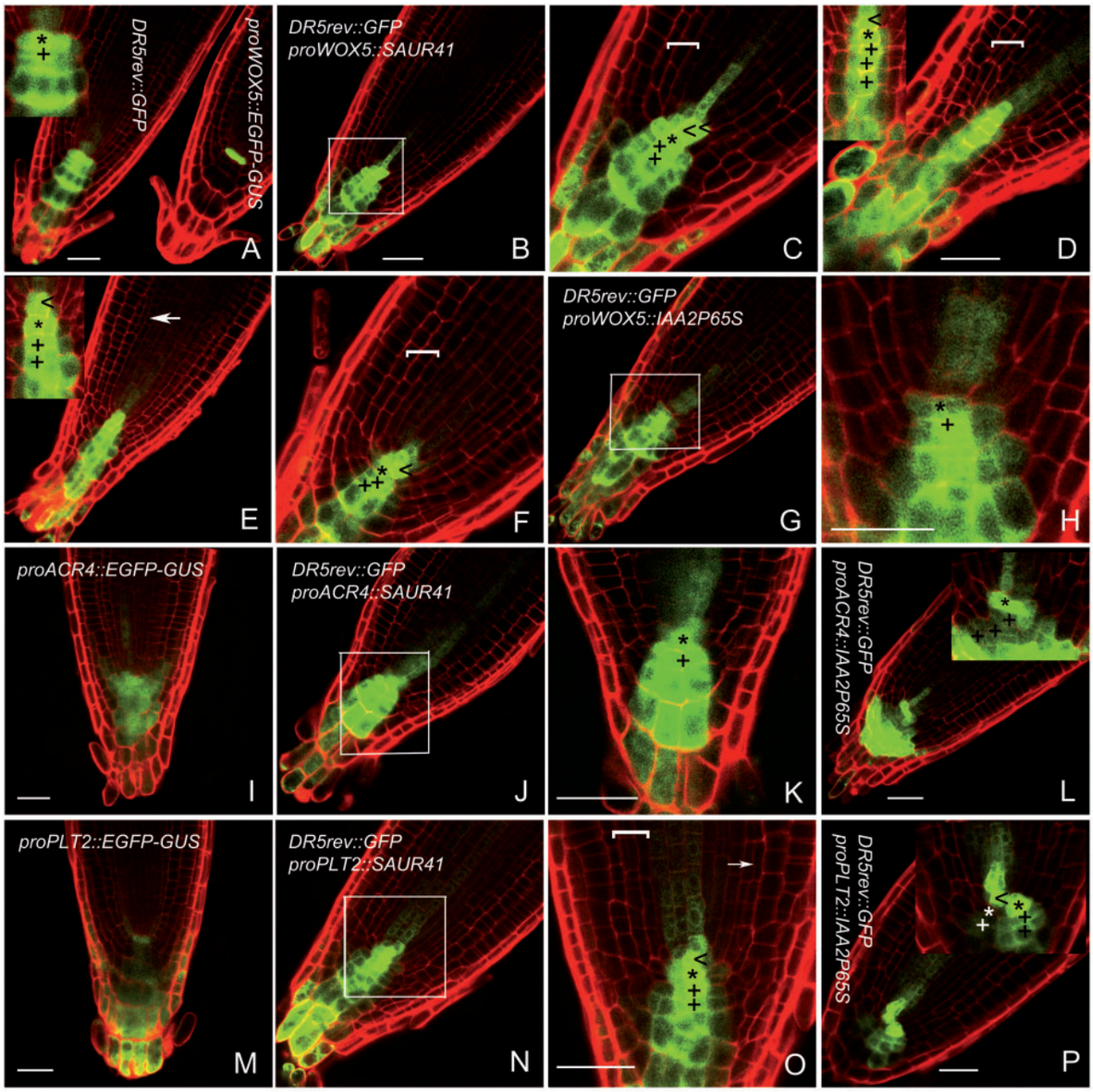

Fig. 5 Tissue-specific expression of *SAUR41* and *IAA2*^{P65S} from promoters of root meristem patterning genes. Green EGFP (enhanced green fluorescent protein) signals and red PI (propidium iodide, staining the cell wall here) signals were viewed by confocal microscopy. Boxed areas were magnified in the subsequent images. Insets were enlargements of root stem cell niches. (A) Auxin accumulation/signaling pattern in root meristems of the *DR5rev::GFP* background line (left) and the promoter activity of *WOX5* (right). (B–F) Tissue-specific expression of *SAUR41* from the *WOX5* promoter. (G, H) Tissue-specific expression of *IAA2*^{P65S} from the *WOX5* promoter. (I) Promoter activity of *ACR4*. (J, K) Tissue-specific expression of *SAUR41* from the *ACR4* promoter. (L) Tissue-specific expression of *IAA2*^{P65S} from the *ACR4* promoter. (M) Promoter activity of *PLT2*. (N, O) Tissue-specific expression of *SAUR41* from the *PLT2* promoter. (P) Tissue-specific expression of *IAA2*^{P65S} from the *PLT2* promoter. The arrow indicates the division of endodermal cells. < indicates additional auxin accumulation/signaling peaks; * indicates the quiescent center; + indicates tiers of distal stem cells; and [indicates the supernumerary cell layers. Bars: 25 μm.

elongation zones in response to auxin treatment (Spartz et al. 2012). *SAUR63* and members of its clade were expressed in growing regions of hypocotyls, cotyledons, petiole, young rosette leaves and inflorescence stems, but not in roots (Chae et al. 2012). Herein, we found that the expression of *SAUR41* was normally restricted to the quiescent center and cortex/endodermis initials of root meristems; upon an auxin or gravitropic stimulation, it was provoked in the endodermis at the proximal meristem region and transition zone of Arabidopsis roots (**Fig. 1A–F**). Furthermore, *SAUR41* was differentially expressed

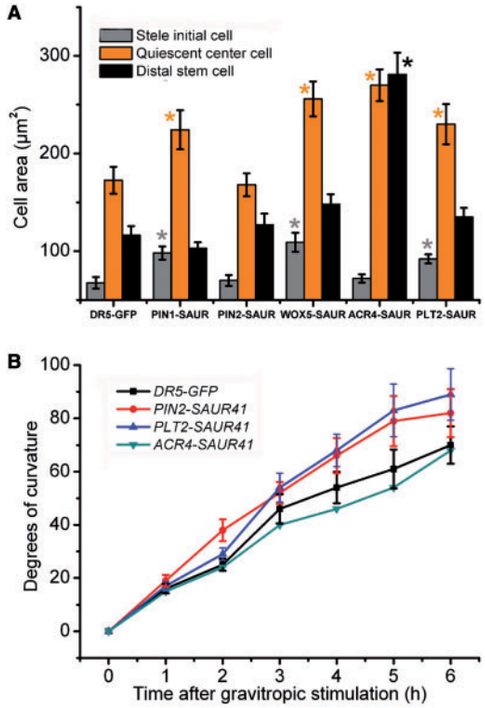

Fig. 6 Ectopic SAUR41 proteins differentially regulated root cell expansion and root gravitropic growth. (A) Cell areas of stele initial cells, quiescent center cells and distal stem cells in roots of 5-day-old seedlings. (B) Root gravitropic responses in 6-day-old seedlings. *$P < 0.05$, *t*-test.

during lateral root development, as manifested by β-glucuronidase (GUS) activity in prospective stem cell niches of lateral root primordia, and in expanding endodermal cells surrounding the lateral root primordia (**Fig. 1G–I**). In previous microarray experiments, the expression of *SAUR41* has been reported to be regulated by multiple environmental signals (Mazzella et al. 2005, Darrah et al. 2006, Zhang et al. 2007, Peltier et al. 2011). Taken together, it seemed that *SAUR41* was actively expressed in response to both developmental and environmental cues.

SAUR41–EGFP fusion proteins localize to the cytoplasm (**Fig. 1M–P**), while EGFP–SAUR19 and SAUR63–EGFP localize predominantly to the plasma membrane (Chae et al. 2012, Spartz et al. 2012). Although the protein localization pattern and the gene expression pattern of *SAUR41* were different from those of *SAUR19* and *SAUR63*, the phenotypes resulting from overexpression of *SAUR41* driven by the CaMV *35S* promoter shared many similarities with those of *SAUR19* and *SAUR63* subfamily genes. In all three cases, transgenic seedlings had elongated hypocotyls, expanded hypocotyl epidermal cells and enhanced hypocotyl basipetal IAA transport compared with the wild type (**Figs. 2A, B, E**, **3**; Chae et al. 2012, Spartz et al. 2012). In the cases of *SAUR41* and *SAUR19*, transgenic seedlings displayed waving roots and increased vegetative biomass (**Fig. 2C, D, H**; Spartz et al. 2012); while in the cases of *SAUR41* and *SAUR63*, transgenic plants had expanded petals and twisted inflorescence stems (**Fig. 2I–L**; Chae et al. 2012). Interestingly, only in the case of *SAUR41* did the transgenic seedlings have increased primary root length and lateral root development compared with wild-type controls (**Fig. 2F, G**). Thus, it seems likely that Arabidopsis SAUR proteins have some similarities but also specificity in terms of molecular functions. Alternatively, SAUR proteins may share a similar molecular function, but different SAUR proteins require different tissue-specific partners.

Tissue-specific expression of *SAUR41* from *PIN1*, *WOX5*, *ACR4* or *PLT2* promoters caused new auxin accumulation/signaling peaks in stele initial cells transporting auxin (**Figs. 4D–G**, **5B–F, N, O**). Roots of *PIN1*::*SAUR41* seedlings had additional tiers of distal stem cells below the quiescent center and supernumerary cell layers in root meristems (**Fig. 4D–H, L, Q**). It has been reported that auxin regulates distal stem cell differentiation in Arabidopsis roots, and defects in auxin transport would lead to additional tiers of distal stem cells (Ding and Friml 2010). Thus, it seemed likely that SAUR41 induced perturbation of auxin transport in root meristems as it was expressed above the stem cell niches (from the *PIN1* promoter). In contrast, tissue-specific expression of *SAUR41* from the *PIN2* promoter did not induce alterations in root meristem patterning, but caused alterations in cell expansion in the corresponding cell lineages (**Fig. 4J, K**). In addition, *PIN2*::*SAUR41* and *PLT2*::*SAUR41* roots had enhanced gravitropic growth (**Fig. 6B**), indicating that ectopic SAUR41 proteins promoted root basipetal auxin transport for root gravitropic responses. Taken together, it seems likely that ectopic SAUR41 proteins retard auxin transport in root stem cell niches, but promote auxin transport in LRC cells and epidermal and cortical cells.

Previously, it has been proposed that rice *SAUR39* acted as a negative regulator of organ growth and auxin transport (Kant et al. 2009), while Arabidopsis *SAUR19* and *SAUR63* acted as positive regulators of cell expansion and auxin transport (Chae et al. 2012, Spartz et al. 2012). Herein, in terms of cell expansion, we found that *SAUR41* promoted cell expansion, as it was constitutively expressed from the CaMV *35S* promoter (**Figs. 2**, **3**). In addition, stele initial cells, quiescent center cells and distal stem cells in root meristems of transgenic seedlings expressing *SAUR41* from promoters of auxin transporter genes and root meristem patterning genes were differentially enlarged (**Fig. 6A**). Thus, similarly to SAUR19 with N-terminal tags and SAUR63 with C-terminal tags, untagged SAUR41 promoted cell expansion, as it was ectopically expressed. However, in terms of auxin transport, the functions of SAUR proteins appeared to be more complicated. The observed higher flow rate of labeled IAA in hypocotyls could be an indirect effect of SAUR protein overexpression. Two questions, why ectopic SAUR41 proteins retarded auxin transport in root stem cell niches but promoted basipetal auxin transport, and why rice OsSAUR39 (analogous to Arabidopsis SAUR63, clade I) inhibited auxin transport but Arabidopsis SAUR63 promoted auxin transport, remained

unanswered. It should be noted that the *DR5::GFP* marker basically indicated the status of auxin signaling but not the auxin transport. Currently, direct measurement of auxin transport in root stem cell niches is unavailable. It was tempting to speculate that SAUR41 proteins used different mechanism to regulate auxin transport for cell elongation and for root meristem patterning.

Tissue-specific expression of *IAA2*^{P65S} from *WOX5*, *ACR4* and *PLT2* promoters displayed fundamentally different effects on root meristem patterning compared with that observed for *SAUR41* (**Fig. 5**). The mechanism of stabilized Aux/IAA proteins is clear. They impaired the SCF^{TIR1} pathway of auxin signaling to regulate cell division, differentiation and elongation. They also disturbed auxin transport by transcriptional modification of the auxin export machinery (Hayashi 2012, Scherer et al. 2012). In contrast, the precise mechanism by which SAUR proteins regulate cell expansion and auxin transport remains unclear. It will be interesting to learn whether there exist epistatic interactions between the *IAA2* and the *SAUR41* gain-of-function phenotypes. We are currently crossing the *IAA2*^{P65S} lines with the corresponding *SAUR41* lines to answer this question.

The *SAUR41* function reported here was solely dependent on the ectopic expression data, while its endogenous role in stem cell maintenance remained unclear. The gene could be involved in the regulation of cell sizes of quiescent center and cortex/endodermis initials, and/or in the modulation of auxin transport in these cells. In addition, the *SAUR41* subfamily contains four members: *SAUR40*, *SAUR41*, *SAUR71* and *SAUR72*. Further investigations on promoter activity and protein localization patterns of other *SAUR41* subfamily members, as well as on loss-of-function phenotypes of the *SAUR41* gene family, are required and of great interest.

Materials and Methods

Plant materials and growth conditions

Arabidopsis thaliana ecotype Columbia-0 and the *DR5rev::GFP* background (Friml et al. 2003) were used as sources of wild-type plant materials. Promoter reporter lines for the *PIN* gene family and the *TIR1/AFB* gene family (She et al. 2010) have been donated to ABRC. Seeds were surface sterilized and cultured aseptically on 9 cm Petri dishes containing Gamborg's B5 medium with 1% (w/v) sucrose and 1% (w/v) agar. The plates were maintained at 4°C for 2 d, and then transferred to a culture room (23°C, 80 μmol m^{-2} s^{-1} irradiance with a 16 h photoperiod and 30–40% relative humidity).

Vector construction and plant transformation

We used the GATEWAY^{TM} system for vector construction. Entry vectors were created using the pENTR^{TM}/D-TOPO kits (Invitrogen). The PCR primers for construction of entry vectors for the coding region of *SAUR41* and for promoter regions of *SAUR41*, *WOX5*, *ACR4* and *PLT2* are listed in **Supplementary Table S1**. *IAA2*^{P65S} was generated by overlapping PCR using the primers given in **Supplementary Table S1**. Each entry clone was confirmed by DNA sequencing. GATEWAY^{TM}-compatible destination vectors for protein subcellular localization, overexpression, MYC tagging and promoter analysis were used (Karimi et al. 2002, Earley et al. 2006, She et al. 2010). The LR reaction was conducted to generate different expression vectors.

To facilitate tissue-specific gene expression from various promoters, the CaMV 35S promoter in the overexpression constructs (*35S::SAUR41* and *35S::IAA2*^{P65S}) was replaced with a *ccdB* fragment by a method described previously (Yang et al. 2012). Briefly, the *ccdB* fragment was PCR amplified using pH7FWG2,0 as a template, with the primers ccdB-Up and ccdB-Dn, containing an introduced *Hin*dIII and *Spe*I site, respectively. The *ccdB* fragment was then digested to replace the 35S promoter sequence, thus forming new destination vectors for tissue-specific expression.

All of the expression vectors were electroporated into *Agrobacterium tumefaciens* strain GV3101. Plants were transformed using the vacuum infiltration method (Bechtold et al. 1993). Transgenic plants were selected on B5 plates with 12.5 μg ml^{-1} hygromycin or 25 μg ml^{-1} kanamycin depending on the selection markers. Single-locus and homozygous transgenic lines were characterized as we described previously (She et al. 2010).

Microscopic analysis and histochemical detection

For histochemical detection of GUS activities, young seedlings at different developmental stages and different parts from transgenic plants were collected. They were stained at 37°C overnight in 1 mM 5-bromo-4-chloro-3-indolyl-β-D-glucuronic acid (X-Gluc), 1 mM potassium ferricyanide, 0.1% Triton X-100 and 0.1 M sodium phosphate buffer, pH 7.0 with 10 mM EDTA. Samples were washed in 70% ethanol to remove Chl. Differential interference contrast (DIC) images were visualized using a microscope (Nikon Eclipse 80i) with a DXM1200 CCD camera and EclipseNet software. For the localization of fluorescence fusion proteins, a confocal microscope system (Zeiss LSM510) was used. Without specification, 5-day-old seedlings were mounted in water. Starch grains in columella cells were stained with I_2–KI as described previously (Ding and Friml 2010).

Hypocotyl IAA transport assay

IAA transport in hypocotyls was measured as previously described (Chae 2012). [^{3}H] IAA was a product of American Radiolabeled Chemicals, Inc. The radioisotope counts of [^{3}H] IAA were detected using a low-noise scintillation counter (MicroBeta 2, Perkin Elmer).

Growth and cell measurement, statistical analysis and image processing

After incubations for the durations indicated in the text, the plates were digitally photographed. Root and hypocotyl length

was measured using magnified images. Lateral root (>1 mm) numbers were counted using each seedling as an individual sample. For hormone treatment, seedlings were transferred onto a medium containing 10 μM NAA or GA_3 for 1 or 12 h. For gravitropism assays, the protocol of Weijers et al. (2005) was adopted. The mean hypocotyl epidermal cell length and the cell area of root stem cell niches were measured as described by Spartz et al. (2012). Each treatment contained 30–50 seedlings and was replicated three times. Statistical analysis of the data was performed using Microsoft Excel and Student's *t*-test. Images were processed using Adobe Photoshop CS2.

Supplementary data

Supplementary data are available at PCP online.

Funding

Q3

This work was supported by the National Natural Science Foundation of China [grant No. 31170211 to J.W.].

Acknowledgments

We are grateful to ABRC and RIKEN-BRC for the distribution of Arabidopsis materials. No conflict of interest is declared.

References

Aichinger, E., Kornet, N., Friedrich, T. and Laux, T. (2012) Plant stem cell niches. *Annu. Rev. Plant Biol.* 63: 625–636.

Aida, M., Beis, D., Heidstra, R., Willemsen, V., Blilou, I., Galinha, C. et al. (2004) The *PLETHORA* genes mediate patterning of the *Arabidopsis* root stem cell niche. *Cell* 119: 109–120.

Bechtold, N., Ellis, J. and Pelletier, G. (1993) *In planta* Agrobacterium-mediated gene transfer by infiltration of adult *Arabidopsis thaliana* plants. *CR Acad. Sci. Ser. III Sci. Vie* 316: 1194–1199.

Bosco, C.D., Lezhneva., L., Biehl, A., Leister, D., Strotmann, H., Wanner., G. et al. (2004) Inactivation of the chloroplast ATP synthase gamma subunit results in high non-photochemical fluorescence quenching and altered nuclear gene expression in *Arabidopsis thaliana*. *J. Biol. Chem.* 279: 1060–1069.

Carrie, C., Giraud, E., Duncan, O., Xu, L., Wang, Y., Huang, S. et al. (2010) Conserved and novel functions for *Arabidopsis thaliana* MIA40 in assembly of proteins in mitochondria and peroxisomes. *J. Biol. Chem.* 285: 36138–36148.

Chae, K., Isaacs, C.G., Reeves, P.H., Maloney, G.S., Muday, G.K., Nagpal, P. et al. (2012) *Arabidopsis SMALL AUXIN UP RNA63* promotes hypocotyl and stamen filament elongation. *Plant J.* 71: 684–697.

Darrah, C., Taylor, B.L., Edwards, K.D., Brown, P.E., Hall, A. and McWatters, H.G. (2006) Analysis of phase of *LUCIFERASE* expression reveals novel circadian quantitative trait loci in *Arabidopsis*. *Plant Physiol.* 140: 1464–1474.

Davuluri, R.V., Sun, H., Palaniswamy, S.K., Matthews, N., Molina, C., Kurtz, M. et al. (2003) AGRIS, Arabidopsis Gene Regulatory Information Server, an information resource of Arabidopsis cis-regulatory elements and transcription factors. *BMC Bioinform.* 4: 25.

De Smet, I., Vassileva, V., De Rybel, B., Levesque, M.P., Grunewald, W., Van Damme, D. et al. (2008) Receptor-like kinase ACR4 restricts formative cell divisions in the Arabidopsis root. *Science* 322: 594–597.

Dharmasiri, N., Dharmasiri, S. and Estelle, M. (2005) The F-box protein TIR1 is an auxin receptor. *Nature* 435: 441–445.

Ding, Z. and Friml, J. (2010) Auxin regulates distal stem cell differentiation in *Arabidopsis* roots. *Proc. Natl Acad. Sci. USA* 107: 12046–12051.

Earley, K.W., Haag, J.R., Pontes, O., Opper, K., Juehne, T., Song, K. et al. (2006) Gateway-compatible vectors for plant functional genomics and proteomics. *Plant J.* 45: 616–629.

Estavillo, G.M., Crisp, P.A., Pornsiriwong, W., Wirtz, M., Collinge, D., Carrie, C. et al. (2011) Evidence for a SAL1–PAP chloroplast retrograde pathway that functions in drought and high light signaling. *Plant Cell* 23: 3992–4012.

Franklin, K.A., Lee, S.H., Patel, D., Kumar, S.V., Spartz, A.K., Gu, C. et al. (2011) PHYTOCHROME-INTERACTING FACTOR 4 (PIF4) regulates auxin biosynthesis at high temperature. *Proc. Natl Acad. Sci. USA* 108: 20231–20235.

Friml, J., Vieten, A., Sauer, M., Weijers, D., Schwarz, H., Hamann, T. et al. (2003) Efflux-dependent auxin gradients establish the apical-basal axis of Arabidopsis. *Nature* 426: 147–153.

Galinha, C., Hofhuis, H., Luijten, M., Willemsen, V., Blilou, I., Heidstra, R. et al. (2007) PLETHORA proteins as dose-dependent master regulators of Arabidopsis root development. *Nature* 449: 1053–1057.

Gleason, C., Huang, S., Thatcher, L.F., Foley, R.C., Anderson, C.R., Carroll, A.J. et al. (2011) Mitochondrial complex II has a key role in mitochondrial-derived reactive oxygen species influence on plant stress gene regulation and defense. *Proc. Natl Acad. Sci. USA* 108: 10768–10773.

Gray, W.M., Kepinski, S., Rouse, D., Leyser, O. and Estelle, M. (2001) Auxin regulates SCF^{TIR1}-dependent degradation of AUX/IAA proteins. *Nature* 414: 271–276.

Hagen, G. and Guilfoyle, T. (2002) Auxin-responsive gene expression: genes, promoters and regulatory factors. *Plant Mol. Biol.* 49: 373–385.

Harrison, B.R. and Masson, P.H. (2008) ARL2, ARG1 and PIN3 define a gravity signal transduction pathway in root statocytes. *Plant J.* 53: 380–392.

Hayashi, K. (2012) The interaction and integration of auxin signaling components. *Plant Cell Physiol.* 53: 965–975.

Jain, M., Tyagi, A.K. and Khurana, J.P. (2006) Genome-wide analysis, evolutionary expansion, and expression of early auxin-responsive *SAUR* gene family in rice (*Oryza sativa*). *Genomics* 88: 360–371.

Jones, B. and Ljung, K. (2012) Subterranean space exploration: the development of root system architecture. *Curr. Opin. Plant Biol.* 15: 97–102.

Josse, E.-M., Gan, Y., Bou-Torrent, J., Stewart, K.L., Gilday, A.D., Jeffree, C.E. et al. (2011) A DELLA in disguise: SPATULA restrains the growth of the developing *Arabidopsis* seedling. *Plant Cell* 23: 1337–1351.

Kant, S., Bi, Y.M., Zhu, T. and Rothstein, S.J. (2009) SAUR39, a small auxin-up RNA gene, acts as a negative regulator of auxin synthesis and transport in rice. *Plant Physiol.* 151: 691–701.

Karimi, M., Inzé, D. and Depicker, A. (2002) GATEWAY^{TM} vectors for Agrobacterium-mediated plant transformation. *Trends Plant Sci.* 7: 193–195.

Kepinski, S. and Leyser, O. (2005) The Arabidopsis F-box protein TIR1 is an auxin receptor. *Nature* 435: 446–451.

Kim, J., Harter, K. and Theologis, A. (1997) Protein–protein interactions among the Aux/IAA proteins. *Proc. Natl Acad. Sci. USA* 94: 11786–11791.

Kodaira, K.-S., Qin, F., Tran, L.-S.P., Maruyama, K., Kidokoro, S., Fujita, Y. et al. (2011) Arabidopsis Cys2/His2 zinc-finger proteins AZF1 and AZF2 negatively regulate abscisic acid-repressive and auxin-nducible genes under abiotic stress conditions. *Plant Physiol.* 157: 742–756.

Leonhardt, N., Kwak, J.M., Robert, N., Waner, D., Leonhardt, G. and Schroeder, J.I. (2004) Microarray expression analyses of Arabidopsis guard cells and isolation of a recessive abscisic acid hypersensitive protein phosphatase 2C mutant. *Plant Cell* 16: 596–615.

Ljung, K., Hull, A.K., Kowalczyk, M., Marchant, A., Celenza, J., Cohen, J.D. et al. (2002) Biosynthesis, conjugation, catabolism and homeostasis of indole-3-acetic acid in *Arabidopsis thaliana*. *Plant Mol. Biol.* 50: 309–332.

Mazzella, M.A., Arana, M.V., Staneloni, R.J., Perelman, S., Batiller, M.J.R., Muschietti, J. et al. (2005) Phytochrome control of the *Arabidopsis* transcriptome anticipates seedling exposure to light. *Plant Cell* 17: 2507–2516.

Nagawa, S., Sawa, S., Sato, S., Kato, T., Tabata, S. and Fukuda, H. (2006) Gene trapping in Arabidopsis reveals genes involved in vascular development. *Plant Cell Physiol.* 47: 1394–1405.

Ottenschläger, I., Wolff, P., Wolverton, C., Bhalerao, R.P., Sandberg, G., Ishikawa, H. et al. (2003) Gravity-regulated differential auxin transport from columella to lateral root cap cells. *Proc. Natl Acad. Sci. USA* 100: 2987–2991.

Ouellet, F., Overvoorde, P.J. and Theologis, A. (2001) IAA17/AXR3, biochemical insight into an auxin mutant phenotype. *Plant Cell* 13: 829–841.

Overvoorde, P., Fukaki, H. and Beeckman, T. (2010) Auxin control of root development. *Cold Spring Harb. Perspect. Biol.* 2: a001537.

Paponov, I.A., Paponov, M., Teala, W., Menges, M., Chakrabortee, S., Murray, J.A.H. et al. (2008) Comprehensive transcriptome analysis of auxin responses in *Arabidopsis*. *Mol. Plant* 12: 321–337.

Park, J.-E., Park, J.-Y., Kim, Y.-S., Sraswick, P.E., Jeon, J., Yun, J. et al. (2007) GH3-mediated auxin homeostasis links growth regulation with stress adaptation response in *Arabidopsis*. *J. Biol. Chem.* 282: 10036–10046.

Peltier, C., Schmidlin, L., Klein, E., Tsconnat, L., Prinsen, E., Erhardt, M. et al. (2011) Expression of Beet necrotic yellow vein virus p25 protein induces hormonal changes and a root branching phenotype in *Arabidopsis thaliana*. *Transgenic Res.* 20: 443–466.

Perilli, S., Mambro, R.D. and Sabatini, S. (2012) Growth and development of the root apical meristem. *Curr. Opin. Plant Biol.* 15: 17–23.

Petricka, J.J., Winter, C.M. and Benfey, P.N. (2012) Control of *Arabidopsis* root development. *Annu. Rev. Plant Biol.* 63: 563–564.

Ramos, J., Zenser, N., Leyser, O. and Callis, J. (2001) Rapid degradation of auxin/indoleacetic acid proteins requires conserved amino acids of domain II and is proteasome dependent. *Plant Cell* 13: 2349–2360.

Reed, J.W. (2001) Roles and activities of Aux/IAA proteins in Arabidopsis. *Trends Plant Sci.* 6: 420–425.

Rogg, L.E., Lasswell, J. and Bartel, B. (2001) A gain-of-function mutation in *IAA28* suppresses lateral root development. *Plant Cell* 13: 465–480.

Sabatini, S., Beis, D., Wolkenfelt, H., Murfett, J., Guilfoyle, T., Malamy, J. et al. (1999) An auxin-dependent distal organizer of pattern and polarity in the *Arabidopsis* root. *Cell* 99: 463–472.

Santner, A. and Estelle, M. (2009) Recent advances and emerging trends in plant hormone signaling. *Nature* 459: 1071–1078.

Sarkar, A.K., Luijten, M., Miyashima, S., Lenhard, M., Hashimoto, T., Nakajima, K. et al. (2007) Conserved factors regulate signaling in *Arabidopsis thaliana* shoot and root stem cell organizers. *Nature* 446: 811–814.

Scherer, G.F.E., Labusch, C. and Effendi, Y. (2012) Phospholipases and the network of auxin signal transduction with ABP1 and TIR1 as two receptors: a comprehensive and provocative model. *Front. Plant Sci.* 3: 56.

She, W., Lin, W., Zhu, Y., Chen, Y., Jin, W., Yang, Y. et al. (2010) The gypsy insulator of *Drosophila melanogaster* together with its binding protein Su(Hw) (Suppressor of Hairy-wing) facilitate high and precise expression of transgenes in *Arabidopsis thaliana*. *Genetics* 185: 1141–1150.

Shirakawa, M., Ueda, H., Shimada, T., Nishiyama., C. and Hara-Nishimura, I. (2009) Vacuolar SNAREs function in the formation of the leaf vascular network by regulating auxin distribution. *Plant Cell Physiol.* 50: 1319–1328.

Spartz, A.K., Lee, S.H., Wenger, J.P., Gonzalez, N., Itoh, H., Inzé, D. et al. (2012) The *SAUR19* subfamily of *SMALL AUXIN UP RNA* genes promote cell expension. *Plant J.* 70: 978–990.

Staswick, P.E., Serban, B., Rowe, M., Tiryaki, I., Maldonado, M.T., Maldonado, M.C. et al. (2005) Characterization of an Arabidopsis enzyme family that conjugates amino acids to indole-3-acetic acid. *Plant Cell* 17: 616–627.

Swarup, R., Friml, J., Marchant, A., Ljung, K., Sandberg, G., Palme, K. et al. (2001) Localization of the auxin permease AUX1 suggests two functionally distinct hormone transport pathways operate in the Arabidopsis root apex. *Genes Dev.* 15: 2648–2653.

Tan, X., Calderon-Villalobos, L.I.A., Sharon, M., Zheng, C., Robinson, C.V., Estelle, M. et al. (2007) Mechanism of auxin perception by the TIR1 ubiquitin ligase. *Nature* 446: 640–645.

Tiwari, S.B., Wang, X.J., Hagen, G. and Guilfoyle, T.J. (2001) AUX/IAA proteins are active repressors, and their stability and activity are modulated by auxin. *Plant Cell* 13: 2809–2822.

Ubeda-Tomás, S., Beemster, G.T.S. and Bennett, M.J. (2012) Hormonal regulation of root growth: integrating local activities into global behavior. *Trends Plant Sci.* 17: 326–331.

Ubeda-Tomás, S., Federici, F., Casimiro, I., Beemster, G.T., Bhalerao, R., Swarup, R. et al. (2009) Gibberellin signaling in the endodermis controls Arabidopsis root meristem size. *Curr. Biol.* 19: 1194–1199.

Ubeda-Tomás, S., Swarup, R., Coates, J., Swarup, K., Laplaze, L., Beemster, G.T. et al. (2008) Root growth in Arabidopsis requires gibberellin/DELLA singaling in the endodermis. *Nat. Cell Biol.* 10: 625–628.

Ulmasov, T., Murfett, J., Hagen, G. and Guilfoyle, T. (1997) Aux/IAA proteins repress expression of reporter genes containing natural and highly active synthetic auxin response elements. *Plant Cell* 9: 1963–1971.

Vanneste, S. and Friml, J. (2009) Auxin: a trigger for change in plant development. *Cell* 136: 1005–1016.

Weijers, D., Benkova, E., Jäger, K.E., Schlereth, A., Hamann, T., Kientz, M. et al. (2005) Developmental specificity of auxin response by pairs of ARF and Aux/IAA transcriptional regulators. *EMBO J.* 24: 1874–1885.

Westfall, C.S., Zubieta, C., Herrmann, J., Kapp, U., Nanao, M.H. and Jez, J.M. (2012) Structural basis for prereceptor modulation of plant hormones by GH3 proteins. *Science* 336: 1708–1711.

Woodward, A.W. and Bartel, B. (2005) Auxin: regulation, action, and interaction. *Ann. Bot.* 95: 707–735.

Worley, C.K., Zenser, N., Ramos, J., Rouse, D., Leyser, O., Theologis, A. et al. (2000) Degradation of Aux/IAA proteins is essential for normal auxin signaling. *Plant J.* 21: 553–562.

Yang, Y., Jin, H., Chen, Y., Lin, W., Wang, C., Chen, Z. et al. (2011) A chloroplast envelope membrane protein containing a putative LrgB domain related to the control of bacterial death and lysis is required for chloroplast development in *Arabidopsis thaliana*. *New Phytol.* 193: 81–95.

Zeng, Y., Zhao, T. and Kermode, A.R. (2012) A conifer ABI3-interacting protein plays important roles during key transitions of the plant life cycle. *Plant Physiol.* 161: 179–195.

Zhang, H., Kim, M., Krishnamachari, V., Payton, P., Sun, Y., Grimson, M. et al. (2007) Rhizobacterial volatile emissions regulate auxin homeostasis and cell expansion in *Arabidopsis*. *Planta* 226: 839–851.

Table S1. Primer sequences used in this study

Primers	Primer Sequence 5'-3'
generating entry clone for coding sequence	
SAUR41-Up	CACCATGAAGCATCTCATCCGC
SAUR41-Dn1	CTACTCTGTAGTTTCAGGTATC (for overexpression)
SAUR41-Dn2	CTCTGTAGTTTCAGGTATC (for protein fusion)
IAA2-Up	CACCATGGCGTACGAGAAAGTC
IAA2-P65S-Dn	AGATCTCACTGGTG**A**CCAAC
IAA2-P65S-Up	AGATCTTCCCGTAAGAACAA
IAA2-Dn	TCATAAGGAAGAGTCTAGAG
generating entry clone for promoter region	
SAUR41P-Up	CACCTAGTTAGCGTATACATGAGA
SAUR41P-Dn	GGTTTAAACTAATGATAGA
WOX5P-Up	CACCTTGGACCATTTTCGTCTTGCTTA
WOX5P-Dn	TCAACTGTTTTACGTTTTAGGGCCT
PLT2P-Up	CACCGTTATTCCTTTTTTCTTCCGTCTC
PLT2P-Dn	CCCTTTTCTTGGAATCAAAGCTTA
ACR4P-Up	CACCTTGATTGATTTTACATCTGCTCC
ACR4P-Dn	CACACGCTTCTTAGTTACTGTCTTC
generating destination clone for tissue-specific expression	
ccdB-Up	GGACTAGTCCACCACTTTGTACAAGAAAGCTGAAC
ccdB-Dn	CCAAGCTTGG ACAAGTTTGTACAAAAAAGCTGAAC

Supplemental Information

Supplemental Experimental Procedures

GFP lines

The GFP lines shown Figure 2 and S1 are the following (except for H1-GFP lines described below): HTR12/CENH3 lines: pHTR12::HTR12-GFP (Fang and Spector, 2005), pCENH3::GFP-CENH3 (Ravi et al., 2011). TFL2/LHP1 line: pLHP1::LHP1-GFP (Nakahigashi et al., 2005). pHTR5::HTR5-GFP, pHTR8::HTR8-CFP (Ingouff et al., 2010), HTA11/H2A.Z: pHTA11::HTA11-GFP (Kumar and Wigge, 2010).

Generation of GFP and RFP -tagged H1 variants

To generate promH1.1::H1.1-EGFP vector, we amplified the promoter (1982 bp) with coding sequence of H1.1 (except the termination codon) with the following primers [5'-GCGTCGACTCATTCTGTGATAGGGATGG-3'; 5'-GCGGATCCCTTCTTAACCCTAGAAGAAGC-3'] and subcloned the fragment in the pCambia1390 vector (carrying a 35S:Hygromycin resistance for in planta selection) using the SalI and BamHI restriction sites introduced in the forward and reverse primers, respectively (underlined), giving pCambia1390/promH1.1::H1.1 vector. The EGFP sequence was subcloned with the BamHI and EcoRI restriction sites into pCambia1390/promH1.1::H1.1 vector, giving pCambia1390/promH1.1::H1.1-EGFP vector. The termination sequence of H1.1 (873 bp) was amplified with the following primers [5'-GCGAATTCTGAAGTTAGGGTTTGTAGGTAG-3'; 5'-GCCCATGGGCTCTCCAAAGGTTAGTTTT-3'] and subcloned in pCambia1390/promH1.1::H1.1-EGFP vector using the EcoRI and NcoI restriction sites introduced in the forward and reverse primers, respectively, giving the final vector promH1.1::H1.1-EGFP.

To generate promH1.2::H1.2-EGFP vector, we amplified the promoter (2191 bp) with coding sequence of H1.2 (except the termination codon) with the following primers [5'-GCCTGCAGTTCGTAAATGGTAGATGGAAAACA-3'; 5'-GCGTCGACCTTCTTAGCCTTCCTAGTCGAA-3'] and subcloned the fragment in the pCambia1390 vector using the PstI and SalI restriction sites introduced in the forward and reverse primers, respectively, giving pCambia1390/promH1.2::H1.2 vector. By using the BamHI and EcoRI restriction sites the EGFP sequence was subcloned in pCambia1390/promH1.2::H1.2 vector, giving pCambia1390/promH1.2::H1.2-EGFP vector. The termination sequence of H1.2 (1187 bp) was amplified with the following primers [5'-GCGAATTCTGAAGAAGATTGGTTTAGGAT-3'; 5'-GCGCTAGCTTCGAGGAATTAGGTGAGAA-3'] and subcloned in pCambia1390/promH1.2::H1.2-EGFP vector using the EcoRI and NheI restriction sites introduced in the forward and reverse primers, respectively, giving the final vector promH1.2::H1.2-EGFP.

To verify that the expression pattern observed was not influenced by the long-range effect of the 35S enhancer, we generated new fusions in a vector carrying a NOS::BAR selection cassette for BASTA selection *in planta*. The NOS::BAR selection cassettewas obtained from pGreenII0229 plasmid (Bendel-Stenzel et al., 1998) using the EcoRV restriction sites and inserted into XmnI-

digested plasmid pCambia0390, giving pCambia0390/NOS::BAR plasmid. Then the whole promH1.1::H1.1-EGFP fragment from pCambia1390 (35S::HYG) was subcloned in pCambia0390 (NOS::BAR) using the AscI and NcoI restriction sites and similarly promH1.2::H1.2-EGFP fragment was subcloned using the AscI and NheI restriction sites. An additional promH1.1::H1.1-RFP vector was generated by swapping the EGFP wit the RFP-T (Maheshwari, 1950) using EcoRI and BamHI restriction sites.

To generate the promH1.1::EGFP-H1.1 vector, we amplified the promoter (2006 bp) with the following primers [5'-GCGTCGACTGTTGGGGAAGATAATCCAA-3'; 5'-GCGGATCCCATCGTCTTCTGAACTTAAGATC-3'] and subcloned the fragment in the pCAMBIA1390 vector using the SalI and BamHI restriction sites introduced in the FWD and REV primers, respectively, giving pCambia1390/promH1.1 vector. The EGFP sequence was subcloned into pCambia1390/promH1.1 vector by using the BamHI and EcoRI restriction sites, giving pCambia1390/promH1.1::EGFP vector. The coding sequence of H1.1 (except the start codon) with its termination sequence (1510 bp) was amplified with the following primers [5'-GCGAATTCTCAGAGGTGGAAATAGAGAACG-3'; 5'-GCCCATGGTGGTAAGCCATCCACAAACA-3'] and subcloned in pCambia1390/promH1.1::EGFP vector using the EcoRI and NcoI restriction sites introduced in the forward and reverse primers, respectively, giving the final vector promH1.1::EGFP-H1.1.

To generate the promH1.1::RFP-H1.1 vector, the GFP sequence from the promH1.1::EGFP-H1.1 vector was replaced using the RFP-T sequence amplified from the pRFP-T_tag plasmid (Shaner et al., 2008) using the following primers [5'-TTAGGATCCGTGTCTAAGGGCGAAGAGC-3'; 5'-ATTAGAATTCCTTGTACAGCTCGTCCATGCC-3'] and subcloned with the respective BamHI and EcoRI restriction sites.

To generate promH1.2::EGFP-H1.2 vector, we amplified the promoter (2191 bp) with the following primers [5'- GCCTGCAGGCAGTTCGTAAATGGTAGATGG-3'; 5'-GCGTCGACCATCTTCTTCTCTCTCAGAAACTG-3'] and subcloned the fragment in the pCAMBIA1390 vector using the PstI and SalI restriction sites introduced in the FWD and REV primers, respectively, giving pCambia1390/promH1.2 vector. The EGFP sequence was subcloned into pCambia1390/promH1.2 vectorusing the BamHI and EcoRI restriction sites, giving pCambia1390/promH1.2::EGFP vector. The coding sequence of H1.2 (except the start codon) with its termination sequence (1044 bp) was amplified with the following primers [5'-GCCAATTGTCTATAGAGGAAGAAAACGTTCC-3'; 5'-GCGCTAGCTCACAAGAGGTTTGCGAATG-3'], digested with the MunI and NheI restriction sites introduced in the FWD and REV primers, respectively and inserted into EcoRI-NheI-pCambia1390/promH1.2::EGFP vector, giving the final vector promH1.2::EGFP-H1.2.

The constructs were introduced into Agrobacterium tumefaciens (GV3101) which were then used to transform Arabidopsis (Col-0) plants with the floral dip method(Seisenberger et al., 2012). Seeds of transformed plants were selected on ½ MS agar plates containing 30 mg/l hygromycin or were grown in soil and selected by spraying with Basta solution (0.05 mg/ml). Plants were selected for single insertion lines and homozygous lines from T3 or T4 generation were eventually used for analysis. Expression of EGFP-tagged H1 was confirmed by fluorescence analysis

Immunostaining in whole-mount ovule primordia

Immunostaining of active polII was done as described in Autran et al (2011). Below is described the method for immunostaining of H3 and H3 modifications as shown in Figure 3, 5.
Young carpels were collected and fixed in freshly made BVO fixation buffer (2mM EGTA pH7.5, 1% Formaldehyde, 10% DMSO, and 0.1%Tween in 1×PBS) at room temperature for 30min. After fixation, the carpels were kept in PBT (1x PBS with 0.1% tween-20) on ice. The ovules were then dissected and embedded in 5% acrylamide + 1.2% APS (ammonium persulfate) + 1.2% NaPS (sodium sulfite) in 1× PBS, and covered with a 20mm x 20mm coverslip. The coverslip was removed after 60min using a razor blade. All subsequent steps are made in coplin jars, under gentle shaking, unless indicated. The samples were treated as follows: 5min methanol, 5min ethanol, 30min ethanol:xylene (1:1), 5min ethanol, 5min methanol, and 15min methanol:PBT(1:1)+ 2.5% Formaldehyde. Following 2×10 min PBT washes, the samples were incubated with an enzyme mix for cell wall digest [0.5% (w/v) cellulose, 1% (w/v) driselase, 0.5% (w/v) pectolyase in PBS], 100µL was applied per slide with a coverslip, for 1-2hrs at 37℃ in a moist-chamber (the incubation time has to be determined empirically for each batch of enzyme mix). After 2×5min PBT washes, the slides were incubated with RNaseA 100µg/ml in PBS + 1%Tween-20 at 37℃ for 1hr. The slide were then washed with 2×5 min PBT and fixed with PBT-F (PBT+ formaldehyde 2.5% (v/v) for 20min. Following 10min PBT wash, the samples were permeabilized in PBS + 2% Tween-20 at 4℃ for 2hrs. After 2×5 min PBT washes, the samples were incubated with 100µL primary antibody dilution (Table S6) in PBS + 0.2% Tween-20 at 4℃ for 16-21hrs in a moist chamber. The slide was then rinsed in PBT for 2-4 hrs and incubated with the secondary antibody 1:200 in PBS + 0.2% Tween-20 at 4℃ for 2days as before. Following 1hr PBT wash, the samples were counterstained with Propidium Iodide at 10µg/ml in PBS for 15min, washed in PBS for 10min and mounted in Prolong Gold (Invitrogen) supplemented with 10µg/ml PI.

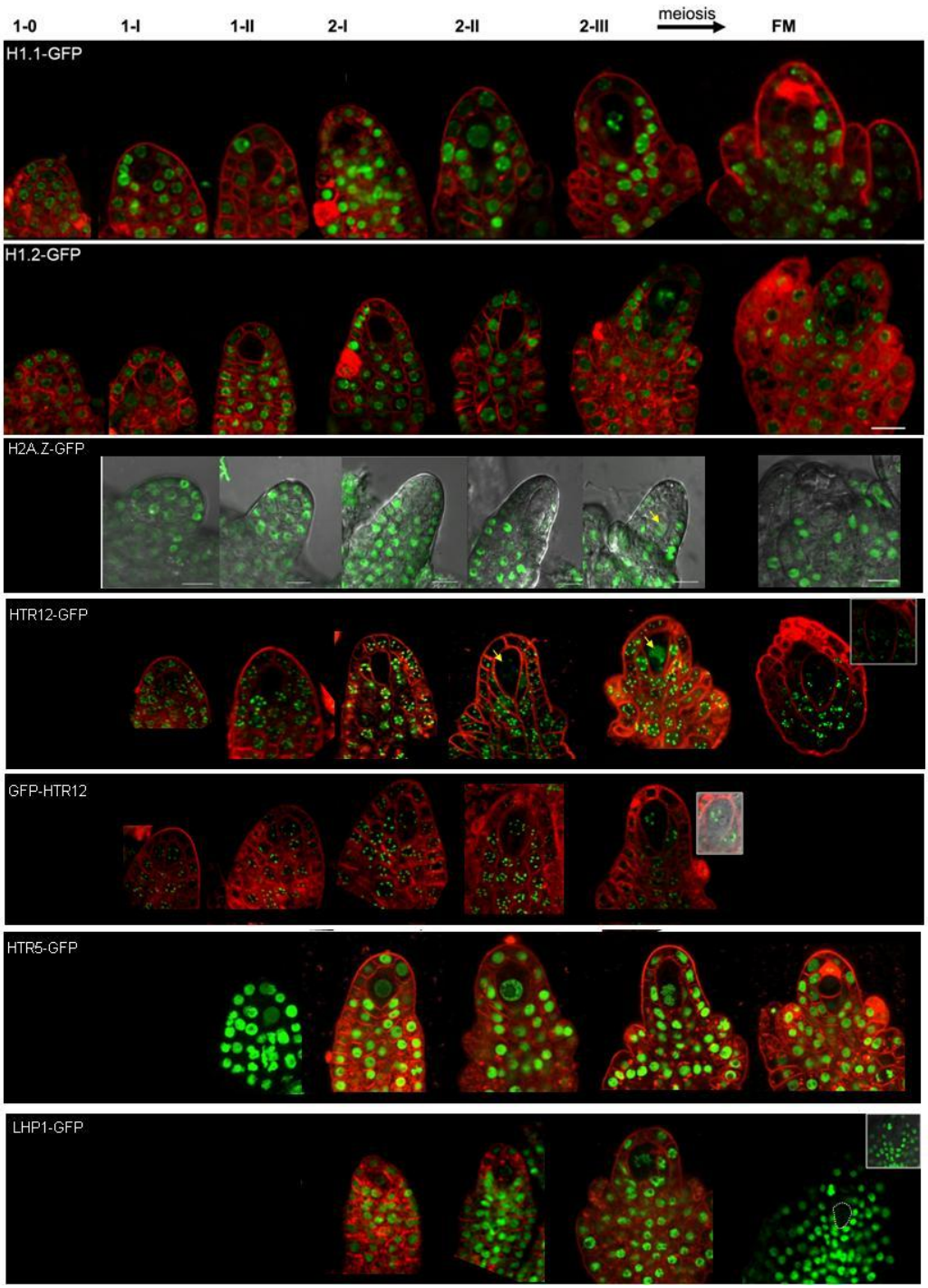

Figure S1. Developmental dynamics of GFP-tagged histone variants and LHP1 during MMC differentiation

The expression dynamics of GFP-tagged histone variants is shown along the stages of ovule primordia development 1-0 until 2-III (onset Prophase I) and in the functional megaspore

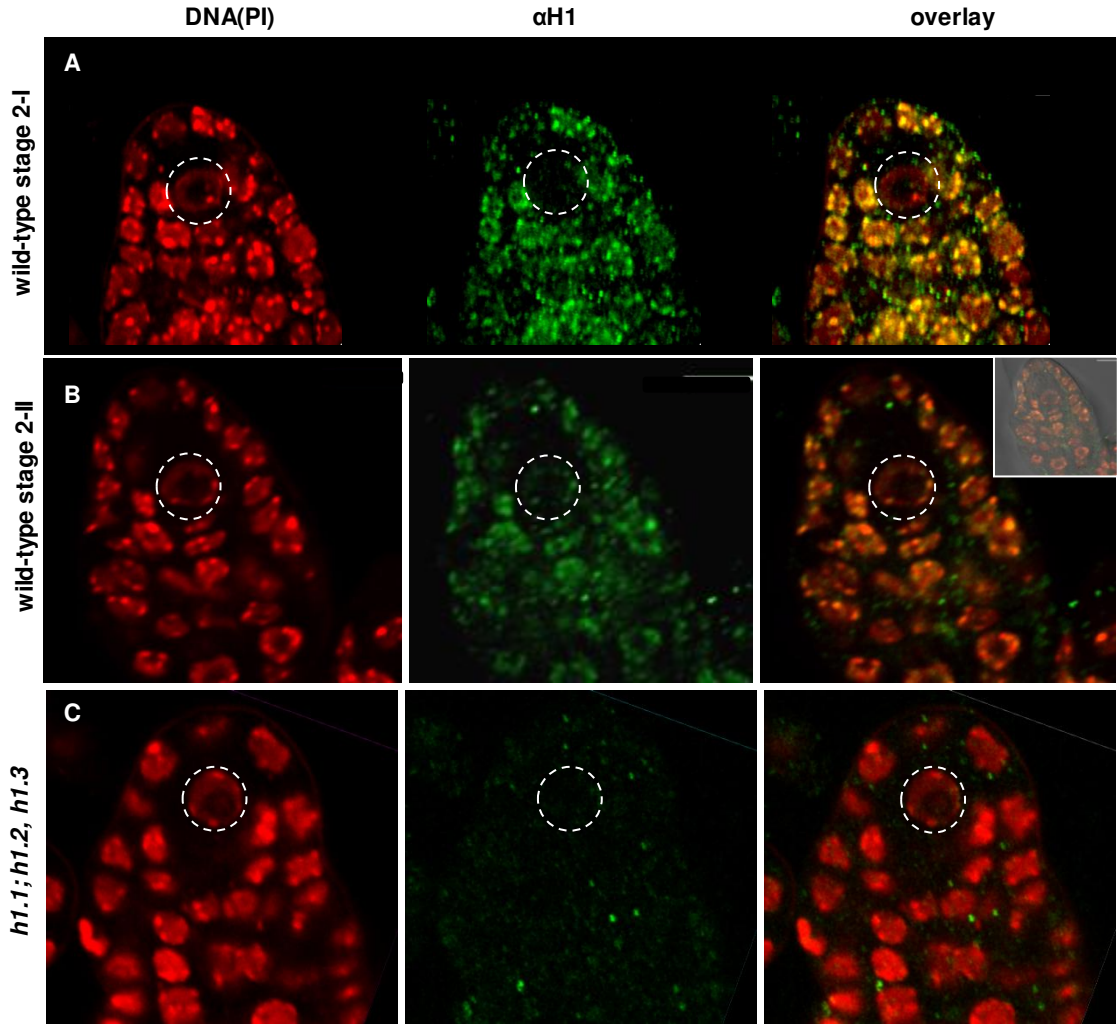

Figure S2. H1 Immunostaining with a novel, plant specific antibody confirms H1 depletion in MMCs

(A) H1 is depleted in MMC (dashed line) at stage 2-I, as revealed by whole-mount immunostaining in wild type ovule primordia.
(B) Reloading of H1 in MMC at stage 2-II in wild-type ovule primordia (faint signals).
(C) H1 is undetectable in the ovule primordia of *h1.1; h1.2,h1.3* triple mutant. The green signals arise from non-specific secondary antibody binding.

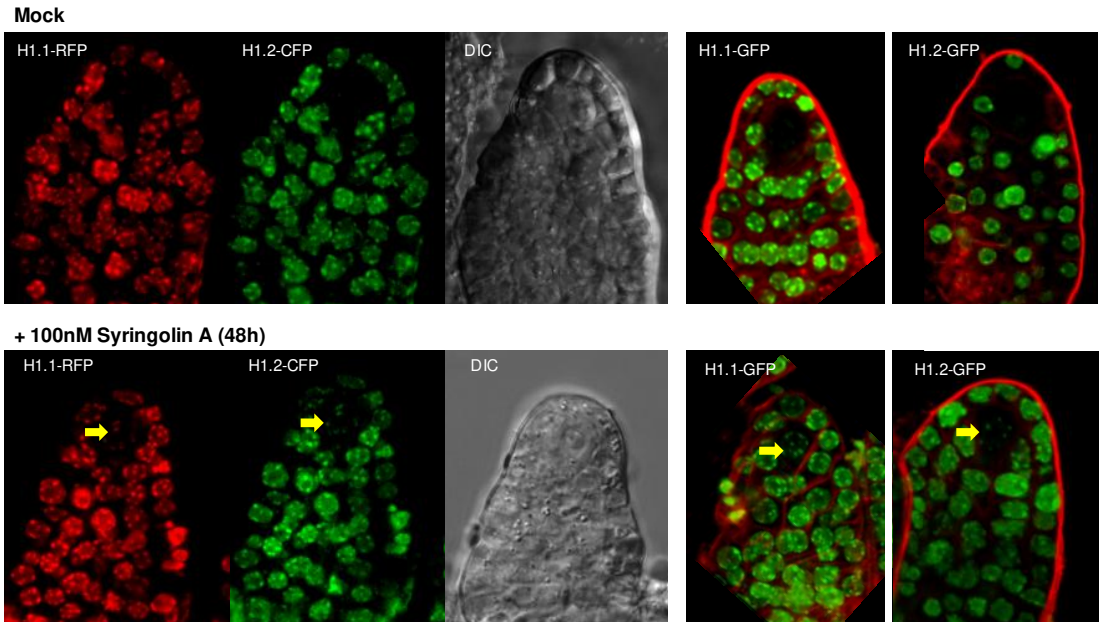

Figure S3. GFP-tagged H1 dynamics is influenced by an inhibitor of the proteasome
Whole inflorescences were incubated in water (Mock) or water containing 100nM Syringolin A (Groll et al., 2008) for 48h before imaging (CSLM, green: GFP, red: FM4-64, grey: DIC). Yellow arrows point to the MMCs where H1 signals clearly remained detectable.

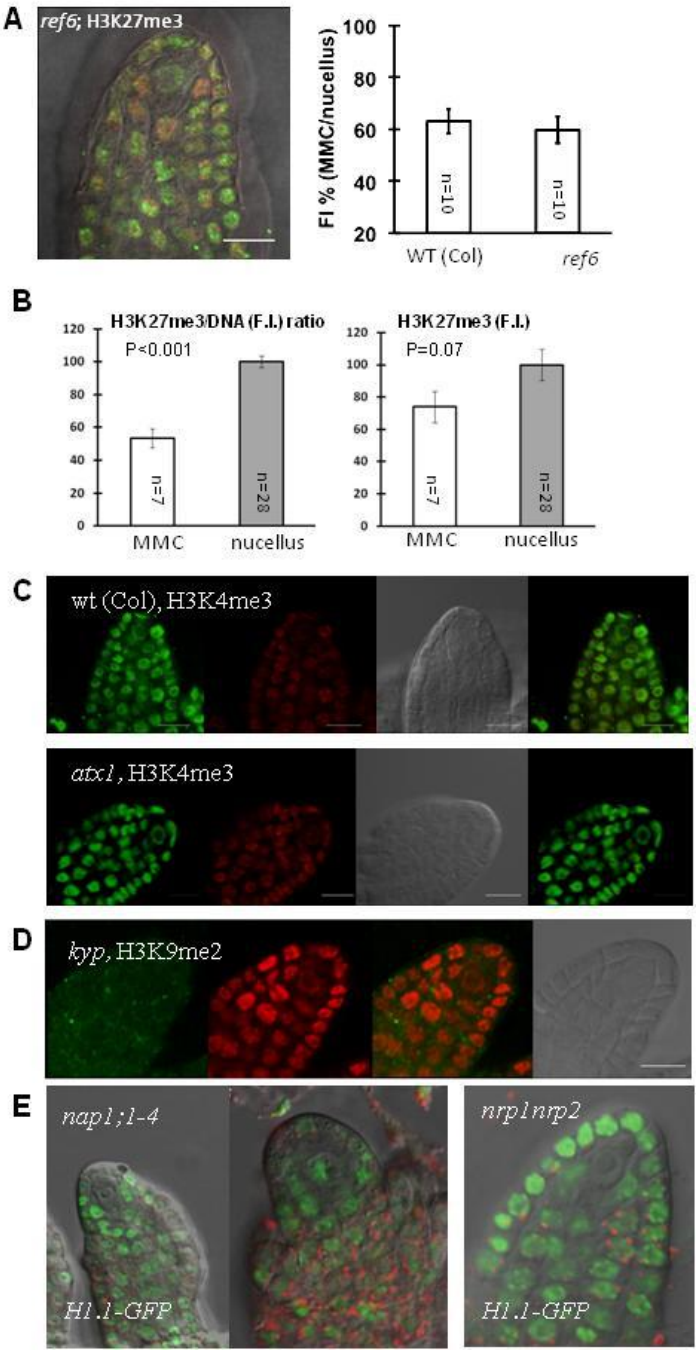

Figure S4. Selected candidate modifiers do not contribute to chromatin dynamics in the MMC

A. H3K27me3 levels in the MMCs relative to the nucellus are stable in the *ref6* mutant (Lu et al., 2011), compared to that in wild type. Representative image is shown for the overlay of antibody (green), DNA (propidium iodide, red) and transmission light (DIC, grey). Detailed quantification is provided in Table S6. **B**. Decreased levels of H3K27me3 in wild-type MMCs relative to the nucellus is visible both after normalization against the DNA content (left graph as in Figure 3) or in absolute values of immunostaining signals (right graph) suggesting both a replication-coupled

passive dilution and a probable active demethylation process **C**. H3K4me3 levels in MMCs which lack ATX1 activity (atx1-1 (Alvarez-Venegas et al., 2003)) are not increased, compared to that in col. Representative images show the antibody (green), DNA (propidium iodide, red), transmission light (DIC, grey), and overlay of antibody (green) with DNA (red). **C.** H3K9me2 immunosignals are drastically decreased in *kyp-2* (Lindroth et al., 2004) ovule primordia both in the MMC and nucellus, yet MMC and gametophyte differentiation proceeds normally. **D.** H1.1-GFP is normally depleted in mutant MMCs of the quadruple mutant lacking NAP1;1-4 activity (Liu et al., 2009) or the double mutant lackig NRP1;NRP2 activity (Zhu et al., 2006) and reloaded at prophase I. Scale bar: 10μm.

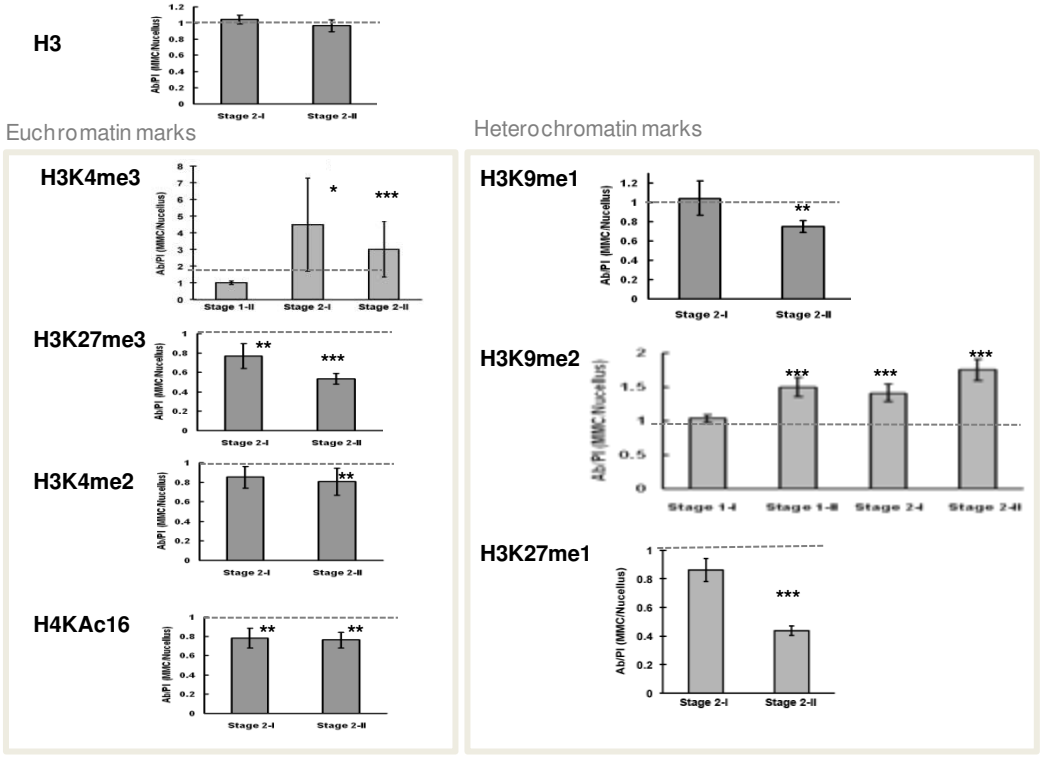

Figure S5. Developmental dynamics of changes in chromatin modification levels in MMCs relative to nucellus' cells.

Graphs represent a MMC/nucellus ratio of relative chromatin modification levels (measured as antibody signal intensity/DNA signal intensity). The stars indicate the level of significance in a Welch'st-test done as for Figure 3 (MMC vs nucellus). Most euchromatin marks are significantly altered in MMC only at stage 2-I or 2-II, while H3K9me2 enrichement is typically measured at stage 1-II.

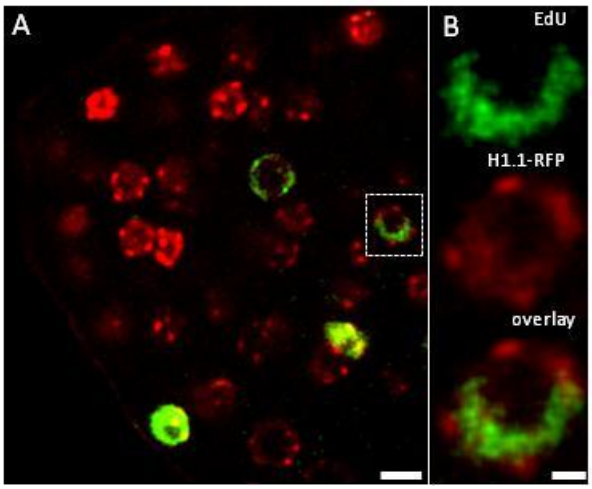

Figure S6. H1.1 is a stable chromatin component during mitotic S-phase

In mitotically active zones of the seedling' root, H1.1::RFP (red) remains incorporated in the chromatin of nuclei engaged in the S-phase as revealed by EdU incorporation (green). (A) confocal section of a root tip (B) close-up on one S-phase nucleus with EdU incorporation in euchromatin. After 2hrs pulse, nuclei showed EdU incorporation in euchromatin only, heterochromatin only, or both. 21/21 nuclei with EdU incorporation in euchromatin only as in (B) showed H1.1-RFP signals. Scale Bar: 10µm.

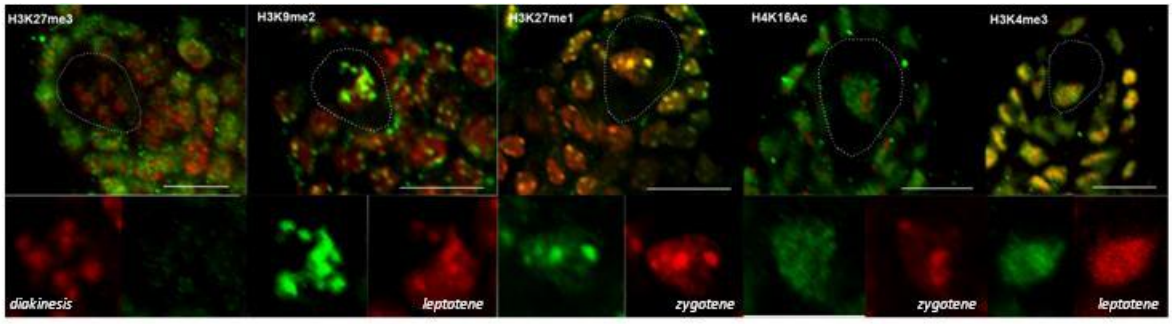

Figure S7. Meiosis entails a novel dynamics in histone modifications

During meiosis I, the dynamic trends for H3K27me3 and H3K9me2 seen during MMC differentiation become more pronounced with a near-loss and high enrichment of immunosignals, respectively, while the trend seems to reverse for H3K27me1 with apparent higher signals than in differentiated MMCs (Figure 3). H3K4me3 and H4K16Ac are well detected, yet the rapid evolution of meiotic chromosomes does not allow precise quantifications for those marks. The upper panel shows immunostaining signals of the indicated histone modifications in primordia tips at stage 2-III (dotted contours: MMC in prophase I). Scale Bar: 10 µm. Lower panel: close-up on MMC nuclei . Red, Propidium iodide, green, antibody signal.

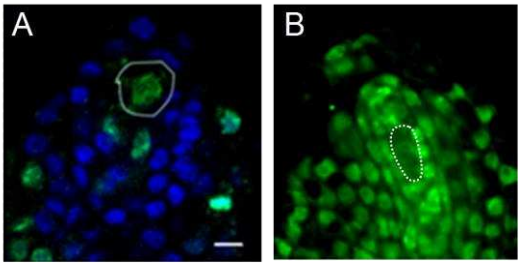

Figure S8. Replication and transcriptional status in the FM

(A) The selected product of female meiosis, the functional megaspore, rapidly engages in mitosis for gametophytic development, with EdU incorporation. (B) Active PolII is detected at low and variable levels by immunodetection, probably due to the rapid transition into the gametophytic stage

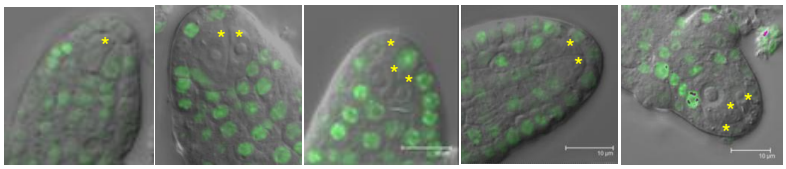

	Wild-type	ago9-3/+	ago9-4/+	rdr6-11/+	sgs3-11/+
Occurence phenotype	~ 5%	26%	31.5%	30.3 %	26.3%
Class A	5%	-	-	-	-
Class B	-	26%	21%	15%	23.6%
Class C	-	-	11.5%	15%	2.7%
n	100	30	57	33	38

Figure S9. Loss of H1.1/GFP is a hallmark of multiple MMCs in *ago9*, *rdr6* and *sgs3* mutants

The number of primordia showing more than one enlarged cell (MMC and MMC-like) was scored in wild-type or mutant primordia with the indicated genotypes. The expression pattern of H1.1-GFP in these MMC and MMC-like cells was scored: class A, primordia with only one H1.1-GFP negative cell (MMC); class B, primordia where all MMC‘s are H1.1-GFP negative; class C: primordia with one H1.1-GFP negative MMC and reduced H1.1-GFP levels in the other(s)

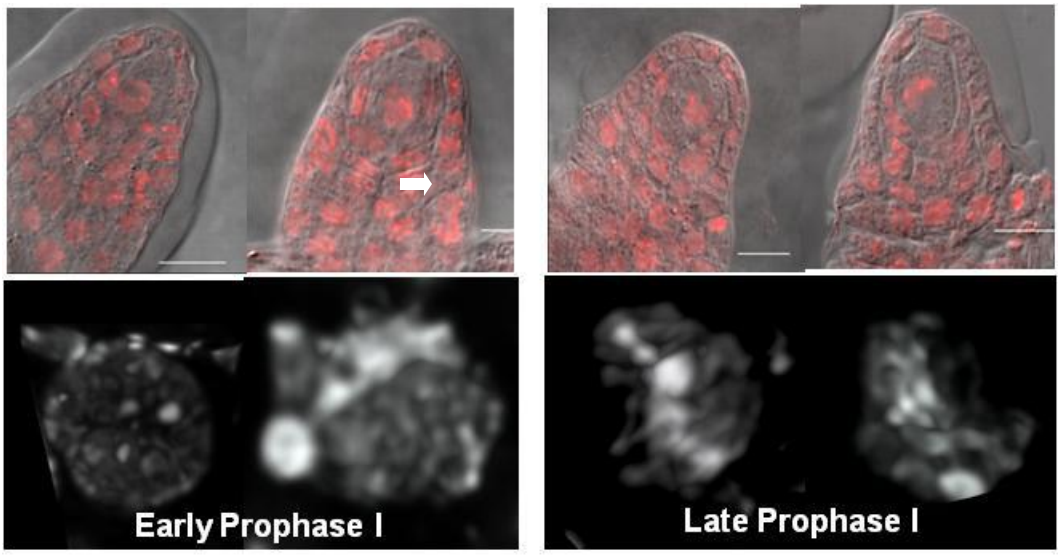

Figure S10. Female meiosis in *sdg2*

Ovule primordia lacking SDG2 activity (Berr et al., 2010) undergo proper meiosis as assessed by clearing and DNA staining and despite reduced H3K4me3 levels compared to that in wild type (Figure 6, this Figure). The lower panel shows deconvolved, 3D-reconstruction of MMC nuclei at different stages of prophase I corresponding to the primordia on the upper panel. Chromosome condensation is initiated during early prophase I (pre-leptotene/leptotene), and becomes more visible at the late prophase during which bivalent are formed. Images in the lower panel were deconvolved using Huygens (SVI).

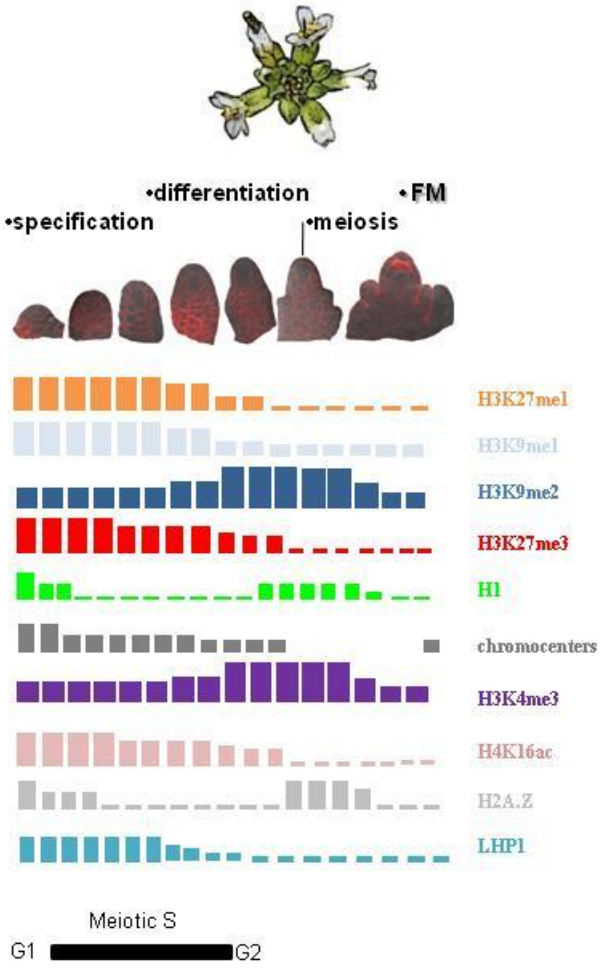

Figure S11. Chromatin reprogramming in plant MMCs

Table S1. Detailed quantification of nuclear size and heterochromatin content in MMC and nucellus cells during ovule primordia development

Nuclear Size (μm^3)	**MMC**			**nucellus**			
stage	**average**	**s.d.**	**n**	**average**	**s.d.**	**n**	
Stage 1-II	44.2	± 16.8	(n=10)	36.698	± 11.46	(n=46)	P=0.206
Stage 2-I	76.127	± 33.66	(n=13)	43.072	± 15.4	(n=63)	P=0.0042
Stage 2-II	90.869	± 25.2	(n=10)	47.382	± 13.92	(n=50)	P=0.0003
RHF	**MMC**			**nucellus**			
stage	**average**	**s.d.**	**n**	**average**	**s.d.**	**n**	
Stage 1-I	24.87	± 6.06	(n=10)	31.517	± 3.58	(n=30)	P=0.007
Stage 1-II	21.24	± 6.08	(n=10)	31.85	± 4.5	(n=30)	P=0.0002
Stage 2-I	18.38	± 7.84	(n=10)	31.38	± 4.44	(n=30)	P=0.0004
Stage 2-II	10.51	± 4.4	(n=10)	32.3	± 5.7	(n=30)	P<0.0001

RHF: Relative Heterochromatin Fraction calculated as a % ratio of fluorescence intensity (propidium iodide) in heterochromatic foci over intensity in the whole nucleus. s.d., standard deviation (note that the graphs show the standard error to mean= s.d/√n). P-value: Welch'st-test (2 tails)

Table S2: Detailed quantifications of relative nuclear immunostaining in MMC and nucellus cells of primordia at stage 2-II

(a) Antibody signal over propidium iodide signal, relative to the nucellus

	MMC			nucellus			
	%	s.d	n	%	s.d	n	
H3	102.51	± 33.48	(n= 9)	100	± 36.46	(n= 43)	P= 0.84
H3K9me1	73.54	± 14.23	(n= 11)	100	± 20.74	(n= 51)	P= 3.57E-06
H3K9me2	171.44	± 47.72	(n= 11)	100	± 31.21	(n= 45)	P= 1.69E-05
H3K27me1	43.57	± 8.25	(n= 6)	100	± 20.23	(n= 26)	P= 6.70E-12
H3K27me3	53.51	± 15.16	(n= 7)	100	± 19.02	(n= 28)	P= 7.58E-08
H3K4me2	74.56	± 17.28	(n= 19)	100	± 28.88	(n= 88)	P= 1.74E-06
H3K4me3	270.17	± 263.77	(n= 12)	100	± 24.30	(n= 60)	P= 0.03
H4KAc16	74.18	± 10.63	(n= 10)	100	± 17.30	(n= 46)	P= 1.10E-07
RNA PolII	61	± 23.00	(n= 7)	100	± 19.00	(n= 25)	P= 2.81E-04

(b) Antibody signal over propidium iodide signal- absolute ratios in the nucellus

	nucellus		
	Ab/PI	s.d	n
H3	0.98664	± 0.36	(n= 43)
H3K9me1	0.72185	± 0.15	(n= 51)
H3K9me2	0.53354	± 0.17	(n= 45)
H3K27me1	0.91792	± 0.19	(n= 26)
H3K27me3	0.83598	± 0.16	(n= 28)
H3K4me2	0.75001	± 0.22	(n= 88)
H3K4me3	0.71775	± 0.17	(n= 60)
H4KAc16	0.81903	± 0.14	(n= 46)

The relative immunostaining signals are calculated as fluorescence intensity ratios of Antibody (Ab) signals over Propidium Iodide (PI) signals. (a) The ratios in nucellus cells are averaged across n samples and set as 100%. Ab/PI ratio in the MMC relative to that in nucellus cells. (b) absolute ratios in nucellus cells. s.d., standard deviation. (note that the graphs show the standard error to mean= s.d/√n). P-value: Welch's t-test (2 tails)

Table S3: Detailed quantifications of relative nuclear immunostaining in MMC and nucellus cells of primordia at stage 1-II and 2-I

A. stage 1-II

(a) Antibody signal over propidium iodide signal, relative to the nucellus

	MMC			nucellus			
	%	**s.d.**	**n**	**%**	**s.d.**	**n**	
H3K9me2	150	± 36.14	(n=8)	100	± 22.43	(n=35)	P= 0.0056

(b) Antibody signal over propidium iodide signal- absolute ratios in the nucellus

	Ab/PI	**s.d.**	**n**
H3K9me2	0.58919	± 0.59	(n=35)

B. stage 2-I

(a) Antibody signal over propidium iodide signal, relative to the nucellus

	MMC			nucellus			
	%	**s.d.**	**n**	**%**	**s.d.**	**n**	
H3	95.45	± 13.17	(n= 10)	100	± 19.71	(n= 48)	P= 0.371
H3K9me1	99.37	± 31.34	(n= 10)	100	± 71.85	(n= 48)	P= 0.965
H3K9me2	138.91	± 30.08	(n= 10)	100	± 23.65	(n= 44)	P= 0.00035
H3K27me3	85.56	± 20.26	(n= 9)	100	± 21.12	(n= 37)	P= 0.064
H3K4me2	86.49	± 32.27	(n= 9)	100	± 25.30	(n= 37)	P= 0.248
H3K4me3	338.32	± 364.38	(n= 6)	100	± 32.22	(n= 29)	P= 0.119
H4KAc16	74.34	± 17.87	(n= 12)	100	± 30.25	(n= 58)	P= 0.000194

(b) Antibody signal over propidium iodide signal- absolute ratios in the nucellus

	Ab/PI	**s.d.**	**n**
H3	0.621242	± 0.06	(n=34)
H3K9me1	0.49682	± 0.18	(n=48)
H3K9me2	0.555674	± 0.07	(n=44)
H3K27me3	0.928	± 0.10	(n=37)
H3K4me2	0.640063	± 0.08	(n=37)
H3K4me3	0.666477	± 0.11	(n=29)
H4KAc16	0.802813	± 0.12	(n=58)

legend: as for Table S2

Table S4. Quantifications of DNA content increase and EdU incorporation in MMCs

(a) Quantification of DNA content (PI fluorescence intensity) in MMC relative to the averaged content in L1-1, L1-0 and L1-2 nucellus cells during ovule primordia development

stage	average	s.d.	n
1-I	1.01	± 0.12	10
1-II	1.24	± 0.32	10
2-I	1.59	± 0.37	10
2-II	1.96	± 0.40	10

s.d., standard deviation. (note that the graphs show the standard error to mean= s.d/√n).

(b) Quantification of MMCs with distinct EdU incorporation patterns (2h pulse)

EdU signal	Stages 1-I + 1-II	Stage 2-II
Euchromatin only (1)	1	16
Heterochromatin only (2)	10	1
Euchromatin and heterochromatin	1	-
Total	**12**	**17**

Table S5: Detailed quantifications of relative nuclear immunostaining in functional megaspore and nucellus cells

(a) Antibody signal over propidium iodide signal, relative to the nucellus

	MMC			nucellus			
	%	**s.d.**	**n**	**%**	**s.d.**	**n**	
H3	101.24	± 17.40	(n= 6)	100	± 20.18	(n= 24)	P= 0.881
H3K9me1	77.72	± 29.65	(n= 10)	100	± 45.06	(n= 50)	P= 0.054
H3K9me2	76.13	± 17.86	(n= 6)	100	± 28.69	(n= 25)	P= 0.015
H3K27me1	66.96	± 15.59	(n= 7)	100	± 25.21	(n= 32)	P= 7.12E-05
H3K4me2	50.34	± 18.05	(n= 11)	100	± 20.62	(n= 54)	P= 2.29E-11
H3K4me3	64.74	± 10.40	(n= 12)	100	± 15.19	(n= 51)	P= 8.84E-14
H4KAc16	56.96	± 13.66	(n= 12)	100	± 35.57	(n= 58)	P= 1.19E-09

(b) Antibody signal over propidium iodide signal- absolute ratios in the nucellus

	Ab/PI	**s.d.**	**n**
H3	0.699	± 0.14	(n=24)
H3K9me1	0.673	± 0.30	(n=50)
H3K9me2	0.663	± 0.19	(n=24)
H3K27me1	0.982	± 0.25	(n=32)
H3K4me2	1.157	± 0.24	(n=54)
H3K4me3	0.920	± 0.14	(n=51)
H4KAc16	1.330	± 0.47	(n=58)

s.d., standard deviation. (note that the graphs show the standard error to mean= s.d/√n).

Table S6: Detailed quantifications of relative nuclear immunostaining in *ago9-4* and *sdg2* mutant megaspore mother cells relative to nucellus cells

General legend: Ab/Pi, Fluorescence intensity sum of the antibody (Ab) relative to the DNA (PI) signals.s.d., standard deviation. (note that the graphs show the standard error to mean= s.d/√n). n, number of cells quantified, P-value: Welch's t-test (2 tails)

A. H3K27me1 relative levels in *ago9-4* MMCs

(a) Antibody signal over propidium iodide signal, relative to the nucellus in *ago9-4/ago9-4* mutant

	Ab/PI	**s.d.**	**n**	
mmc1	38.43	±11.61	(n= 5)	P= 0.7
mmc2	39.65	±8.31	(n= 5)	
nucellus	100	±30.24	(n= 24)	

In each primordia, the mmc with the highest intensity was called mmc1, while the one with the lowest was called mmc2. The distribution of fluorescence intensity in individual mmc's (white and black dot) per ovule primordia is as follows:

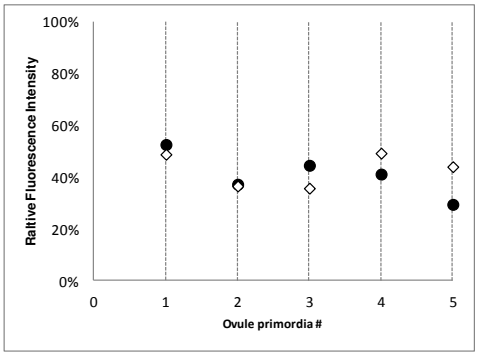

(b) Antibody signal over propidium iodide signal- absolute ratios in the nucellus*ago9-4/ago9-4* mutant

	Ab/PI	**s.d.**	**n**
nucellus	0.997043	± 0.3016	(n= 24)

B. H3K27me3 relative levels in *ago9-4* MMCs

(a) Antibody signal over propidium iodide signal, relative to the nucellus in *ago9-4/ago9-4* mutant

	Ab/PI	**s.d.**	**n**	
mmc1	62.82	±38.01	(n= 10)	P= 0.38
mmc2	48.63	±32.7	(n= 10)	
nucellus	100	±48.25	(n= 50)	

In each primordia, the mmc with the highest intensity was called mmc1, while the one with the lowest was called mmc2. The distribution of fluorescence intensity in individual mmc's (white and

black dot) per ovule primordia is as follows:

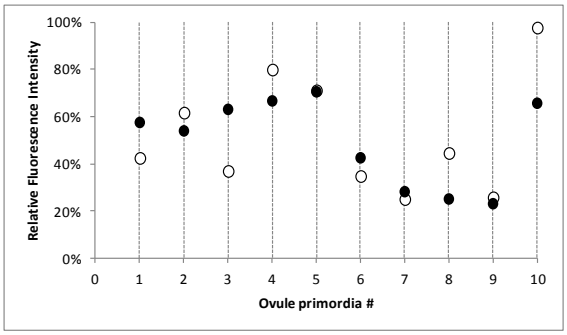

(b) Antibody signal over propidium iodide signal- absolute ratios in the nucellus of the *ago9-4/ago9-4* mutant

	Ab/PI	**s.d.**	**n**
nucellus	1.9505	± 0.89	(n= 50)

C. H3K4me3 relative levels in *sdg2 vs* wild-type (Col) MMCs

(a) Antibody signal over propidium iodide signal, relative to the nucellus in *sdg2/sdg2* mutant

MMC			**nucellus**			
%	**s.d.**	**n**	**%**	**s.d.**	**n**	
163.29	± 48.59	(n= 12)	100	± 54.16	(n= 59)	P= 0.0001

(b) Antibody signal over propidium iodide signal- absolute ratios in the nucellus of the *sdg2/sdg2* mutant

Ab/PI	**s.d.**	**n**
1.26	± 0.68	(n=59)

(c) Comparison of H3K4me3 relative levels (MMC/nucellus) in *sdg2* and wild-type (col) primordia

	average	**s.d.**	**n**	
Col	270.17	131.89	12	P= 0.0152
sdg2	163.29	48.59	12	

D. H3K27me3 relative levels in *ref6 vs* wild-type (Col) MMCs

(a) Antibody signal over propidium iodide signal, relative to the nucellus of the *ref6/ref6* mutant

MMC			**nucellus**			
%	**s.d.**	**n**	**%**	**s.d.**	**n**	
59.77	± 16.3	(n= 10)	100	± 17.15	(n= 50)	P= 0.004

(b) Antibody signal over propidium iodide signal- absolute ratios in the nucellus of the *ref6/ref6* mutant

Ab/PI	**s.d.**	**n**
0.79	± 0.14	(n=50)

(c) Comparison of H3K4me3 relative levels (MMC/nucellus) in *ref6* and wild-type (col) primordia

	average	**s.d.**	**n**
Col	63.16	30.8	10
ref6	59.77	32.6	10

legend: as for Table S2

Table S7. List of antibodies and test of immunostaining signals' reliability in whole-mount ovule primordia in serial dilutions

				Dilution for immunostaining			
Antibody Target	**Provider**	**Cat#**	**(concentration)**	**1/1000**	**1/500**	**1/200**	**1/100**
H3	Abcam	ab1791	(1mg/ml)	-	-	+	nd
H3K27me1	Upstate	07-448	(1mg/ml)	nd	-	+	nd
H3K27me3	Upstate		(1mg/ml)	-	-	+	+
H3K4me2	Abcam	ab32356	(0.04mg/ml)	-	-	+	nd
H3K4me3	Upstate	07-473	(0.1-0.5 mg/ml)	+	+	+	+
H3K9me1	Upstate	07-450	(1mg/ml)	nd	-	+	nd
H3K9me2	Upstate	07-441	(1mg/ml)	nd	-	+	nd
H4K16Ac	Millipore	07-329	(1mg/ml)	-	-	+	nd
H1	Agrisera	AS111801	(1mg/ml)	nd	nd	+	nd

Immunostaining results on whole-mount primordia: +, stable signal. -: unstable signals (not reproducible across replicates). Grey: dilutions used for the quantifications in Figure 3, 5, 6, S2, Table S2, S3, S5, S6.

References related to Supplemental Information

Alvarez-Venegas, R., Pien, S., Sadder, M., Witmer, X., Grossniklaus, U. and Avramova, Z. (2003) 'ATX-1, an Arabidopsis homolog of trithorax, activates flower homeotic genes', *Curr Biol* 13(8): 627-37.

Bendel-Stenzel, M., Anderson, R., Heasman, J. and Wylie, C. (1998) 'The origin and migration of primordial germ cells in the mouse', *Semin Cell Dev Biol* 9(4): 393-400.

Berr, A., McCallum, E. J., Menard, R., Meyer, D., Fuchs, J., Dong, A. and Shen, W. H. (2010) 'Arabidopsis SET DOMAIN GROUP2 is required for H3K4 trimethylation and is crucial for both sporophyte and gametophyte development', *Plant Cell* 22(10): 3232-48.

Fang, Y. and Spector, D. L. (2005) 'Centromere positioning and dynamics in living Arabidopsis plants', *Mol Biol Cell* 16(12): 5710-8.

Groll, M., Schellenberg, B., Bachmann, A. S., Archer, C. R., Huber, R., Powell, T. K., Lindow, S., Kaiser, M. and Dudler, R. (2008) 'A plant pathogen virulence factor inhibits the eukaryotic proteasome by a novel mechanism', *Nature* 452(7188): 755-8.

Ingouff, M., Rademacher, S., Holec, S., Soljic, L., Xin, N., Readshaw, A., Foo, S. H., Lahouze, B., Sprunck, S. and Berger, F. (2010) 'Zygotic resetting of the HISTONE 3 variant repertoire participates in epigenetic reprogramming in Arabidopsis', *Curr Biol* 20(23): 2137-43.

Kumar, S. V. and Wigge, P. A. (2010) 'H2A.Z-containing nucleosomes mediate the thermosensory response in Arabidopsis', *Cell* 140(1): 136-47.

Lindroth, A. M., Shultis, D., Jasencakova, Z., Fuchs, J., Johnson, L., Schubert, D., Patnaik, D., Pradhan, S., Goodrich, J., Schubert, I. et al. (2004) 'Dual histone H3 methylation marks at lysines 9 and 27 required for interaction with CHROMOMETHYLASE3', *EMBO J* 23(21): 4286-96.

Liu, Z., Zhu, Y., Gao, J., Yu, F., Dong, A. and Shen, W. H. (2009) 'Molecular and reverse genetic characterization of NUCLEOSOME ASSEMBLY PROTEIN1 (NAP1) genes unravels their function in transcription and nucleotide excision repair in Arabidopsis thaliana', *Plant J* 59(1): 27-38.

Lu, F., Cui, X., Zhang, S., Jenuwein, T. and Cao, X. (2011) 'Arabidopsis REF6 is a histone H3 lysine 27 demethylase', *Nat Genet* 43(7): 715-9.

Maheshwari, P. (1950) *An introduction to the embryology of angiosperms (1950)*: New York, McGraw-Hill.

Nakahigashi, K., Jasencakova, Z., Schubert, I. and Goto, K. (2005) 'The Arabidopsis heterochromatin protein1 homolog (TERMINAL FLOWER2) silences genes within the euchromatic region but not genes positioned in heterochromatin', *Plant Cell Physiol* 46(11): 1747-56.

Ravi, M., Shibata, F., Ramahi, J. S., Nagaki, K., Chen, C., Murata, M. and Chan, S. W. (2011) 'Meiosis-specific loading of the centromere-specific histone CENH3 in Arabidopsis thaliana', *PLoS Genet* 7(6): e1002121.

Seisenberger, S., Andrews, S., Krueger, F., Arand, J., Walter, J., Santos, F., Popp, C., Thienpont, B., Dean, W. and Reik, W. (2012) 'The Dynamics of Genome-wide DNA Methylation Reprogramming in Mouse Primordial Germ Cells', *Mol Cell* 48(6): 849-62.

Shaner, N. C., Lin, M. Z., McKeown, M. R., Steinbach, P. A., Hazelwood, K. L., Davidson, M. W. and Tsien, R. Y. (2008) 'Improving the photostability of bright monomeric orange and red fluorescent proteins', *Nat Methods* 5(6): 545-51.

Zhu, Y., Dong, A., Meyer, D., Pichon, O., Renou, J. P., Cao, K. and Shen, W. H. (2006) 'Arabidopsis NRP1 and NRP2 encode histone chaperones and are required for maintaining postembryonic root growth', *Plant Cell* 18(11): 2879-92.